Analysis of
the Role of TRF1 and SMG6 in Telomere Length Maintenance

ANALYSIS

OF

THE ROLE OF TRF1 AND SMG6 IN TELOMERE LENGTH MAINTANCE

BY

SICHUN LIN, B.Sc.

A Thesis

Submitted to the School of Graduate Studies

in Partial Fulfillment of the Requirement

For the Degree

Master of Science

Master University

MASTER OF SCIENCE (2011) McMaster University

(Biology) Hamilton Ontario

TITLE	Analysis of the role of TRF1 and SMG6 in telomere length maintenance
AUTHOR	Sichun Lin, B.Sc. (University of Toronto Scarborough)
SUPERVISOR	Professor Xu-Dong Zhu
NUMBERS OF PAGES	xiii, 129

Abstract

TRF1, a shelterin protein, is a negative mediator of telomere length maintenance. Phosphorylation has been shown to play an important role in modulating TRF1 function. T137 and S249 of TRF1 have been indentified to be candidate phosphorylation sites *in vivo*, and one of my thesis objectives was to examine their role in regulating TRF1 function. Both T137 and S249 have each been changed to either alanine (nonphosphorylatable) or phosphomimic mutation. The TRF1 mutants were introduced into a TRF1-depleted cell line. Southern analysis revealed that neither T137 nor S249 of TRF1 is involved in telomere length maintenance. Immunoprecipitation studies showed that T137 and S249 are not required for TRF1 interaction with TIN2. *In vitro* gel-shift assays indicated that T137 and S249 are not important for TRF1 binding to telomeric DNA. Taken together, these results suggest that T137 and S249 may not be required for TRF1 function in telomere length maintenance.

Human Est1A has been suggested to play a role in telomere length maintenance. To identify the domain of hEst1A involved in telomere length maintenance, a number of deletion constructs were generated and retrovirally introduced into HT1080 cells. Southern analysis revealed that the RID domain may positively regulate telomere length maintenance whereas the first 220 amino acids at the N-terminus may be a negative mediator of telomere length maintenance.

In *S. cerevisiae*, Est1 recruits telomerase to telomeres in a Tel1- (homolog of ATM) and MRX-dependent manner. To assess whether *atm-1* and *smg-6* may function in the same genetic pathway of regulation of telomere length in *C.elegans*, the single mutant

strain *atm-1(gk186)* was crossed with three of *smg-6* mutant strains *(tm1308, ok1794 and r896)* to generate double mutants. Southern analysis revealed that deletion of ATM-1 or SMG-6 *(tm1308)* results in telomere shortening, suggesting that atm-*1* and *smg-6* may function in the same genetic pathway to regulate telomere length maintenance.

Acknowledgements

Firstly, I would like to thank my supervisor Dr. Xu-Dong Zhu for allowing me to complete my graduate studies under her supervision. Dr. Zhu is an excellent and experienced professor. Dr. Zhu has provided me with all around training needed to be successful in the field of molecular and cellular biology. From experimental design to data analysis, she has taught me how to perform independent research and how to critically evaluate other research in the filed. She has constantly challenged me to make progress and to improve my abilities. She is always available and her help is greatly appreciated.

I would like to express my thanks to my committee members Dr. Guarné and Dr. Gupta. Thank you for all the time you spent with me and your critical comments on my projects. Both of you have enhanced my learning experience and shown me how research could be done from different point of view. Furthermore, Dr. Gupta spent numerous of hours passing me his knowledge and skills on how the genetic experiment is conducted and for that I am grateful.

I am also grateful to Dr. Rainbow for his advice on my projects during our lab meetings. I want to thank the members of the Zhu laboratory, Taylor, Megan, Kajapanran, and Nicole. I have enjoyed working with you. I am also grateful to have opportunity to know other students in the department. In addition, I would like to thank the other faculty and staff in Biology Department who helped me.

Lastly, I would like to thank my family members who have always been my biggest supporters and who have always loved me.

Table of Contents

List of Figures

Abbreviations

2-D – 2-dimensional
A – Alanine
AA – Amino acid
ALT – Alternative lengthening of telomeres
ATM – Ataxia telangiectasia mutated
ATP – Adenosine triphosphate
ATR – Ataxia telangiectasia and Rad3 related
BCS – Bovine Calf Serum
BLM – Bloom's syndrome protein
BP – Base pairs
Cdc13 – Cell division cycle 13
C-rich – Cytosine rich strand of DNA
ChIP – Chromatin immunoprecipitation
CK2 – Casein kinase II
D-loop – Displacement loop
DMEM – Dulbecco's Modified Eagle Medium
DNA – Deoxyribonucleic acid
DNA-PK – DNA dependent protein kinase
DTT – Dithiothreitol
E – Glutamic acid
EDTA – Ethylenediaminetetraacetic acid
EGTA – Ethylene Glycol Tetraacetic Acid
EST – Even shorter telomeres
FBS – Fetal bovine serum
FISH – Fluorescent in situ hybridization
G2 – Gap 2 phase
GAR domain – Glycine and arginine-rich domain
G-rich – Guanine rich strand of DNA
HBS – Hepes Buffered Saline
HEPES – 4-(2-hydroxyethyl)-1-piperazineethanesulfonic acid
hRap1 – Human transcriptional repressor/activator protein 1
hTERT – Human telomerase reverse transcriptase
hTR – Human telomerase RNA component
KDa – Kilodalton
M – Mitosis
MOPS – 3-(N-morpholino)propanesulfonic acid
MRN – Mre11/Rad50/Nbs1
MRX – Mre11/Rad50/Xrs2
mRNA – Messenger RNA
NHEJ – Nonhomologous End Joining
NMD – Non-sense mediated mRNA decay
NT – Nucleotide

OB – Oligonucleotide/oligosaccharide binding
PABP – Poly-A-binding protein
PBS – Phosphate buffer saline
PCR – Polymerase chain reaction
PD – Population doubling
PI3-K – Phosphatidylinositol-3 kinase
PMSF – Phenylmethanesulfonylfluoride
POT1 – Protection of telomeres
Q – Glutamine
pRS – pRetroSuper-puro
Rap1 – Repressor-activator Protein 1
RNA – Ribonucleic acid
RTEL1 – Regulator of telomere elongation helicase 1
S – Serine
S-phase – Synthesis phase
SDS – Sodium dodecyl sulphat
PAGE – Polyacrylamide gel electrophoresis
siRNA – Small interfering RNA
shRNA – Small hairpin interfering RNA
SMG – Suppressor with Morphological effect on Genitalia
T or Thr – Theronine
T-loop – Telomere loop
TBE – Tris borate EDTA
TE – Tris EDTA
TERRA – Telomeric repeat–containing RNA
TIN2 – TRF1 Interacting Nuclear Protein 2
TRF1 – Telomere repeat binding factor 1
TRF2 – Telomere repeat binding factor 2
TRFH – TRF homo dimerization domain
UPF1 – Up-Frameshift protein 1
WT – Wild type

Chapter 1-Introduction

1.1 Telomeres and Telomerase

Telomeres, specialized DNA-protein structures found at the ends of linear chromosomes, play an essential role in maintaining genome integrity (de Lange, 2002). The chromosome ends undergo erosion with each cell cycle due to end replication problem (Olovnikov, 1973), which is stemmed from the fact that the conventional DNA replication machinery could not completely synthesize the end of linear chromosomes (Olovnikov, 1973). DNA polymerases need a RNA primer to initiate DNA replication and the primer needs to be removed (Olovnikov, 1973; Watson, 1972). Upon the removal of the last RNA primer from the lagging strands, DNA polymerase is unable to fill the gap, and therefore chromosome ends become shorter with the each of the replicative cycle (Harley et al., 1990; Olovnikov, 1973). Telomeres function as a buffer to combat the end replication problem and ensure the coding DNA is not lost.

The mammalian telomeres are composed of repetitive TTAGGG sequence ranging from 3 to 20 kb ending in a 3' single-stranded overhang ranging from 50-500 nt (Fig. 1.1A) (Makarov et al., 1997; Moyzis et al., 1988; Wellinger & Sen, 1997). The 3' G-rich overhang is thought to fold back into the duplex DNA and base pair with the complementary C-rich strand of double-stranded DNA to displace the G-rich strand, forming a large loop structure, termed the t-loop (Fig. 1.1B) (Griffith et al., 1999). The t-loop structure masks the natural chromosomal ends from being recognized as damaged DNA (Griffith et al., 1999).

Progressive telomere shortening limits cell proliferation potential and is regarded as a tumor suppressor mechanism (Palm & de Lange, 2008). In human somatic cells, telomeres shorten with each cell cycle, which ultimately leads to an induction of a replicative senescence (Blackburn et al., 1989; Greider & Blackburn, 1987; Greider & Blackburn, 1989). Thus, telomere length serves as a cellular "clock" to limit cell proliferative ability and has been implicated in ageing (Harley et al., 1990; Wright & Shay, 2002). However, most cancer cells can overcome the replicative barrier and gain the potential of unlimited growth by activating telomerase (Broccoli et al., 1995; Kim et al., 1994; Meyerson et al., 1997).

Telomerase is a ribonucleoprotein containing a reverse transcriptase, a template RNA, and accessory components (Greider & Blackburn, 1985). Human telomerase hTERT (telomerase reverse transcriptase) uses its RNA component (hTR or hTERC) to elongate telomeres by adding of TTAGGG repeats onto the chromosome ends (Feng et al., 1995; Meyerson et al., 1997). Telomerase activity is low or absent in most human cells, but active in germ line cells and stem cells (Broccoli et al., 1995; Kim et al., 1994).

1.2 Shelterin Complex

Human telomeres are bound by a protein complex termed shelterin. Shelterin complex regulates telomere length maintenance and protects the natural chromosome ends from being recognized as double-strand DNA breaks (de Lange, 2005). The shelterin complex comprises TRF1, TRF2, and hRap1, TIN2, TPP1 and POT1 (Fig. 1.2). TRF1 and TRF2 bind specifically to double-stranded telomeric DNA whereas POT1 binds to single-stranded telomeric DNA (Baumann & Cech, 2001; Bianchi et al., 1997; Chong et

al., 1995). TPP1 and POT1 form a heterodimer whereas hRap1 interacts with TRF2 (Hockemeyer et al., 2007; Li et al., 2000; Ye et al., 2004). TIN2 bridges TRF1 and TRF2 and connects POT1 to TRF1 by interacting with TPP1 (de Lange, 2005; O'Connor et al., 2006; Ye et al., 2004). The shelterin complex controls telomere length maintenance and limits the access of telomerase through a negative feedback mechanism (Palm & de Lange, 2008; van Steensel & de Lange, 1997). The more telomere-bound TRF1 and other shelterin components, the shorter the telomeres are, in part due to a decrease in the accesses of telomerase to the end of telomeres (Smogorzewska et al., 2000; Palm & de Lange, 2008; van Steensel & de Lange, 1997).

TRF1 is the first mammalian telomeric protein isolated based on its *in vitro* binding specificity to TTAGGG repeats (Zhong et al., 1995). TRF2 was identified as a telomeric protein based on the sequence and structural similarities between TRF1 and TRF2. Both TRF1 and TRF2 contain a TRF-specific dimerization domain (TRFH), a linker region, and a C-Myb DNA binding domain (Bianchi et al., 1999; Bilaud et al., 1997; Chong et al., 1995; Broccoli et al., 1997; Fairall et al., 2001). TRF1 has an acidic domain at its N-terminus (Fig. 1.3.A). TRF2 contains an N-terminal basic domain (or GAR domain, Gly/Arg rich domain) (Smogorzewska et al., 2000; Smogorzewska & de Lange, 2004). Both TRF1 and TRF2 bind telomeric DNA as a homodimer (Broccoli et al., 1997). However, they don't form a heterodimer despite the similarity of their TRFH (Broccoli et al., 1997; Fairall et al., 2000).

TRF2 has been shown to preferentially bind to double-stranded DNA with a 3' single-stranded overhang (Stansel et al., 2001). The GAR domain of TRF2 has a high

affinity for binding DNA junctions, including Holiday junctions (Amiard et al., 2007; Fouche et al., 2006). TRF2 has been demonstrated to promote t-loop formation *in vitro* (Stansel et al., 2001). TRF2 negatively regulates telomere length maintenance since overexpression of TRF2 results in telomere shortening in telomerase positive and negative cells (Smogorzewska et al., 2000). In addition, TRF2 suppresses ATM-dependent DNA damage response at telomeres (Celli & de Lange, 2005; Denchi & de Lange, 2007; Karlseder et al., 1999).

The interaction of TRF2 with hRap1 (Repressor-activator protein 1) was uncovered through a yeast two-hybrid analysis which revealed that the C-terminus of Rap1 mediates the interaction with TRF2 at TRFH domain and linker region (Li et al., 2000). Rap1 was found to form ~1: 1 complex with TRF2 (Zhu et al., 2000). The TRF2 and Rap1 interaction is responsible for telomeric localization and stability of hRap1. Both TRF2 and Rap1 are required to prevent chromosome ends from undergoing NHEJ (Bae & Baumann, 2007; Li & de Lange, 2003; Sarthy et al., 2009; van Steenel et al., 1998). However, it has also been suggested that Rap1 can function to inhibit homologous recombination at telomeres (Sfeir et al., 2010).

TIN2 (TRF1 interacting nuclear protein 2) was identified as a TRF1 interacting protein through a yeast two-hybrid analysis (Kim et al., 1999). TIN2 is able to bind TRF1, TRF2 and TPP1 to hold the shelterin complex together. The C-terminal domain of TIN2 and TRFH domain of TRF1 mediates TRF1-TIN2 interaction whereas the N-terminal domain of TIN2 is associated with the linker region of TRF2. TIN2 recruits TPPI through its N-terminal domain (Chen et al., 2008; Kim et al., 2004).

TPP1 was first identified as a TIN2 interacting protein (Houghtaling et al., 2004). Its C-terminus mediates TPP1 and TIN2 interaction whereas its centrally located POT1 interaction domain recruits the single-stranded telomeric binding protein POT1 to telomeres (Ye et al., 2004). The interaction of TPP1 with TIN2 connects single-stranded DNA binding protein POT1 to the double-stranded proteins TRF1 and TRF2 (Liu et al., 2004; Ye et al., 2004). POT1 interacts with TRF1 and it has been suggested to sever as a transducer of TRF1 in telomere length maintenance (Loayza & de Lange). An OB-fold domain at the N terminus of TPP1 has been shown to interact with telomerase (Xin et al., 2007). A role of TPP1 in the recruitment and stimulation of telomerase activity at telomeres has been suggested (Xin et al., 2007). Recently, the TIN2-TPP1 interaction has been shown to be important for the recruitment of telomerase to the chromosome ends (Abreu et al., 2010).

POT1 contains two OB folds at the N terminus through which it can recognize and bind the G-rich telomeric DNA *in vitro* and *in vivo* (Baumann & Cech, 2001; Kelleher et al.,2005; Loayza et al., 2004). POT1-TPP1 interaction is required for POT1 function in telomere length regulation and suppression of ATR-dependent DNA damage response at telomeres (Denchi & de Lange; 2007; Hockemeyer et al., 2007).

Aside from shelterin, human telomeres are also associated with many telomere non-specific proteins, including Mre11/Rad50/Nbs1 (MRN) and ATM which play important roles in maintaining genomic stability (Kishi et al., 2001; Verdun et al., 2005; Zhu et al., 2000).

1.3 TRF1 and TRF1 Phosphorylation

1.3.1 The HumanTRF1 Protein (Telomere Repeat Binding Factor 1)

TRF1 is a ubiquitously expressed protein and consists of 439 amino acids. TRF1 is localized in the nucleus and binds telomeric DNA as a dimer (Bianchi et al., 1997; Chong et al., 1995; van Steensel & de Lange, 1997; Zhong et al., 1992). The linker region of TRF1 is high flexible and the C-terminal Myb domain of TRF1 has the ability to loop, bend telomeric DNA, and bind duplex 5'TAGGGTT3' sequence in parallel and anti-parallel orientations, implicating that TRF1 may facilitate t-loop formation (Bianchi et al., 1997; Broccoli et al., 1997; Griffith et al., 1998).

TRF1 has been shown to associate with telomeres throughout the cell cycle. Its association with telomeres has been reported at lowest in S phase and an increase at G2/M phase (Verdun et al., 2005). A role of TRF1 in mitosis has also been suggested (Dynek & Smith, 2004; Nakamura et al., 2002).

PIN2 is a protein that is identical to TRF1 except for a 20 amino acids (amino acids 296-316) deletion in the linker region of TRF1. PIN2 and TRF1 form heterodimers because of the identical dimerization domain (Shen et al., 1997). PIN2 has been suggested to be more abundant than TRF1 (Shen et al., 1997), however, functional differences between PIN2 and TRF1 are yet to be defined (Zhou et al., 2003).

TRF1 has been suggested to regulate telomere length by acting in *cis* to limit the access of telomerase to telomere ends (Ancelin et al., 2002; van Steensel & de Lange, 1997). Overexpression of TRF1 results in telomere shortening in telomerase positive cells. Expression of dominate-negative TRF1 allele promotes telomere elongation (Ancelin et al., 2002; Smogorzewska et al., 2000; van Steensel & de Lange, 1997).

TRF1 interacts with TIN2 via the TRFH F142 of TRF1 and the FxLxP motif located at C-terminus of TIN2 (Chen et al., 2008). TIN2 has been shown to stabilize the shelterin complex at telomeres (O'Connor et al., 2006). TIN2 and TRF1 can form a subcomplex (Kim et al., 2008). N-terminus of TRF1 mediates TRF1 interaction with tankyrase 1 (a TRF1-interacting ankyrin-related ADP-ribose polymerase) through which it recruits the tankyrase 1 and tankyrase 2 to telomeres (Smith et al., 1998). Poly(ADP-ribose)ylation of TRF1 by tankyrase 1 prevents TRF1 from binding to telomeric DNA, resulting in reduction of telomere-associated TRF1 (Chang et al., 2003). The telomere-unbound TRF1 has been suggested to be ubiquitinated, followed by proteolysis (Chang et al., 2003). The ubiquitination of TRF1 is mediated by Fbx4 which is a substrate of ubiquitin E3 ligase (Lee et al., 2006). TIN2 interaction with TRF1 inhibits tankyrase 1 activity (Ye & de Lange, 2004).

TRF1 is an essential gene. TRF1 knockout mice are embryonic lethal (Karlseder et al., 2003). This phenotype is independent of telomerase, and exhibits no obvious telomere length defect, indicating that TRF1 plays a role in development (Karlseder et al., 2003). TRF1 has been implicated to play a role in facilitating telomere DNA replication. Mouse conditional knockout of TRF1 resulted in a fragile-telomere phenotype, characterized with multiple telomeric signals and occasional breakages at chromatid ends, implicating a replication-dependent defect (Sfeir et al., 2009). TRF1 has been suggested to recruit helicases BLM and RTEL1 to the replication fork, which resolve replicative barriers at telomeres (Sfeir et al., 2009).

TRF1 has been suggested to play a role in telomere transcription. Human telomeres have been shown to be transcribed into non-coding telomeric-repeat-containing RNAs, referred as TERRA, which was found in the nucleus and form foci with telomeres in interpahse as well as metaphase (Azzalin et al., 2007). TRF1 has been suggested to interact with DNA dependent RNA polymerase II to transcribe the C-rich strand of the telomeres (Schoeftner & Blasco, 2008). Knockdown of TRF1 decreases the level of telomere transcription, but has no effect on TRF1 interaction with RNA polymerase II (Schoeftner & Blasco, 2008).

1.3.2 TRF1 Phosphorylation

TRF1 is subjected to posttranslational modification. A few of kinases were found to be responsible for TRF1 phosphorylation and phosphorylation has been showed to play an important role in modulating TRF1 function. ATM (a phosphatidylinositol-3 kinase) is activated by DNA double stranded breaks and phosphorylates consensus S/TQ sites. ATM has been demonstrated to be associated with TRF1 by immunoprecipitation (Kishi et al., 2001). ATM preferentially phosphorylates TRF1 at serine 219 in response to ionizing irradiation. This phosphorylation suppresses the mitotic entry and apoptosis (Kishi et al., 2001) .

Threonine 122 of TRF1, phosphorylated by CK2, plays an important role for TRF1 biding to telomeric DNA and regulates telomere length (Kim et al., 2008). Akt, a serine/threonine protein kinase, well known for its function in regulating cell proliferation, survival and cell growth signaling, has been shown to interact with TRF1. Akt-mediated phosphorylation of TRF1 at threonine 273 causes telomere shortening (Chen et al. 2009).

Previously, cyclin dependent kinase 1 (Cdk1) has been suggested to act as a priming kinase to phosphorylate TRF1 at threonine 371, generating a docking site for the phosphorylation of TRF1 at serine 435 mediated by Polo-like kinase 1 (Plk1). Phosphorylation at S435 has been suggested to increase TRF1 binding to telomeric DNA (Wu et al., 2008). However, recent work demonstrated that Cdk 1 mediated phosphorylation of T371 of TRF1 in early mitosis keeps it off telomeres to facilitate the resolution of sister telomeres. In addition, this phosphorylation stabilizes the telomere-unbound TRF1 and makes it readily available for telomere protection upon dephosphorylation of T371 at late mitosis. This phosphorylation decreases TRF1 binding to telomeric DNA (McKerlie & Zhu, 2011).

PIN1 (a prolyl isomerase) regulates TRF1 function through binding phosphorylated threonine 149-proline (Thr 149-Pro) motif of TRF1 at TRFH. This interaction has been suggested to promote TRF1 degradation, resulting in a reduction of telomere-bound TRF1 at telomeres in human and mice cells (Lee et al., 2009).

Mass spectrometry has been performed on TRF1 immunoprecipitated from HT1080 cells and has identified additional TRF1 phosphorylation sites *in vivo*. Threonine 137 and serine 249 are two putative phosphorylated sites at TRFH domain (Zhu, unpublished data). F142 of TRF1 interacts with TIN2 and other FxLxP motif containing proteins (Fig. 1.4) (Palm & de Lange, 2008). It is speculated that phosphorylation at T137 might play a role in TRF1 interaction with TIN2.

Crystal structure revealed that each TRF1 momomer consists of nine α helices at the TRFH domain (Fig. 1.3B) (Fairall et al., 2001). The dimerization occurs via three

helices from each monomer, in which helix 1 and helix 2 of each monomer pack in an antiparallel orientation, while two helix 9 packing against each other stabilize the dimer by forming a perpendicular crossbrace (Fig. 1.3C) (Fariall et al.,2001). S249 of TRF1 is located at the C-terminal end of helix-8 (Fairall et al., 2001). Phosphorylation at this site might play a role in the formation of a stabilizing perpendicular crossbrace by helix-9. It was hypothesized that phosphorylation at T137 and/or S249 may modulate TRF1 function in telomere length maintenance.

1.4 Human Est1A (SMG6)

1.4.1 Human Est1A (SMG6) and NMD

Human Est1A (also named SMG6) was isolated as a human homolog of *Caenorhabditis elegans* and *Drosophila melanogaster* NMD protein SMG-6 (Chiu et al., 2003; Reichenbach et al., 2003; Snow et al., 2003). Eukaryotic cells have evolved a RNA quality control mechanism termed non-sense mediated mRNA decay (NMD). NMD recognizes and degrades mRNAs carrying premature termination codons (PTCs), and prevents the accumulation of truncated proteins which could have deleterious functions (Yamashita et al., 2005). The SMG protein family, including SMG1, UPF1, UPF2, UPF2, SMG5, SMG6 and SMG7, plays an essential role in NMD. UPF1 (an ATP-dependent helicase and a nucleic acid-dependent ATPase) is a central player of NMD. The cycle of phosphorylation and dephosphorylation of UPF1 is thought to drive NMD (Wilkinson, 2003). Current model of the assembly of RNA surveillance complex is viewed as follow. During the first round of translation, SMG1 (a phosphatidylinositol-3 kinase) and UPF1 are recruited by ribosome through interactions with release factors eRF1 and eRF3 when

a premature termination codon (an exon junction complex located 50-55 nt downstream a stop codon) is recognized (Yamashita et al., 2005). The phosphorylation of UPF1 mediated by SMG1 (maybe in the presence of UPF2 and UPF3, presumably UPF2 binding to EJC complex-bound UPF3) represents the key signaling for the induction of mRNA decay (Yamashita et al., 2005). Phosphoserine of UPF1 interacts with 14-3-3 like domain of SMG5, SMG6 and SMG7 (Ohnishi et al., 2003). SMG5, SMG6 and SMG7 facilitate UPF1 dephosphorylation by the recruitment of protein phosphatase 2A (PP2A) (Chiu et al., 2003; Ohnishi et al., 2003), and promote mRNA degradation by recruitment of deadenylation and/or decapping associated exonucleases mediated by SMG7 (Behm-Ansmant & Izaurralde, 2006; Unterholzner & Izaurralde, 2004). Alternatively mRNA degradation could be initiated by SMG6 endonucleolytic cleavage, followed by exonuclease activities (Eberle et al., 2009; Nicholson et al., 2009).

The PIN domain (PilT-N-terminus) was originally named after a protein involved in type IV pili biosynthesis due to sequence similarity (Wall et al, 1999). The nuclease activity of PIN domain was discovered through bioinformatic analysis (Clissold & Ponting, 2000), and crystallography studies. Crystallography of the PIN domain revealed that it resembles that of the nuclease domain of T4 RNase H (Arcus et al., 2004; Glavan et al., 2006; Levin et al., 2004; Takeshita et al., 2006), a protein of FLAP family. The PIN domain at the C-terminus of SMG6 (hEst1A) has been shown to have *in vitro* ssRNA degradation ability and *in vivo* nuclease activity (Glavan et al., 2006). Recent studies suggested that SMG6 is an endonuclease responsible for cleaving the targeted mRNAs in *Drosophila melanogaster* S2 cells and in human cells during NMD (Eberle et al., 2009;

Huntzinger et al., 2008). However, the linker region flanked by 14-3-3 like domain and the PIN domain is not important for its endonuclease activity (Huntzinger et al., 2008).

Recently, two conserved EBM (exon junction complex binding motif) motifs were uncovered at the N-terminal domain of SMG6 and its orothologs (Kashima et al., 2010). The EBM is related to the C-terminus of UPF3b which was known to bind to the EJC complex (Buchwald et al., 2010). The N-terminus of SMG6 has been shown to mediate interactions of SMG6 with all NMD factors, and directly interacts with EJC complex (Fig. 1.5). Mutations in these two motifs impair SMG6 function in NMD, suggesting EJC complex may play a role in recruitment of the SMG6 endonuclease to the PTC containing mRNAs (Kashima et al., 2010).

Aside from NMD, UPF1 and SMG1 have been suggested to play important roles in maintaining genome stability. UPF1 has been illustrated to associate with DNA polymerase delta and it is essential for S phase progression (Azzalin & Lingner, 2006). Like ATM, SMG1 kinase activity is also activated by cellular stress induced DNA damage and regulates G1 checkpoint (Brumbaugh et al., 2004; Gehen et al., 2008). SMG1 was found to be required for p53 (a checkpoint protein) phosphorylation *in vivo* upon γ-irradiation (Brumbaugh et al., 2004; Gehen et al., 2008). In addition, SMG1 promotes UPF1 phosphorylation in response to γ-irradiation, suggesting that SMG1 and UPF1 play a role in DNA damage response (Brumbaugh et al., 2004).

RNA surveillance complexes have been found at telomeres. ChIP assays indicated the seven SMG proteins including UPF1, SMG1, SMG6 (hEst1A) are associated with telomeres *in vivo* (Azzalin et al., 2007). Telomeres are transcribed into TERRA which is

associated with telomeres (Azzalin et al., 2007). It has been shown that knockdown of hEst1A, UPF1 and SMG1 by shRNA increases TERRA's association with telomeres without affecting either the half life of TERRA or the total TERRA levels (Azzalin et al., 2007), suggesting that SMG1, UPF1 and hEst1A negatively regulate TERRA's association with telomeres.

1.4.2 *S.cerevisiae* Est1 and hEst1A (SMG6)

Human Est1 was also identified as one of the three human homologs of the *S.cerevisiae* telomerase subunit Est1p through sequence similarity (Reichenbach et al., 2003; Snow et al., 2003). The similarity led to the identification of three human Est1 related proteins: hEst1A, hEst1B and hEst1C. Human Est1A showed 17.5% identity and 28.9% similarity to Est1p. Human Est1B (SMG5) exhibited 13.5% identity and 27% similarity to Est1p. Human Est1C (SMG7) shared 15.4% identity and 25.4% similarity with Est1p (Reichenbach et al., 2003; Snow et al., 2003).

S. cerevisiae telomerase is composed of four subunits: the catalytic subunit Est2 (the reverse transcriptase) (Lingner et al., 1997), the RNA component TLC1 (Singer & Gottschling, 1994), and two cofactors Est1 (Lundblad & Szostak, 1989), and Est3 (Hughes et al., 2000). All of the subunits are required for telomerase enzymatic activity *in vivo*. A loss of function of any Est gene results in progressive telomere shortening (ever shorter telomeres) characterized by gradual telomere loss and eventual cell death after ~50-100 generations (Bianchi et al., 2004; Lendvay et al., 1996; Lundblad & Szostak, 1989; Singer & Gottschling, 1994).

The budding yeast *S. cerevisiae* telomeres contain about 350 base pairs of TG1–3 repeats (Wellinger et al., 1993). In yeast, Rap1 is the double-stranded telomeric DNA binding protein (Conrad et al., 1990), whereas Cdc13 binds to single-stranded overhangs (Nugent et al., 1996). Est1 binds specifically to G-rich single-stranded DNA *in vitro*, and it associates with telomerase (Est2) *in vivo* by binding to the RNA component TLC1 at its bulged stem-loop (Seto et al, 2002; Virta-Pearlman et al., 1996). Est1 has been suggested to recruit telomerase to telomeric DNA through a direct interaction with Cdc13 (Pennock et al., 2001; Qi & Zakian, 2000). Genetic experiments suggested that Est1 has the ability to activate telomerase enzymatic activity once telomerase is telomere-bound (Taggart et al., 2002).

Est1 has been suggested to be involved in a rate limiting step of telomere elongation. Overexpression of Est1 or co-overexpression Est1 with other subunits of telomerase promoted telomere elongation, whereas co-overexpression of other subunits alone had little effect on telomere length change (Zhang et al., 2010). Est1 has been implicated in a role for promoting G-quadruplex (a high order of DNA structure) formation, and the G-quadruplex appears to positively regulate telomerase-dependent telomere lengthening (Zhang et al., 2010).

Three human Est1 proteins were tested for the association with telomerase RNA. Human Est1A (hEst1A) and hEst1B were found to associate with endogenous telomerase (Reichenbach et al., 2003). Human Est1A has been shown to interact with telomerase RNA (hTR) through its RID domain (RNA interaction domain), which has a high affinity but a low specificity for RNA (Redon et al., 2007). Human Est1A interacts with

telomerase catalytic subunit (hTERT) through a specific protein-protein interaction (Redon et al., 2007). It has been suggested that the EID domain (hEst1A interaction domain) of hTERT mediates both the protein-RNA and protein-protein interaction (Redon et al., 2007).

Overexpression of hEst1A causes telomere shortening in human embryonic kidney 293 cells, but lengthening while co-expressed with hTERT (Snow et al., 2003). However, overexpression of hEst1A in human fibrosarcoma-derived HTC75 cells results in telomere uncapping and genome instability characterized with chromosome fusions and anaphase bridges (Reichenbach et al., 2003). Knockdown of hEst1A causes cell cycle arrest, loss of telomeric tract at some chromosome ends and activates DNA damage response (Azzalin et al., 2007; Chawla & Azzalin, 2008). It is noted that depletion of hTR by siRNA results in telomerase independent cell cycle arrest, and ATR-dependent DNA damage response (Kedde et al., 2006).

Co-expression of hEst1A with hTERT results in telomere elongation, suggesting that hEst1A plays a role in telomere length maintenance. The domains of SMG6 involved in NMD have been identified. However, the domain(s) involved in telomere length maintenance has not been fully characterized. It was hypothesized that the N-terminal of hEst1A promotes telomere lengthening.

1.5 *C.elegans* telomeres, SMG-6 and ATM-1

The nematode *C.elegans* telomeres contain 2 to 9 kb of TTAGGC repeats (Raices et al., 2005). The homologs of mammalian telomeric proteins TRF1, TRF2, TIN2, and TPP1 have not uncovered despite the fact that the whole genome of *C.elegans* has been

completely sequenced. *C. elegans trt-1*, encoding one of shortest telomere reverse transcriptase proteins, was identified, and its deletion leads to progressive telomere shortening and results in chromosome end to end fusions (Meier et al., 2006).

Mammalian telomeres end with G-rich overhangs and form t-loop structures. Recently, it has been suggested that human telomeric DNA can contain both G-rich and C-rich overhangs (Oganesian & Karlserder, 2011). Southern blotting and 2-D gel analysis showed that *C.elegans* telomeres contain both G-rich and C-rich overhangs, as well as telomeric circles (Raices et al., 2008). The G-rich and C-rich overhangs are bound by specific proteins containing an OB fold similar to that of POT1. The G-tail is bound by CeOB1, a protein shares similarity with the second OB fold of POT1, whereas C-tail is bound by CeOB2, which is similar to the first OB fold of POT1. Deletion of CeOB1 causes telomere elongation as well as G-overhang elongation, suggesting a telomerase dependent telomere lengthening (Raices et al., 2008). Deletion of CeOB2 leads to more heterogeneous in telomere length, indicating a recombination dependent telomere length regulation (ALT phenotype) (Raices et al., 2008). STELA (single telomere length analysis) analysis indicates that the majority of G-rich overhang ends in TTA-3' (Raices et al., 2008) whereas the C-rich overhang ends in TTC-5' (Cheung et al., 2004), implicating a well-regulated mechanism for generation of the overhangs (Raices et al., 2008).

Like hEst1A (SMG6), *C.elegans* SMG-6 was identified as a NMD factor, and it functions to facilitate UPF-1 dephosphorylation (SMG-2) during NMD (Chiu et al., 2003). It also contains a conserved 14-3-3 domain and a PIN domain (Reichenbach et al, 2003).

ATM and ATR are PI-3 kinases responsible for transducing DNA damage signals (Abraham, 2001; Cimprich & Cortez, 2008). ATM and ATR along with other DNA repair proteins are found to be associated with telomeres (Smogorzewska & de Lange, 2004; Verdun et al., 2005). In human, mutations of *ATM* gene result in ataxia-telangectasia (AT) syndrome, and cells from AT patients have short telomeres (Metcalfe et al., 1996).

Deletion of the homolog of ATM in *S.cerevisiae* (Tel1) causes telomere shortening, whereas deletion of Mec1 (ATR) has little effect on telomere length (Ritchie et al., 1999). The kinase activity of ATM is required for its telomere function (Mallory & Petes, 2000). In budding yeast, telomerase was found to preferentially elongate short telomeres. Est1 is the first telomerase cofactor identified, and it is required for telomerase activity *in vivo* but not *in vitro*. *S. cerevisiae* telomere overhangs are bound by single-stranded DNA binding protein Cdc13. Est1 interacts with Cdc 13 to recruit telomerase to telomeres. The recruitment of telomerase by Est1 is Tel1- and MRX- dependent (Bianchi & Shore, 2008). *C. elegans* ATM-1 is a homolog of ATM. ATM-1 and SMG-6 are conserved proteins. It is of interest to understand whether ATM-1 or SMG-6 plays a role in telomere length maintenance, and whether *atm-1* and *smg-6* act in the same genetic pathway of telomere length regulation.

Table 1.1 Summary of proteins that are discussed and involved in telomere length maintenance

Proteins	Function
Human	
Shelterin component	
TRF1	Duplex telomeric DNA binding protein
TRF2	Duplex telomeric DNA binding protein
hRap1	TRF2 interacting proteins
TIN2	Bridging molecule that interacts with TRF1, TRF2 and TPP1
TPP1	TIN2 and Pot1 interacting protein
POT1	Single-stranded telomeric DNA binding protein
Telomerase component and associated proteins	
hTERT	Human telomerase reverse transcriptase
hEst1A (SMG6)	Homolog of Est1
hEst1B (SMG5)	Homolog of Est1
Other proteins	
tankyrase 1	TRF1-interacting ankyrin-related ADP-ribose polymerase 1
tankyrase 2	TRF1-interacting ankyrin-related ADP-ribose polymerase 2
ATM	A member of PI-3 kinase
ATR	A member of PI-3 kinase
S.cerevisie	
Rap1	Duplex telomeric DNA binding protein
Cdc13	Single stranded telomeric DNA binding protein
Est2	Telomerase reverse transcriptase
Est1	Telomerase associating factor that recruits and activates telomerase
Est3	Associated with Est2
Tel1	Homolog of ATM
Mec1	Homology of ATR
C.elegans	
CeOB1	Single-stranded (G-rich) telomeric DNA binding protein
CeOB2	Single-stranded (C-rich) telomeric DNA binding protein
TRT-1	Telomerase reverse transcriptase
SMG-6	Homolog of hEst1A
ATM-1	Homolog of ATM

Table 1 .2 Summary of proteins that are discussed and are involved in NMD

Proteins	Function
Human	
SMG1	A member of PI-3 kinase responsible for phosphorylation of UPF1
UPF1	A key component of NMD
UPF2	Interacts with both UPF1 and UPF3
UPF3	Interacts with EJC complex
SMG5	Interacts with PP2A
SMG6 (hEst1A)	Interacts with EJC complex, and the PIN domain of SMG6 is an endonuclease responsible for cleaving targeted mRNA
SMG7	Interacts with SMG5
C.elegans	
UPF-1	Homolog of UPF1
SMG-6	Homolog of hEst1A

Figure 1.1: The structure of human telomeres. (A) Human chromosomes end in TTAGGG repeats that varies in length and contains a 3' overhang ranging from 50-500 nt. Proximal to the telomeric repeats is degenerate TTAGGG repeats and subtelomeric repeats region (Palm & de Lange, 2008). (B) Schematic of the t-loop. The size of the t-loop varies in length. The 3' overhang invades the duplex telomeric DNA and forms a large loop structure (Palm & de Lange, 2008).

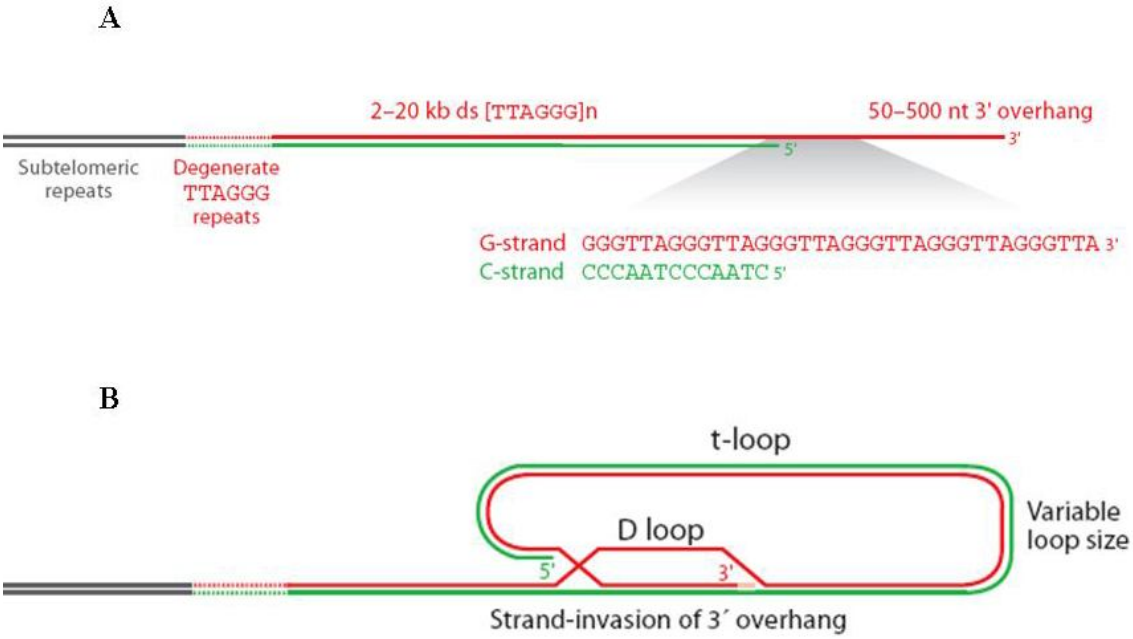
A
2–20 kb ds [TTAGGG]n
50–500 nt 3' overhang
3'
5'
Subtelomeric repeats
Degenerate TTAGGG repeats
G-strand GGGTTAGGGTTAGGGTTAGGGTTAGGGTTAGGGTTA 3'
C-strand CCCAATCCCAATC 5'
B
t-loop
D loop
Variable loop size
5'
3'
Strand-invasion of 3´ overhang

Figure 1.2: Depiction of the shelterin complex binds to the telomeric repeats. Shelterin complex consist of six subunits. TRF1 and TRF2 bind to double stranded telomeric DNA. POT1 binds to single-stranded telomeric DNA. TIN2 bridges TRF1, TRF2 and connects POT1 with TRF1 by interaction with TPP1. Rap1 forms (~ 1: 1) complex with TRF2 (de Lange, 2005).

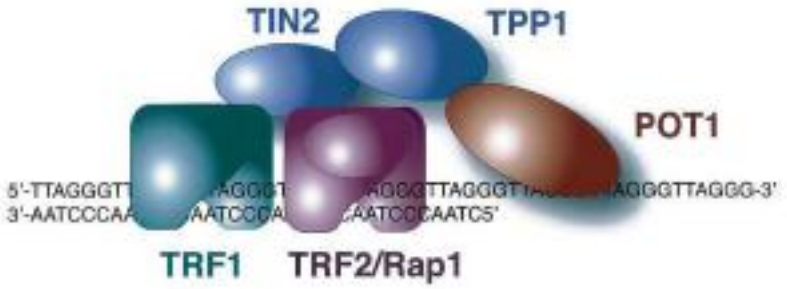
TIN2
TPP1
POT1
TRF1
TRF2/Rap1

Figure 1.3: TRF1 domain organization and TRF1 dimerization domain structure. (A) Schematic of TRF1 domain organization. TRF1 consists of an N-terminal acidic domain, a central dimerization domain (TRFH) and C-Myb domain (adapted from Broccoli et al., 1997). (B) Structure of TRFH monomer. Each monomer consists of nine α helices at the TRFH domain (Fairall et al., 2001). (C) The structure of TRFH dimer. The dimerization occurs via three helices from each monomer. Helix-1 and helix-2 of each monomer pack in an antiparallel manner to form a four-helix bundle, while two helix 9 packing against each other stabilize the dimer by forming a perpendicular crossbrace at the top and the bottom (Fairall et al., 2001).

A


Linker region
N
Acidic
TRFH
C-Myb
C
19
66
263
337
356
378
439

B

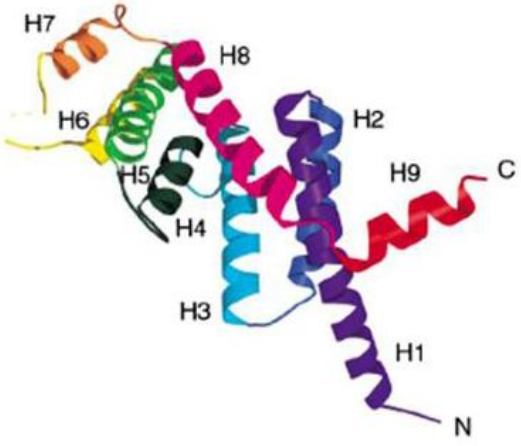
H7
H8
H6
H2
H5
H9
C
H4
H3
H1
N

C

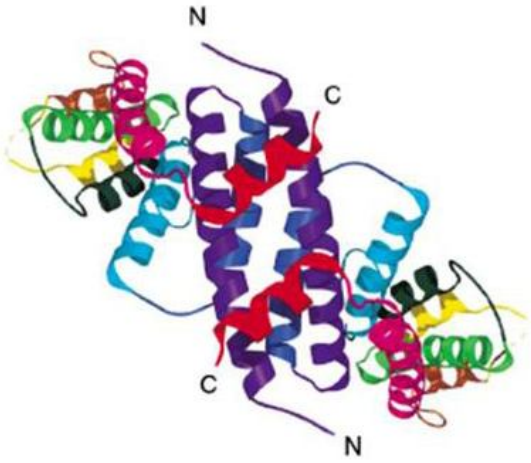
N
C
C
N

Figure 1.4: Schematic of TRF1 binding proteins. The F142 at TRFH of TRF1 interacts with FxLxP containing proteins. TIN2 interaction with this site has been verified *in vivo*. Candidate interactions are shown as dotted lines which connect FxLxP containing interaction partners of TRF1 with F142. The interaction of TRF1 with tanykyrase 1 and 2, and Fbx4 are not involved in FxLxP motif (adapted from Palm & de Lange, 2008).

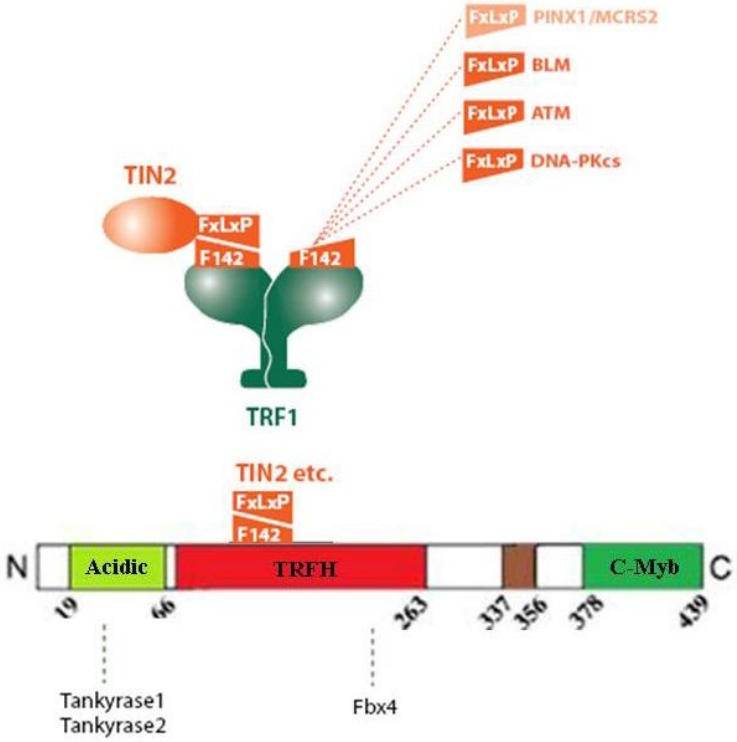
FxLxP PINX1/MCRS2
FxLxP BLM
FxLxP ATM
FxLxP DNA-PKcs
TIN2
FxLxP
F142
F142
TRF1
TIN2 etc.
FxLxP
F142
N
Acidic
TRFH
C-Myb
C
19
66
263
337
356
378
439
Tankyrase1
Tankyrase2
Fbx4

Figure 1.5: Model illustrating SMG6 interactions with NMD factors. During the first round of translation, SMG1 and UPF1 are recruited by ribosome through interactions with release factors eRF1 and eRF3 when a premature termination codon (an exon junction complex located 50-55 nt downstream a stop codon) is recognized. The phosphorylation of UPF1 mediated by SMG1 in the presence of UPF2 and UPF3 represents the key signaling for the induction of mRNA decay. Phosphoserine of UPF1 interacts with 14-3-3 like domain of SMG5, SMG6 and SMG7. In turn, SMG5, SMG6 and SMG7 promote UPF1 dephosphorylation by the recruitment of protein phosphatase 2A (PP2A), and promote mRNA degradation by recruitment deadenylation and/or decapping associated exonucleases mediated by SMG7. Alternatively the mRNA degradation could be initiated by SMG6 endonucleolytic cleavage. EJC complex has been suggested to play role in recruitment of SMG6 endonuclease to the targeted mRNA (Kashima et al., 2010).

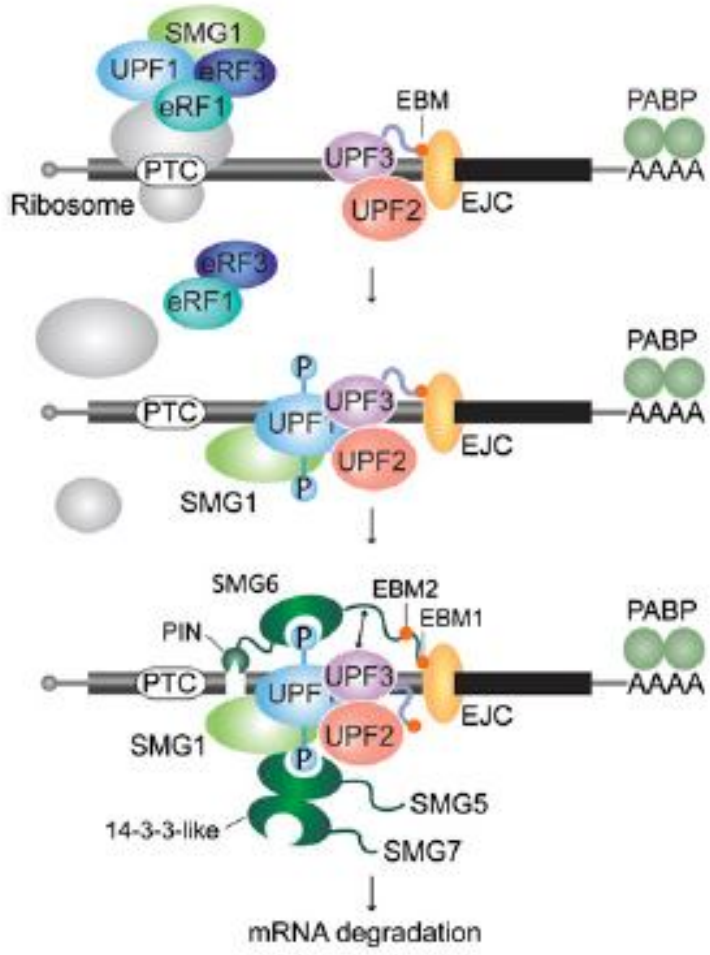
SMG1
UPF1
eRF3
eRF1
EBM
PABP
PTC
UPF3
AAAA
Ribosome
UPF2
EJC
eRF3
eRF1
PABP
P
PTC
UPF
UPF3
AAAA
EJC
UPF2
P
SMG1
SMG6
EBM2
EBM1
PABP
PIN
P
PTC
UPF
UPF3
AAAA
EJC
SMG1
UPF2
P
SMG5
14-3-3-like
SMG7
mRNA degradation

Chapter 2-Materials and Methods

2.1 Cloning of Constructs

2.1.1 Transformation

Half a microliter of mini-prep plasmid DNA was incubated with 30 μl Top10 competent *E. coli* cells on ice for 30 minutes. The sample was heat shocked at 42°C for 45 seconds and then incubated on ice for 2 minutes. One mililiter of LB media (1% Bacto™ tryptone, 0.5% Bacto™ yeast extract, 17.1 mM NaCl, and 2.8 mM NaOH) was added to the tube and cells were incubated in a 37°C shaker at 200 rpm for 1 hour. Twenty microliter of bacteria was spread on LB agar plates containing 0.1 mg/ml ampicillin. Plates were incubated for 16 hours at 37°C. For transformation of ligated DNA, 10 μl of ligated DNA was incubated with 100 μl *E.coli* Top10 competent cells on ice for 30 minutes. Nine hundred microliter of LB media was added to the tube after heat shock, cells were spun down 13,000 rpm for 30 seconds after 1 hour incubation at 37°C. Cell pellets were resuspended in 100 μl of the LB, and plated on LB agar plates containing 0.1 mg/ml ampicillin, followed by overnight incubation at 37°C.

2.1.2 Isolation of Plasmid DNA with Alkaline Lysis Solution

A single transformed bacterial colony was inoculated into 2 ml of LB media containing 0.1 mg/ml ampicillin and placed in a 37°C shaker at 200 rpm for 16 hours. The bacterial cells were collected by centrifugation at 13,000 rpm for 1 minute at 4°C. The supernatant was removed and the pellet was resuspended in 100 μl of solution I (50 mM glucose, 25 mM Tris-HCl[PH8.0], 10 mM EDTA[PH8.0]) , followed by addition of 200

μl of freshly made solution II (200 mM NaOH, 1% SDS), mixed by inversion, and incubated at room temperature for 3-4 minutes. One hundred and fifty microliter of chilled solution III (3.0 M potassium acetate [pH 5.0]) was added to the samples, mixed and incubated on ice for 5 minutes. Samples spun at 13000 rpm for 5 minutes at 4°C, the supernatant was transferred to a fresh tube, followed by addition of 450 μl of phenol/chloroform/isoamylalcohol (25:24:1), mixed by vortexing, and spun at 13,000 rpm for 2 minutes at 4°C. The supernatant was transferred to a new tube, and 900 μl of chilled 95% of ethanol was added to precipitate DNA. The sample was spun at 13,000 rpm for 5 minutes at 4°C, the supernatant was removed, and the DNA pellet was washed with 70% ethanol, air dried, and resuspended in 1X TE buffer (10 mM Tris-HCl [pH 8.0], 1 mM EDTA [pH 8.0]) with 20 μg/ml of RNase A.

2.1.3 QIAGEN® Plasmid Purification Maxiprep Kit

The Maxiprep purification was carried out according to the manufacturer's instruction. In brief, a single transformed bacterial colony was inoculated in 3 ml of LB media containing 0.1 mg/ml ampicillin and placed in a 37°C shaker at 200 rpm for 8 hours. The culture was then diluted 1:1000 in 200 ml of LB media containing 0.1 mg/ml ampicillin and was kept shaking at 200 rpm for 16 hours at 37°C. The bacterial cells were collected by centrifugation at 4000 rpm for 15 minutes at 4°C. The supernatant was removed and the pellets were resuspended in 10 ml of buffer P1 (50 mM Tris-HCl [pH 8.0], 10 mM EDTA, and 100 μg/ml RNase A). Ten mililiter of buffer P2 (200 mM NaOH, 1% SDS) was added, mixed thoroughly by inversion, and incubated at room temperature for 5 minutes. Ten mililiter of chilled buffer P3 (3.0 M potassium acetate [pH 5.0]) was

added to the samples and incubated on ice for 20 minutes. The samples were spun at 12,500 rpm for 30 minutes at 4°C to remove the cell debris, the supernatant was centrifuged again at 12,500 rpm for 15 minutes at 4°C, and the final remaining supernatant was loaded into a QIAGEN column equilibrated with 10 ml of buffer QBT (750 mM NaCl. 50 mM MOPS [pH 7.0], 15% iso-propanol, 0.15% TritonX-100). The columns were washed twice with 30 ml of buffer QC (1.0 M NaCl, 50 mM MOPS [pH 7.0], 15% iso-propanol). The plasmid DNA was then eluted with 15 ml of buffer QF (1.25 M NaCl, 50 mM Tris-HCl [pH8.5], 15% iso-propanol). Ten and half mililiter of iso-propanol was added to the plasmid DNA and centrifuged at 12,500 rpm for 30 minutes at 4°C. The DNA pellet was washed with 5 ml of 70% ethanol and centrifuged at 12,500 rpm for 10 minutes at 4°C. The DNA was dried and resuspended in 1ml of 1X TE buffer (10 mM Tris-HCl [pH 8.0], 1 mM EDTA [pH 8.0]). The concentration of the DNA was measured.

2.1.4 Illustra GFX™ PCR DNA and Gel Band Purification Kit

The extraction of DNA from agarose gel was performed with a commercial kit (GE Healthcare: illustra GFX™ PCR DNA and Gel Band Purification Kit). After running on the gel, the band of interest was excised with a razor blade and placed in a weighted 1.5 ml microcentrifuge tube. The gel band plus the tube was weighted again to determine the weight of the agarose gel slice. Ten microliter of capture buffer type 3 for each 10 mg of the gel was added to the tube, mixed by inversion, and incubated at 60°C to dissolve agarose completely. The capture buffer type 3 and sample mix was transferred to assembled GFX MicroSpin^{TM} column with collection tube, and spun at 13,000 rpm for 1

minute. The column was washed with 500 μl wash buffer type 1, spun at 13,000 rpm for 1 minute. The column was transferred to a clean 1.5 ml microcentrifuge tube, and 40 μl of 1X TE (10 mM Tris-HCl [pH 8.0], 1 mM EDTA [pH 8.0]) buffer was added into the column, followed by incubation for 1 minute at room temperature, and spun at 13,000 rpm for 1 minute to collect purified sample DNA.

2.1.5 Cloning Constructs

pRS-shTRF1 (plasmid#3007, targeted nucleotides 596-614 of TRF1): Annealed oligo 145/146 (the oligos are listed in table 2.1) was ligated into pSuperRetro-puro (pRS for short, plasmid# 2041) vector previously digested with BglII and HindIII. The ligated DNA was transformed into Top 10 cells. Mini-prep DNAs were digested with BglII, and HindIII to screen putative positive clones, and the positive clone was verified by sequencing. All enzymes were purchased from New England BioLab Inc.

pWZL-N-Myc-TRF1SM (wild type with silent mutation, plasmid# 3034): Site directed mutagenesis was preformed to generate pWZL-N-Myc-TRF1SM by using oligos 170/171 as primers and pLPC-N-Myc-TRF1 (plasmid# 1069) as a template. After the parental strands were digested with DpnI, 20 μl of PCR product was transformed. Mini-prep DNAs were digested with EcoRI to screen for positive clones. The plasmid DNA carrying desired mutation was digested with BglII and XhoI to release ~ 1 kb fragment. This fragment was purified and ligated into the vector (~ 6.1 kb in size) generated by digesting pWzl-N-Myc TRF1 wild type (plasmid# 3033) with BglII and XhoI, resulting in pWZL-N-Myc TRF1SM. The presence of mutation was verified by sequencing.

pWZl-N-Myc-TRF1S249E (plasmid# 3041): pWZL-N-Myc-TRF1SM was digested with EcoRI, followed by alkali phosphatase treatment. A large fragment about 6.5 kb in size was purified as a vector. This vector was ligated with an insert containing S249E about 700 bp in size. This insert was generated through PCR, followed by digesting the PCR product with EcoRI. The PCR was carried out by using oligos 170/175 as primers, pLPC-Myc-TRF1S249E (plasmid# 3022) as a template. The ligated vector and insert gave rise to pWZL-N-Myc-TRF1S249E. Positive clones were screened by XhoI, EcoRI and SalI digestion. The positive clone was verified by sequencing.

pWZL-N-Myc-TRF1S249A (plasmid# 3042): pWZL-N-Myc-TRF1SM was digested with EcoRI and SalI. A large fragment about 6.5 kb in size was purified to as a vector. This vector was ligated with an insert containing S249A (about 700 bp). This insert was generated by PCR, followed by digesting the PCR product with EcoRI and XhoI. The PCR was performed by using oligos 170/175 as primers, and pLPC-N-Myc-TRF1-S249A (plasmid# 3021) as a template. The ligated vector and insert resulted in pWZL-N-Myc-TRF1S249A. The positive clones were screened by Bmt1, EcoRI, and SalI digestion, and verified by sequencing.

pWZL-N-Myc-TRF1T137D (plasmid# 3037): This construct was generated in two steps. Step 1: pWZL-N-Myc (plasmid# 1059, 5.9 kb in size) was linearized by BamHI and EcoRI digestion to serve as a vector. This vector was ligated with an insert containing T137D (about 600 bp in size). The insert was produced through PCR, followed by digesting the PCR product with BamHI and EcoRI. The PCR was carried out by using oligos 172/171 as primers, and pLPC-N-Myc-TRF1T137D (plasmid# 3020) as a

template. The ligated vector and insert gave rise to an intermediate containing the first 614 bp of TRF1 including T137D and the desired silent mutations. The positive clones were screened by BglII, BamHI and EcoRI digestion. Step 2: The positive DNA was linearized by EcoRI and SalI digestion to produce a new vector (about 6.4 kb in size). This vector was ligated with an insert about 700 bp in size (also used as an insert for cloning pWZL-N-Myc-TRF1T137A). This insert was generated through PCR, followed by digesting the PCR product with EcoRI and XhoI. The PCR was performed by using oligos 170/175 as primers, pLPC-Myc-TRF1 as a template. The ligated vector and insert gave rise to pWZL-N-Myc-TRF1T137D. The positive clones were screened by EcoRI, and SalI digestion, and verified by sequencing.

pWZL-N-Myc-TRF1T137A (plasmid# 3036): The cloning strategy was essential the same as that of pWZL-N-Myc TRF1T137D other than the template for PCR was replaced by pLPC-N-Myc-TRF1T137A (plasmid# 3003) at step 1, as a result, the intermediate containing first 614 bp of TRF1 including T137A and desired silent mutations.

pLPC-N-Myc-hEst1A wild type (plasmid# 4021): hEst1A wild type was generated in 3 steps. Step 1: An insert about 2.3 kb in size (bp 1981 to 4260 of hEst1A) was generated by digesting pWZL-N-Myc-hEst1A ($AA^{32\text{-}1419}$) (plasmid# 1072) with BamHI and EcoRI. This insert was ligated into the vector pLPC-N-Myc (plasmid # 1061, 5.6 kb in size) which was linearized by BamHI and EcoRI digestion. Upon transformation of the ligated DNA in Top 10 cells, positive clones were screened by digesting mini-prep DNAs with BamHI and EcoRI. The positive clone was the intermediate pLPC-N-Myc-

hEst1A bp 1981-4260 (also used for cloning hEst1A#6 and #7). Step 2: Annealed oligos 219/220 (containing bp 1-51 of hEst1A) was ligated into BamHI-linearized vector pLPC-N-Myc-hEst1A bp 1981-4260 (about 7.9 kb in size). The ligated DNA was transformed, and the positive clones were screened by PCR using oligos 219 and 80 as primers, verified by sequencing, and termed as pLPC-N-Myc-hEst1A bp 1-51+1918-4260 (also used for cloning hEst1A#5). Step 3: An insert (bp 52-1980 of hEst1A, used for cloning hEst1A#5 as well) was generated by PCR, followed by digesting the PCR product with BamHI. The PCR was carried out by using oligo 221/80 as primers, pWZL-N-Myc-hEst1A ($AA^{32\text{-}1419}$) as a template. This insert was ligated into the BamHI-linearized vector pLPC-N-Myc-hEst1A bp 1-51+ 1981-4260. The ligated DNA gave rise to pLPC-N-Myc-hEst1A wild type. Mini-prep DNAs were digested with BamHI to screen for insertion, digested with BglII to determine the orientation. The positive clone was verified by sequencing.

pLPC-N-Myc-hEst1A#5 (plasmid# 5029): An insert (bp 1981-3714 of hEst1A) was generated through PCR, followed by digesting the PCR product with BamHI and EcoRI. The PCR was performed by using oligos 108/245 as primers, wild type hEst1A as a template. This insert was ligated into the vector pLPC-N-Myc-hEst1A bp 1-51. The vector was generated by digesting pLPC-N-Myc-Est1A bp 1-51+1981-4260 with BamHI and EcoRI, followed by purifying a large fragment. Upon transformation of the ligated DNA, mini-prep DNAs were digested with BamHI and EcoRI to screen positive clones. The positive clone (pLPC-N-Myc-hEst1A bp 1-51+ 1981-3714) was digested with BamHI to generate a new vector (about7.4 kb in size). This vector was ligated with the

insert (bp 52-1980, generated while cloning wild type hEst1A at step 3). The ligated DNA gave rise to pLPC-N-Myc-hEst1A#5. Following the transformation of the ligated DNA, mini-prep DNAs were digested with BamHI to screen for insertion, and digested with BglII to determine the orientations. The positive clone was verified by sequencing.

pLPC-N-Myc-hEst1A#6 (plasmid# 6024): An insert (bp 1237-1980 of hEst1A) generated through PCR , followed by digesting the PCR product with BamHI. The PCR was carried out by using oligos 246/80 as primers, wild type hEst1A as a template. This insert was ligated into BamHI-linearized vector pLPC-N-Myc-hEst1A bp 1981-4260 (about 7.9 kb). The ligated DNA gave rise to pLPC-N-Myc-hEst1A#6. Upon transformation of the ligated DNA, mini-prep DNAs were digested with BamHI to screen for insertion, and PCR was performed by using oligos 246/80 as primers to determine orientation. The positive clone was verified by sequencing.

pLPC-N-Myc-hEst1A#7 (plasmid#6021): An insert (bp 661 to 1980 of hEst1A) was generated through PCR, followed by digesting the PCR product with BamHI. The PCR was carried out by using oligos 264/80 as primers, wild type hEst1A as a template. This insert was ligated into BamHI-linearized vector pLPC-N-Myc-hEst1A bp 1981-4260 (about 7.9 kb). Followed by transformation of the ligated DNA, mini-prep DNAs were digested with BamHI to screen for insertion, and PCR was performed by using oligos 264/80 as primers to determine orientations. The positive clone (pLPC-N-Myc-hEst1A#7) was verified by sequencing.

2.2 Tissue Culture

2.2.1 Growth of Cell Lines

Phoenix cells and hTERT-BJ cells were grown in DMEM medium containing 10% FBS, supplemented with L-glutamine, penicillin (100 U/ml), streptomycin (0.1 mg/ml), and non-essential amino acids. HeLaII cells stably expressing pRS, or pRS-shTRF1 were grown in the presence of 2 μg/ml puromycin in 10% of BCS containing DMEM medium. HeLaII cell stably expressing pWZL-N-Myc, and pWZL-N-Myc-TRF1 (wild type and mutants) were cultured in the presence of 2 μg/ml puromycin or 900 μg/ml hygromycin in 10% FBS containing DMEM medium for the first long-term culturing, and in 5% of FBS containing DMEM medium for the second long-term culturing. HT1080 cell stably expressing pLPC-N-Myc, pLPC-N-Myc-hEst1A (wild type and mutants) were cultured in the presence of 2 μg/ml puromycin in 5% FBS containing DMEM medium. All cell lines were grown in 37°C incubator containing 5% CO2 and 100% humidity.

2.2.1 Transfection and Retroviral Infection-Calcium Phosphate Method

Three and half to four million of phoenix amphotropic retroviral package cells were seeded 16-24 hours preceding transfection experiments on 10 cm plates. Twenty microliter of plasmid DNA (1 μg/μl) was mixed with 438 μl of ddH2O and 62 μl of 2 M CaCl2. While bubbling, 500μl of 2X HBS [pH 7.05] (50 mM HEPES, 10 mM KCl, 12 mM dextrose, 280 mM NaCl, 1.5 mM Na2PO4) was added dropwise to the DNA. The mixture was bubbled for 30 seconds following the addition of the last drop of 2X HBS [pH 7.05], and a total of 1 ml of mix was added dropwise to the phoenix cells. Twelve hours post-transfection, the medium was replaced with 9 ml of fresh medium and 12 hours later to 4 ml of fresh medium. Thirty six hours post transfection, the virus containing medium was collected, supplemented with 400 μl FBS and 100 μg/ml of

polybrene, and filtered though a 0.45μm filter. The filtered medium was then plated on recipient cells which were seeded on 10 cm plate 24 hours prior to the first infection (seeding 750,000 for HeLaII or hTERT-BJ cells, and 200,000 for HT1080 cells). A total of 6 infections with an interval of 6 hours were carried over the period of 48 hours. Following the last infection, the medium was changed with 9 ml of fresh medium and 12 hours later the cells were placed in selection medium.

2.2.2 Transfection and Retroviral Infection- Lipofectamine™ Method

For Lipofectamine transfection (Invitrogen), 4 to 4.5 million of phoenix cells were seeded in 6 cm plates 16-24 hours prior to transfection. Twenty microliter of Lipofectamine™ reagent was mixed with 480 μl of 1X reduced medium (Opti-MEM® I Reduced Serum Medium) and incubated at room temperature for 5 minutes. Eight microliter of plasmid DNA (1 μg/μl) was added into 492 μl 1X reduced medium, and then Lipofectamine™ and DNA was mixed and incubated for 20 minutes at room temperature. A total of 1 ml of DNA and Lipofectamine™ mix was added dropwise to phoenix cells. The medium was replaced with 4 ml fresh medium 24 hour post transfection. The infection was carried the same as calcium phosphate method other than phoenix cells were transferred to 10 cm plates after virus was collected for the first infection.

2.3 Protein Study

2.3.1 Whole Cell Extract

Confluent plates of cells grown on 10 cm plates were scraped and the cells were collected. The cells were spun in a 15 ml falcon tube at 1000 rpm for 5 minutes at 4°C.

The cells were then transferred to a microcentrifuge tube, washed in 1 ml of 1X PBS [pH 7.4], and collected by centrifugation at 3000 rpm for 2 min at 4°C. Cell pellets were resuspended in buffer C (20 mM Hepes-KOH [pH7.9], 0.42 M KCl, 25% glycerol, 0.1 mM EDTA, 5 mM MgCl2, 0.2% NP40, 1 mM DTT, 0.5 mM PMSF, 1 μg/ml leupeptin, 1 μg/ml aprotinin, 1 μg/ml pepstatin, 10 mM NaF, 1mM NaVO4, 20 mM Na-β-glycerol phosphate) such that the final concentration of cells was $4x10^4$/μl for HeLaII cells, and $2x10^4$ /μl for hTERT-BJ and HT1080 cells. The cell mix incubated on ice for 30 minutes, followed by centrifugation at 13,000 rpm for 10 minutes at 4°C. The supernatant was transferred to a fresh tube, followed by addition of 2X Laemmli buffer (100 mM Tris-HCl [pH 6.8], 20% glycerol, 3% SDS, 0.01% bromophenol blue, 0.02% β-mercaptoethanol) to allow for a final cell concentration of $2x10^4$ cells/μl for HeLaII and $1x10^4$ cells/μl for hTERT-BJ and HT1080 cells. Samples were stored at -20°C.

2.3.2 Bradford Assay

The concentration of the protein extract was determined using Bradford assay. One microliter of protein extract was added to 199 μl of water, followed by 800 μl of Bradford (BioRad) prior to vortexing. The mixture was incubated at room temperature for 15 minutes and an absorbance reading was done at 595 nm. As a blank control, 200 μl of water was mixed with 800 μl of (BioRad) reagent. The concentration of the protein extract was determined based on the standard curve of the Bradford reagent by using BSA as the standard protein.

2.3.3 Western Immunoblotting

Protein extract was heated for 5 min at 90°C and loaded onto an 8% SDS polyacrylamide gel (SDS-PAGE gel) and run in buffer (25 mM Tris, 250 mM glycine, 1% SDS) for 1.5 to 2 hours at 100 V. The proteins were then transferred to a nitrocellulose membrane at 90 V for 1.5 hours in blotting buffer (25 mM Tris, 125 mM glycine, 20% methanol, 0.02% SDS). The membranes were blocked for a minimum of 45 minutes at room temperature in 1X PBS containing 10% skim milk and 0.5% Tween-20. The membranes were washed 3 times each for 5 minutes in incubation buffer (1X PBS containing 0.1% skim milk and 0.1% Tween-20) and followed by incubation with primary antibody for 2 hours at room temperature or overnight at 4°C. The membrane was subsequently washed 3 times each for 10 minutes at room temperature in the incubation buffer. The membrane was then incubated in the appropriate horse radish peroxidase-conjugated secondary anti-rabbit or anti-mouse secondary antibody at a 1:20-000 dilution for 1 hour at room temperature. The membrane was then washed 3 times each for 10 minutes with the incubation buffer. The membranes were exposed using enhanced chemiluminescence reagent (GE Heathcare). Membranes were stripped for 1 hour at room temperature in 2 M glycine [pH 2.2] and subsequently blocked.

2.3. 4 Immunoprecipatation: Myc- IP for pWZL-N-Myc TRF1

Five to six subconfluent plates (10 cm plates) per cell line were scraped and transferred into 50 ml falcon tube. Samples were spun at 1000 rpm for 5 minutes, and the cell pellet was resuspended in 1X PBS buffer (cold), and processed to extract protein with buffer C as described in 2.3.1. The supernatant was transferred to a fresh cold tube, and dialyzed in buffer D (20 mM Hepes-KOH, 100 mM KCl, 20% glycerol, 0.2 mM EGTA,

and 1 mM DTT and 0.5 mM PMSF were added right before the dialysis) overnight at 4ºC. The proteins were transferred to pre-chilled eppendorf tubes and the concentrations were determined by Bradford assay. One miligram of protein extract with 0.1% of NP-40 was transferred to an eppendorf tube and incubated with 3.5 μl of anti-Myc antibody in the cold room overnight. Thirty microliter of pre-blocked protein-G bead was added to the tube and incubated for another 2 hours in the cold room, and then spun to remove the supernatant. The beads were washed six times each in 1 ml buffer D (0.1% NP-40, 150 mM KC, 1 mM DTT, 0.5 mM PMSF). After the final wash, the beads were resuspended with 50 μl of 2X Laemmili buffer, boiled for 5 minutes, and spun at 3000 rpm for 2 minutes. The supernatant was transferred to a new tube. The samples were loaded on an 8% SDS-PAGE gel along with the input (saved after the concentration was determined), and continued with Western protocol.

2.3.5 Antibodies

Anti-Myc mouse (9E-10) monoclonal antibody was purchased from Calbiocam, and used at a dilution of 1:1000 in incubation buffer. Antibodies to TRF1 (371.2), and TIN2 (864) were generous gifts from Titia de Lange (Rockefeller University), and they were used at a dilution of 1:1000 for TFR1, 1:2000 for TIN2 in incubation buffer. Mouse monoclonal anti γ-tubulin used at 1:20,000 was from Sigma. Anti-mouse and anti-rabbit IgG peroxidase-linked secondary antibodies were purchased from Amersham Biosciences.

2.4 Proliferation Assays

Seven hundred and fifty thousand HeLaII cells or two hundred thousand HT1080 cells were seeded in a 10 cm plate within one week since the start of selection. Every 4

days, the cells were trypsinized and counted using a Beckman Z1 Coulter® Particle Counter. The same density of cell was reseeded.

2.5 Genomic DNA Analysis

2.5.1 Isolation of Genomic DNA

Confluent plates of HeLaII, or HT1080 cells grown on 10 cm plates were scraped and the cells were collected. The cells were spun in a 15 ml Falcon tube at 1000 rpm for 5 minutes at 4°C. The cells were then transferred to a microcentrifuge tube, washed in 1 ml of cold 1X PBS [pH 7.4], and collected by centrifugation at 3000 rpm for 2 minutes at 4°C. After removing the supernatant, the cell pellets were stored in -80°C.

For isolation of human genomic DNA, cell pellets were quickly thawed at room temperature, resuspended in 1 ml of TNE (10 mM Tris [pH 7.4], 100 mM NaCl, 10 mM EDTA), and squired into a 15 ml phase lock tube (5 Prime) containing 1 ml of freshly prepared TENS buffer containing proteinase K (10 mM Tris [pH 7.4], 100 mM NaCl, 10 mM EDTA, 1% SDS, 100 μg/ml proteinase K). The mixtures were incubated overnight at 37°C.

The next day, 2 ml of phenol/chloroform/isoamylalcohol (25:24:1) was added to the tubes and they were mixed until the phases were indistinguishable. The mixtures were spun at 3000 rpm for 10 minutes at 4°C. The aqueous phase was then transferred into a new phase lock tube, 2 ml of phenol/chloroform/isoamylalcohol was added, and the tubes were inverted several times until one phase was apparent, and spun at 3000 rpm for 10 minutes at 4°C. The aqueous phase was then transferred into a 15 ml tube containing 2 ml iso-propanol and 220 μl of 2 M NaAc [pH 5.5]. Genomic DNA was fished out and

transferred to a microcentrifuge tube containing 300 μl of 1X TNE with 100 μg/ml RNase A. The DNA was incubated for 2.5 hours at 37°C. Subsequently, 300 μl of 1X TENS buffer containing proteinase K was added to the DNA and the DNA was incubated for another hour at 37°C. Six hundred microliter of phenol/chloroform/isoamylalcohol was then added to the microcentrifuge tube and the tubes were mixed until one phase appeared. The DNA was then spun at 13,000 rpm for 10 minutes at 4°C. The aqueous phase was transferred with a blue tip (tip cut) to a microcentrifuge tube containing 600 μl of iso-propanol with 66 μl of 2 M NaAc [pH 5.5]. The genomic DNA was then fished out and placed in 200 μl of $T_{10}E_{0.1}$ (10 mM Tris-HCl [pH 8.0], 0.1 mM EDTA). The DNA was left to dissolve for one hour at 37°C and left in 4°C overnight. Samples were ready to be digested.

2.5.2 Digestion of Genomic DNA

A total of 30 μl of dissolved genomic DNA was digested with 2.5 μl of RsaI, Hinf1, and 0.2 ng RNase A overnight at 37°C. The DNA concentration was measured using Hoechst fluorometry using calf thymus DNA as a standard.

2.5.3 Southern Blotting and Detection of Telomere Restriction Fragments

Based on the Hoechst measurement, 4 μg of digested genomic DNA was loaded onto a 20x20 cm 0.7% agarose gel in 0.5X TBE (45 mM Tris-borate, 1 mM EDTA). The gel was run for 1000 voltage hours until the 1 kb marker almost ran off the gel. The gel was dried for 2 hours at 50°C using a gel drier (SGD200 Slab Gel Drier model #QS2576). The dried gel was denatured for 30 minutes in denaturing solution (1.5 M NaCl, 0.5 M

NaOH) and neutralized two times for 15 minutes in neutralization buffer (3 M NaCl, 0.5 M Tris-HCl [pH 7.0]). The gel was rinsed in ddH2O for 3 minutes and placed in 25 ml (for a full gel) of Churchmix (0.5M NaPi [pH7.2], 1 mM EDTA [pH 8.0], 7% SDS, 1% BSA) for a minimum of 1 hour at 55°C. The gel was hybridized overnight with a γ-^{32}P end labeled telomere C-rich probe $(AATCCC)_4$.

The next day, the gel was washed three times each for 30 minutes in 4X SSC (0.6 M NaCl, 60 mM sodium citrate) and then 30 minutes in 4X SSC containing 0.1% SDS. The gel was placed in a PhosphorImager screen (GE Healthcare) overnight and scanned using a PhosphorImager (Storm 820, Amersham Pharmcia Biotech). The Southern blots were quantified using ImageQuant software version 5.2.

2.6 Gel Shift Assay

pHis-parallel-2-TRF1SM (plasmid# 5043), pHis-parallel-2-TRF1-T137A (plasmid# 5067), pHis-parallel-2-TRF1-T137D (plasmid# 5058), pHis-parallel-2-TRF1-S249A (plasmid# 5056) and pHis-parallel-2-TRF1 S249E (plasmid#5067) were cloned, and the recombinant proteins were purified by Kajaparan. For gel shift assays, 60, 120, 240, 360 ng of purified TRF1 protein (wild type or mutant) was incubated with 10 μl of 2X GS buffer (10% glycerol, 8% Ficoll, 40 mM Hepes [PH7.9], 300 mM KCl, 2 mM MgCl2, 0.2 mM EDTA,1 mM DTT), 0.5 μl of β-casein (100 ng/μl), 0.5 μl of sheared *E.coli* DNA (1 μg/μl), and 0.5 μl of labeled pTH12 probe in a total volume of 20 μl for 20 minutes at room temperature. The samples were loaded on 1% of agarose gel (0.1X TBE running buffer), run at 130 V for 1 hour, dried at 80°C in a gel dryer for 2 hours, placed in a PhosphorImager screen overnight, and scanned.

2.7 Worm Strains

Worms were grown at 20°C and maintained as described (Brenner, 1974). The strains used in this study include the following: wild type strain N2, mutant strains *atm-1(gk186)*, *smg-6 (tm1308)*, *smg-6 (ok1794)* and *smg-6 (r896)* (obtained from the Caenorhabditis Genetics Center).

2.8 Single Worm PCR

One worm (or one to five worms) was picked from a plate and transferred into a 0.7 ml ice chilled microcentrifuge tube with 5 μl of lysis buffer (50 mM KCl, 10 mM Tris [PH 8.2], 2.5 mM $MgCl_2$, 0.45% NP-40, 0.45% Tween-20, 0.001% Gelatin, and fresh thawed proteinase K 2 μg/μl). The microcentrifuge tube with worms to be lysed was incubated at -80ºC for at least 15 minutes or overnight or even longer, worm genomic DNA was then extracted by incubating the frozen tube at 60 ºC for 1 hour, 95 ºC for 15 minutes. The genomic DNA was store at 4 ºC or added into PCR mix to process PCR.

2.9 Crosses

2.9.1 Crossing *atm-1* Male with *smg-6 (ok1794 or tm1308)* Hermaphrodites to Generate Double Mutant

Ten of *atm-1 (gk186)* males were crossed with two of *smg-6 (ok1794)* or *smg-6 (tm1308)* hermaphrodites. Eight of F1 worms were cloned in 8 plates (1 worm/plate). Five or six worms were randomly picked from each of the cloned F1 plate to extract genomic DNA which serviced as template for PCR and used to screen *atm-1*$^{-}$*/atm-1*$^{+}$; *smg-6 (ok1794)*$^{-}$*/smg-6 (ok1794)*$^{+}$or *atm-1*$^{-}$*/atm-1*$^{+}$; *smg-6 (tm1308)*$^{-}$*/smg-6 (tm1308)*$^{+}$ heterozygous. Thirty two of worms were then cloned from the heterozygous plate (1

worm/plate). Five or six worms were randomly picked from each of those 32 cloned plates to extract genomic DNA which serviced as template for PCR and used to screen both *atm-1* and *smg-6* deletion. The worms derived from putative deletion plates were subjected to be further verified by PCR.

2.9.2 Crossing *atm-1* Male with *smg-6 (r896)* Hermaphrodites to Generate Double Mutant

Smg-6 (r896) hermaphrodites have protrusive vulva. For cross between *atm-1* and *smg-6 (r896)*, wild type phenotypic F1 worms were picked to extract genomic DNA. Genomic DNA served as a template to screen *atm-1*$^{-}$*/atm-1*$^{+}$ genotype by PCR. Sixteen worms were cloned from *atm-1* heterozygous plate. Five or six F2 worms were randomly picked from each of the cloned plates in which worms have protrusive vulva to extract genomic DNA. Genomic DNA served at a template to screen *atm-1* deletion by PCR. Primers used for PCR are listed in table 2.2.

2.10 Isolation of Genomic DNA from *C.elegans* and Southern Blotting

Worm genomic DNA isolation was carried as described (Raices et al, 2005). Briefly, nematodes were floated off the bacterial lawns with M9 buffer (0.3% KH_2PO_4, 0.6% Na_2HPO_4, 0.5% NaCl, 1 mM $MgSO_4$), collected through centrifugation at 2800 rpm for 2 minutes, and washed twice with M9 buffer. After harvesting, worms were lysed in 2 ml freshly made buffer containing 100 mM Tris HCl [pH 8.5], 100 mM NaCl, 50 mM EDTA, 1% SDS, 100 μg/ml proteinase K, and 1% β-mercaptoethanol for 2 hours at 50°C. The mixtures were transferred to a 15 ml Phase Lock Gel tube, and DNA was isolated by phenol/chloroform/isoamylalcohol extraction, followed by isopropanol precipitation.

Genomic DNA fished out and dissolved in 0.3 ml buffer containing 100 mM Tris-HCl [pH 8.5], 100 mM NaCl, 50 mM EDTA with 100 μg/ml RNase A, and incubated at 37 °C for 2.5 hours. Followed by the addition of 0.3 ml of the proteinase K buffer and incubation at 50°C for 1 hour, DNA was isolated by phenol/chloroform/isoamylalcohol extraction and isopropanol precipitation. The genomic DNA was dissolved in 100 μl of T_{10} $E_{0.1}$ (10 mM Tris-HCl [pH 8.0], 0.1 mM EDTA) buffer, and stored at 4 °C. Genomic DNA isolated from worm was digested with MboI and AluI. Southern blotting was carried out the same as described in 2.5.3 except the end labeled probe for detected *C.elegans* telomeres is $(AATCCG)_4$.

Table 2.1 Oligos used for cloning

Oligo number	Sequence
80	GCGCAAGCTTCCTCCTCGTATACACTGCCAGC
108	GCGCGGATCCGAATGTTGAGAACCC
145	GATCCCCGAATATTTGGTGATCCAAATTCAAGAGATTTGGATCACC AAATATTC TTTTTGGAAA
146	AGCTTTTCCAAAAAGAATATTTGGTGATCCAAATCTCTTGAATTTGG ATCACCAAATATTCGGG
170	GCAGAAGAAGTCTTTGAAAGAATATTCGGCGATCCGAATTCTCATA TGCC
171	GGCATATGAGAATTCGGATCGCCGAATATTCTTTCAAAGACTTCTTC TGC
172	GCGCGGATCCGCGGAGGATGTTTCCTCAGCGGCC
175	GGCATATGAGAATTCGGATCGCCGAATATTCTTTCAAAGACTTCTTC TGC
219	GATCTAGATCTGCGGAAGGGCTGGAGCGTGTGCGGATCTCCGCGTC GGAGCTGCGCGG
220	GATCCCGCGCAGCTCCGACGCGGAGATCCGCACACGCTCCAGCCCT TCCGCAGATCTA
221	GCGCGGATCCTGGCTACTCTGGCCCCGCAGGCCGGGAGCAGAGAAA ACATGAAGGAATTAAAGGAGGCCAGGCCGCGCAAAGATAAC
245	GCGCGAATTCTCACTGCCTCATCTGACTGTGGTCCTCCAG
246	GCGCGGATCCGCCCATACCACCCTATCTGTCAATTC
327	GCGCGGATCCAGCCCTCTGCCTACCAGCACCATGAG

Table 2.2 Oligos used for worm single worm PCR

Primer	sequence
oligo#238 (*atm-1*)	ATTCTGAGAATGCGTACCGCGCAA
oligo#239 (*atm-1*)	ATTTAGCCGCCGTATGTACC
oligo#252 (*ok1794*)	GCGGAGCACAAATATCAGTCAGGCTG
oligo*# 253 (ok1794*)	CTTGCTCTTTGAGCCAAGCCACAGCGAT
oligo#254 (*tm1308*)	GTGTGGGATGTGAAGTGATCAGTAAGG
oligo#255 (*tm1308*)	GTGCTAAACCGCACTTGTGTAGAT

Chapter 3-Results and Discussion: Analysis of the Role of Potential Phosphorylation Sites T137 and S249 of TRF1 in Telomere Length Maintenance

3.1 Generation of Cell Lines Stably Depleted for Endogenous TRF1

Phosphorylation has been shown to play an important role in modulating TRF1 function. Mass spectrometric analysis revealed two putative phosphorylation sites on TRFH of TRF1 at T137 and S249. To study the function of potential phosphorylation sites T137 and S249 of TRF1 *in vivo*, we decided to examine the effect of a nonphosphorylatable (alanine) or a phosphomimic (aspartic acid or glutamic acid) mutation on each of the respective site. We chose to analyze the function of these mutations in a cell line with persistent depletion of endogenous TRF1 to minimize the interference from endogenous TRF1. pSuperRetro (pRS) was used as the vector to generate pRS-shTRF1.

To knockdown TRF1, plasmid DNA pRS and pRS-shTRF1 were transfected into phoenix retroviral packaging cells and the retrovirus carrying pRS or pRS-shTRF1 was used to infect HeLaII (or hTERT-BJ) cells. Western analysis showed that TRF1 was depleted in both HeLaII and hTERT-BJ cells (Fig. 3.1).

3.2 Depletion of TRF1 Does Not Affect Cell Proliferation in HeLaII Cells

It has been implicated that depletion of TRF1 induces apoptosis and growth defects in cells with short telomeres (such as HeLa cells) (Wu et al., 2008). To assess the effect of TRF1 depletion on cell proliferation, HeLaII cells stably expressing pRS or pRS-shTRF1 were cultured for up to 70 population doublings (PDs). Growth curves of pRS

and pRS-shTRF1 HeLaII cell lines showed that HeLaII cells depleted for TRF1 grew similarly to those expressing the vector alone (Fig. 3.2).

3.3 Depletion of TRF1 Results in Telomere Elongation

TRF1 binds to double stranded telomeric DNA and has been suggested to limit the access of telomerase to the telomere ends (Chong et al., 1995; de Lange, 2005; van Steensel & de Lange, 1997). The removal of TRF1 from telomeres promotes telomerase-dependent telomere elongation.

To determine the role of TRF1 depletion in telomere length dynamics, HeLaII cells stably expressing shTRF1 or pRS were cultured for up to 70 PDs. Genomic DNA was extracted and telomere restriction fragments were analyzed by Southern blotting. Southern analysis demonstrated that depletion of TRF1 resulted in telomere elongation at a rate of about 170 bp/PD, in which the average telomere length increased drastically between PD 2 (6 kb) and PD 34 (14 kb), and then became plateau at about PD 50 (17 kb) in HeLaII-shTRF1 cells. The average telomere length of the vector control cell line remained little changed over the period of 70 PDs (Fig. 3.3).

TRF1 was stably depleted by shTRF1 in HelaII cell line (Fig. 3.1). The depletion of TRF1 didn't alter the cell proliferation (Fig.3 .2), but resulted in telomere elongation (Fig. 3.3), the latter is consistent with previous finding (van Steensel & de Lange, 1997). Thus, the HeLaII TRF1 knockdown cell line (HelaII-shTRF1) can be used as a tool to study the functions of phosphorylation at T137 and S249 of TRF1 in telomere length maintenance.

3.4 Overexpression of TRF1 Carrying Mutation at T137 or S249 Does Not Affect Cell Proliferation in TRF1-depleted HeLaII Cells

To study the role of phosphorylation at T137 or S249 of TRF1 on telomere length maintenance, wild type and mutant TRF1 were retrovirally introduced into HeLaII-shTRF1 cells. HeLaII-shTRF1 cells were infected with retrovirus expressing the vector alone (pWZL-N-Myc), Myc-tagged TRF1SM, Myc-tagged TRF1T137A, Myc-tagged TRF1T137D, Myc-tagged TRF1S249A, or Myc-tagged TRF1S249E, giving rise to six stable cell lines (shTRF1-vector, shTRF1-TRF1SM, shTRF1-TRF1T137A, shTRF1-TRF1T137D, shTRF1-TRF1S249A, and shTRF1-TRF1S249E). As a control, HeLaII-pRS cells were also infected with retrovirus expressing the vector alone, generating a stable HelaII-pRS-vector cell line. The seven cell lines were generated two times independently.

It has been implicated that overexpression of TRF1 induces mitotic entry and apoptosis in cells with short telomeres (Kishi et al., 2001). To assess the effect of overexpression of TRF1SM and mutants on growth dynamics and telomere length dynamics, these seven cell lines were subjected for long-term culturing up to 60-80 population doublings. Overexpression of T137A, T137D, S249A, and S249E in HeLaII-shTRF1 cells had no impact on cell proliferation compared to overexpression of wild type TRF1 or the vector alone as shown in Figure 3.4.

3.5 T137 of TRF1 Doesn't Appear to Be Involved in Telomere Length Maintenance

3.5.1 Analysis of the TRF1 Protein Expression Level during the Course of Long-term Culturing

Western blotting was performed to examine whether HeLaII-shTRF1 cells experienced a similar level of TRF1 protein expression at early and late population doublings. During the first long-term culturing, the level of all the TRF1 expression including TRF1SM, T137A, T137D, S249A and S249E decreased with increasing population doublings as revealed by Western analysis (Fig. 3.5A). The level of protein expression at PD 5 was higher than that of PD 35, and the level of protein expression at PD 35 was higher than that of PD 80 as shown in Figure 3.5A. The loss of TRF1 expression was not due to a lack of protein expression as revealed by γ- tubulin blots (Fig. 3.5A). These results indicate a loss of protein expression throughout the long-term cell culturing.

During the course of second long-term culturing, the expression level of TRF1SM, T137A, T137D and S249A appeared to be maintained from early to late population doublings (PD 3 to PD 78), whereas a decrease of S249E expression was detected at PD 40 (Fig. 3.5B). In addition, a degradation product was detected in shTRF1-T137D cell line from PD 3 to PD 78 (Fig. 3.5B).

3.5.2 Overexpression of T137A and T137D Suppresses Telomere Elongation Mediated by shTRF1 in HeLaII Cells

To determine whether the phosphomimic or nonphosphorylatable mutation at T137 or S249 may play a role in telomere length maintenance, Southern blotting was performed to examine the telomere dynamics in these seven stable cell lines which were generated two times independently. I have shown that HeLaII cells depleted for TRF1 (HeLaII-shTRF1) experienced rapid telomere lengthening. The average telomere length

increased from 6 kb at PD 2 to about 14 kb at PD 35 (Fig. 3.1), and became plateau at about PD 50 (17 kb). Telomere dynamics in HeLaII-shTRF1-vector cells was similar to that of HeLaII pRS-shTRF1 cells. The average telomere length of HeLaII-pRS-vector cells stayed constantly as that of HeLaII-pRS cells (Fig. 3.5C and 3.5E). Overexpression of wild type TRF1 resistant to shTRF1 resulted in suppression of telomere lengthening in HelaII-shTRF1 cells (Fig. 3.5C and 5E). The average telomere length in HeLaII shTRF1-TRF1SM cell was maintained at about 7.5 kb (Fig. 3.5G and 3.5H).

Southern analysis indicated that T137 of TRF1 is not involved in telomere length maintenance. Two independent experiments revealed that overexpression of T137A and T137D suppressed telomere elongation in HeLaII-shTRF1 cells (Fig. 3.5D and 3.5F), compared to that of overexpression of TRF1SM (Fig. 3.5C and 3.5E). The first genomic blots revealed that the average telomere length in shTRF1-T137D cell line was maintained constantly and similar to that of TRF1SM over the period of 62 PDs (Fig. 3.5D). The average telomere length in HeLaII shTRF1-T137A cell line appeared to increase with increasing population doublings (Fig. 3.5D), nonetheless, it is much shorter than that of shTRF1-vector cell line. The second genomic blot showed that T137A appeared to suppress telomere elongation more effectively than TRF1SM (Fig. 3.5E and 5F). On the other hand, T137D appeared to be as effective as TRF1SM in suppressing telomere elongation in HeLaII-shTRF1 cells (Fig. 3.5E and 3.5F). The average telomere length in shTRF1-T137A cell line was maintained at about 7.1 kb (Fig. 3.5G). The average telomere length in shTRF1-T137D cell line was maintained at about 7.2 kb (Fig.

3.5H). Telomere length dynamics were very similar in shTRF1-T137A, shTRF1-T137D and shTRF1-TRF1SM cell lines (Fig. 3.5G).

3.6 S249 of TRF1 Is Not Involved in Telomere Length Maintenance

Two independent genomic blots suggested that S249 of TRF1 is not involved in telomere length maintenance. The first genomic blot demonstrated that overexpression of S249A and S249E suppressed telomere elongation in HeLaII-shTRF1 cells. The average telomere length in shTRF1-S249A or shTRF1-S249E cell line was maintained fairly constant and similar to that of wild type TRF1 (Fig. 3.5C and 3.5D).

The second genomic blot showed that overexpression of S249A and S249E in HeLaII-shTRF1 cells suppressed telomere lengthening mediated by shTRF1 as effectively as TRF1SM did (Fig. 3.5E and 3.5F). Overall, in shTRF1-S249A cell line, average telomere length was maintained at about 8 kb (Fig. 3.5H), and in shTRF1-S249E cells, the average telomere length was maintained at approximately 8.4 kb (Fig. 3.5H). There was no significantly difference in telomere length dynamics between HeLaII-shTRF1 cells overexpression of TRF1SM and S249 mutant ofTRF1 (Fig. 3.5H).

3.7 T137 and S249 Are Not Involved in TRF1-TIN2 Interaction

It has been shown that TRFH domain of TRF1 contains a peptide docking site through which it recruits its interaction partners (FxLxP motif containing proteins) to telomeres (Chen et al., 2008). TIN2 and TRF1 interaction is mediated by F142 of TRF1 TRFH domain. T137 is located close to F142 and it is speculated that a mutation in T137 might affect TRF1 interaction with TIN2. Immunoprecipitation was performed to examine TRF1 interaction with TIN2 in the stable cell lines used for analysis of telomere

length dynamics. Anti-Myc was used as the antibody to pull down Myc-tagged TRF1 proteins (SM, T137A, T137D, S249A and S249E), and shTRF1-pWZL served as a negative control. The presence of endogenous TIN2 was analyzed by Western blot with anti-TIN2 antibody. Expression of Myc-tagged wild type TRF1 was indistinguishable from those of TRF1 mutants. As depicted in Figure 3.6, TIN2 (arrow in Fig. 3.6) was pulled down by Myc-tagged TRF1SM, T137A, T137D, S249A and S249E at a comparable level, and there was no defect in TRF1-TIN2 interaction detected.

3.8 T137 and S249 Are Not Important for TRF1 Binding to Telomere DNA

TRF1 binds to double stranded telomeric DNA (Chong et al., 1992). To examine whether the phosphomimic or the alanine mutation at T137 or S249 may impair TRF1 binding to telomeric DNA, *in vitro* gel-shift assays using bacteria-expressed recombinant TRF1 proteins were performed. As depicted in Figure 3.7, all TRF1 mutants bound telomeric DNA and their binding was indistinguishable from that of wild type TRF1.

3.9 Discussion and Conclusions

Southern analysis showed that overexpression of wild type TRF1 suppressed telomere elongation mediated by shTRF1 in HeLaII cells. However, the variations were observed between two experiments, in which the average telomere length in TRFSM cell line in the second experiment appeared to be longer than that of the first one. These results may be caused by the subtle difference in protein expression, the difference of the culture media as described in the method (10% FBS vs 5% of FBS), or the length cells left in falcon tubes between counting and seeding.

Both T137A and T137D suppressed the telomere elongation in HeLaII-shTRF1 cells. However, a difference in telomere length dynamics between T137A and T137 D cell line was observed, and the difference seemed to differ from experiment to experiment. The first genomic blot indicated that overexpression of T137D seemed to suppress telomere elongation better than that of T137A, whereas it appeared to be just the opposite in the second genomic blot. The variation may be caused by the difference in the protein expression in two experiments. In the first experiment, protein expression decreased (Fig. 3.5A), whereas a degradation product of TRF1T137D was produced in the second experiment (Fig. 3.5B).

Despite the fact that expression of TRF1 proteins decreased during the course of the first long-term culturing, Southern blotting revealed that the phosphomimic mutation and non-phosphorylatable mutation T137 or S249 (before PD52) of TRF1 suppressed telomere elongation as effective as that of wild type TRF1 in HeLaII-shTRF1 cells, suggesting that the phosphorylation at T137 or S249 may have no impact on telomere length maintenance. In addition, Southern analysis from the second long-term culturing indicated that T137 and S249E of TRF1 had no effect on telomere length dynamics.

Southern analysis suggests that both phosphomimic and alanine mutants of T137 and S249 suppressed telomere elongation mediated by shTRF1 as effective as that of wild type TRF1. The gel-shift assays indicated that the mutation at T137 or S249 doesn't affect TRF1 binding to telomeric DNA (Fig.3.7). Immunoprecipitations revealed that T137 and S249 are not involved in TRF1-TIN2 interaction (Fig. 3.6). Taken together,

these results suggest T137 and S249 of TRF1 are not important for TRF1 function in telomere length maintenance.

Figure 3.1: TRF1 is depleted by shTRF1 in hTERT-BJ and HeLaII cell lines. pSuperRetro (pRS, vector control) or pRS-shTRF1 was retrovirally introduced into hTERT-BJ and HeLaII cells to generate stable cell lines. Cells were lysed to extract protein after 8 days selection (hTERT-BJ, left) and cultured for 34 PDs (HeLaII, right). Protein extracts from $2x10^5$ cells of each sample were loaded on an 8% SDS-PAGE gel. Anti-TRF1 was used to detect endogenous TRF1, and anti γ-tubulin served as a loading control.

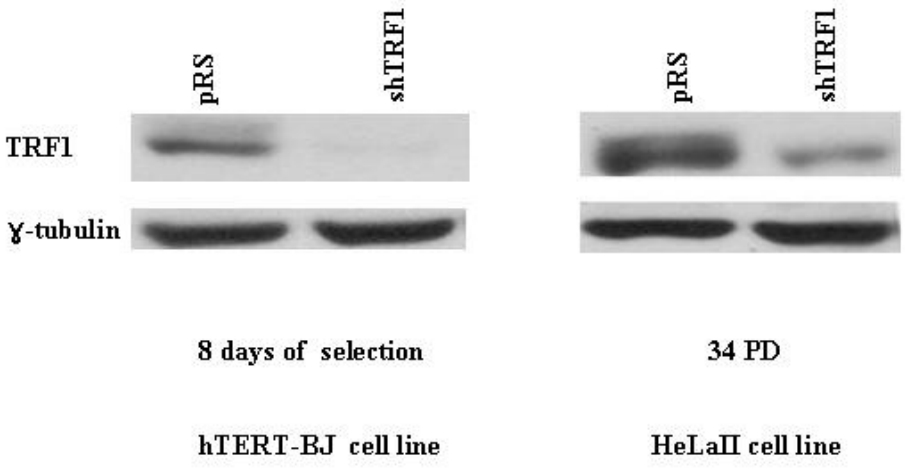
pRS
shTRF1
pRS
shTRF1
TRF1
γ-tubulin
8 days of selection
34 PD
hTERT-BJ cell line
HeLaII cell line

Figure 3.2: HeLaII cells depleted for TRF1 do not exhibit any defect in cell proliferation compared to control cells. HeLaII cells stably expressing pRS or shTRF1 were cultured up to 70 PDs. The number of population doublings was plotted against the number of days in culture.

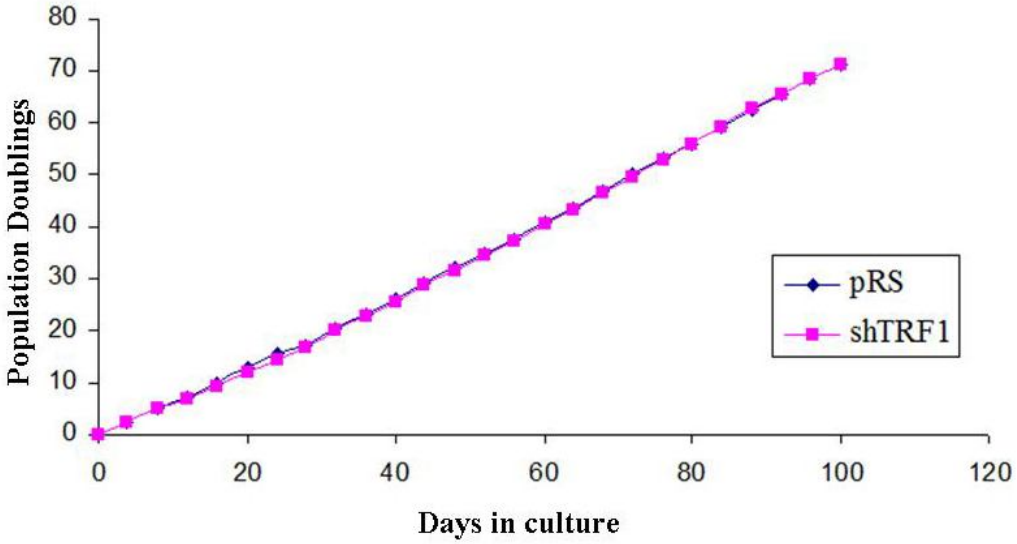
Population Doublings
80
70
60
50
40
30
20
10
0
0
20
40
60
80
100
120
Days in culture
pRS
shTRF1

Figure 3.3: Depletion of TRF1 results in telomere elongation in HeLaII cells. HeLaII cells stably infected with the indicated viruses were cultured for up to 70 PDs. Genomic DNA was isolated from different population doublings and digested with HinfI and RsaI. The DNA was run on a 0.7 % agarose gel. The gel was dried, denatured, and hybridized with a radioactively-labeled telomere specific probe. Southern blot analysis (A) and the quantification (B) reveal that cells depleted for TRF1 show telomere elongation compared to control cells. Loading control (ethidium bromide staining) is shown below the Southern blot.

A

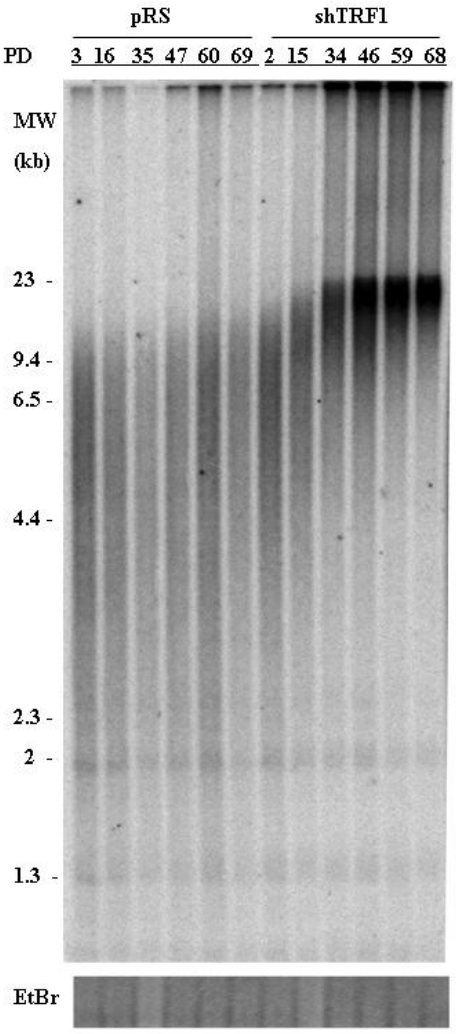
pRS
shTRF1
PD
3 16 35 47 60 69
2 15 34 46 59 68
MW
(kb)
23 -
9.4 -
6.5 -
4.4 -
2.3 -
2 -
1.3 -
EtBr

B

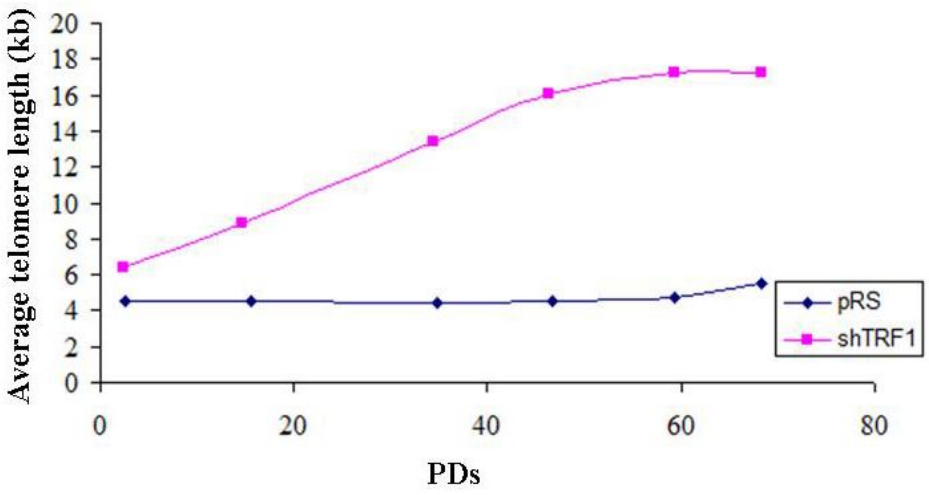
Average telomere length (kb)
20
18
16
14
12
10
8
6
4
2
0
0
20
40
60
80
PDs
pRS
shTRF1

Figure 3.4: Overexpression of various TRF1 mutants has no effect on cell proliferation in HeLaII-shTRF1 cell line. HeLaII-pRS and HeLaII-shTRF1 cells were retrovirally infected with retrovirus expressing the vector alone, HeLaII-shTRF1 cells infected with retrovirus expressing Myc-tagged TRF1SM, Myc-tagged TRF1T137A, Myc-tagged TRF1T137D, Myc-tagged TRF1S249A, or Myc-tagged TRF1S249E, resulting in seven stable cell lines. These cell lines were cultured up to 80 PDs. The number of population doublings was plotted against the number of days in culture.

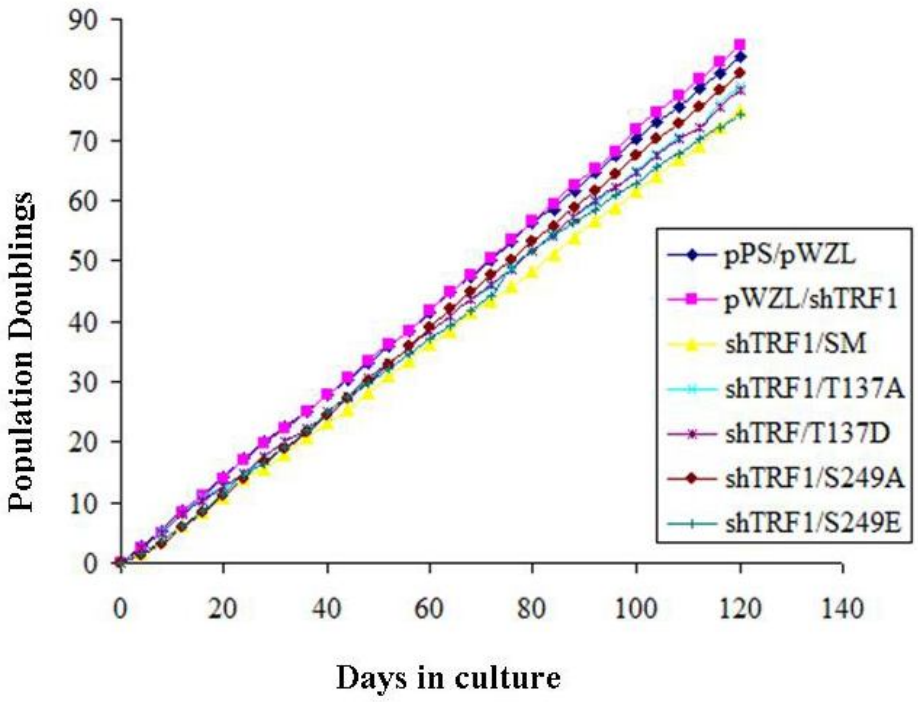
Population Doublings
Days in culture
0
10
20
30
40
50
60
70
80
90
0
20
40
60
80
100
120
140
pPS/pWZL
pWZL/shTRF1
shTRF1/SM
shTRF1/T137A
shTRF/T137D
shTRF1/S249A
shTRF1/S249E

Figure 3.5: Overexpression of Myc-tagged TRF1SM, Myc-tagged TRF1T137A, Myc-tagged TRF1T137D, Myc-tagged TRF1S249A or Myc-tagged TRF1S249E in HeLaII-shTRF1 cells suppresses the telomere elongation mediated by shTRF1. The seven cell lines described in Figure 3.4 were generated twice independently, cultured up to 80 PDs, and their telomere length dynamics were measured by Southern blotting. The expression of various TRF1 proteins was analyzed by Western blot. Anti-Myc antibody was used to detected Myc-tagged TRF1, and anti γ-tubulin served as a loading control. The expression of wild type and various TRF1 mutants at indicated PDs during the course of the first (A), the second (B) long-term culturing. Two independent genomic blots of telomeric restriction fragments of HeLaII shTRF1 cells expressing TRF1 proteins after indicated numbers of PDs were shown in (C) and (D) for the first, (E) and (F) for the second experiments. Loading control (ethidium bromide staining) is shown below the Southern blot. (G) and (H) Average telomere length of indicated cell lines was plotted against PDs. Standard deviations were derived from two independent experiments .

A

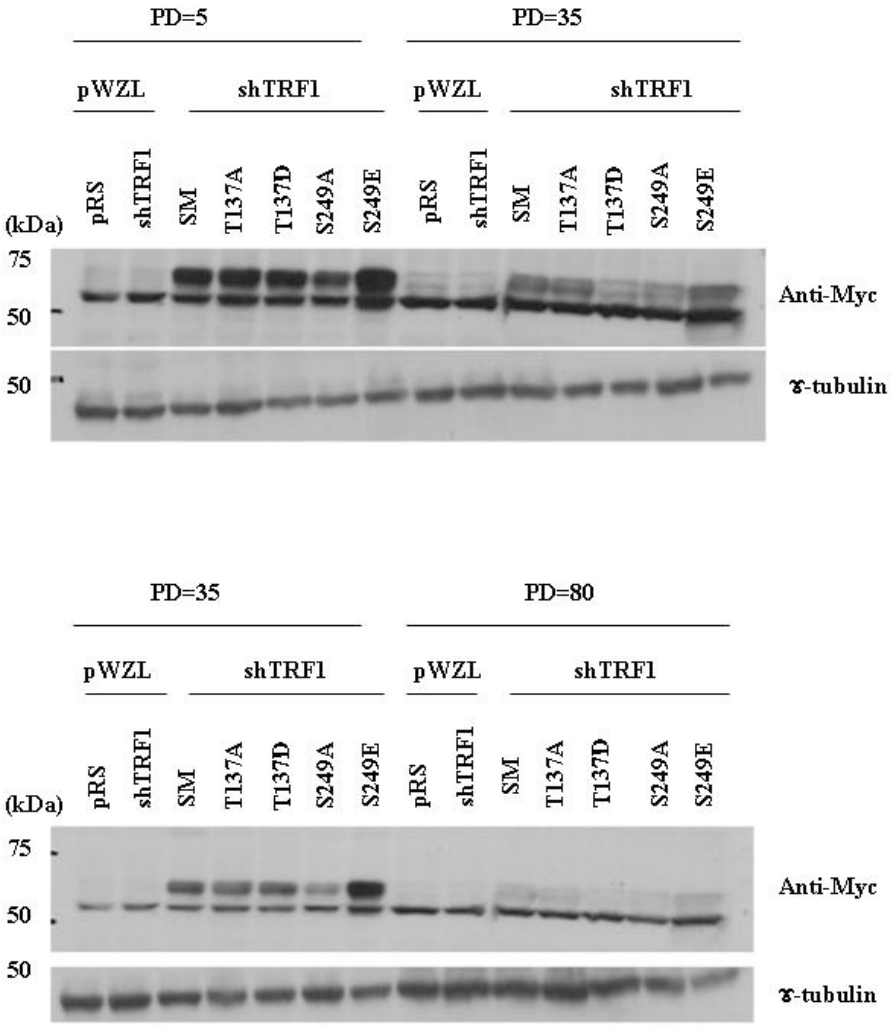
PD=5
PD=35
pWZL
shTRF1
pWZL
shTRF1
pRS
shTRF1
SM
T137A
T137D
S249A
S249E
pRS
shTRF1
SM
T137A
T137D
S249A
S249E
(kDa)
75
50
Anti-Myc
50
α-tubulin
PD=35
PD=80
pWZL
shTRF1
pWZL
shTRF1
pRS
shTRF1
SM
T137A
T137D
S249A
S249E
pRS
shTRF1
SM
T137A
T137D
S249A
S249E
(kDa)
75
50
Anti-Myc
50
α-tubulin

B

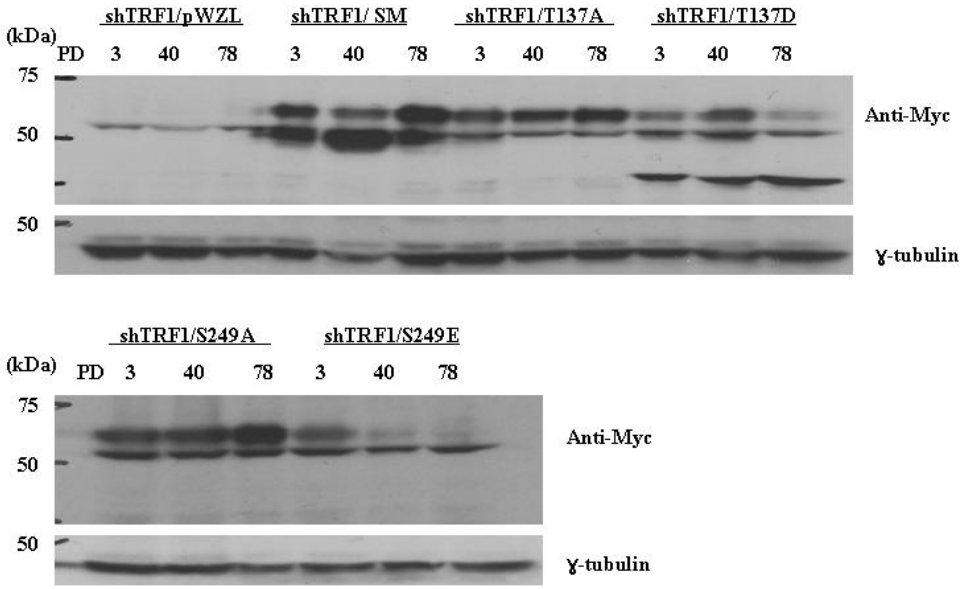
shTRF1/pWZL
shTRF1/ SM
shTRF1/T137A
shTRF1/T137D
(kDa)
PD 3 40 78 3 40 78 3 40 78 3 40 78
75
50
Anti-Myc
50
γ-tubulin
shTRF1/S249A
shTRF1/S249E
(kDa)
PD 3 40 78 3 40 78
75
50
Anti-Myc
50
γ-tubulin

C

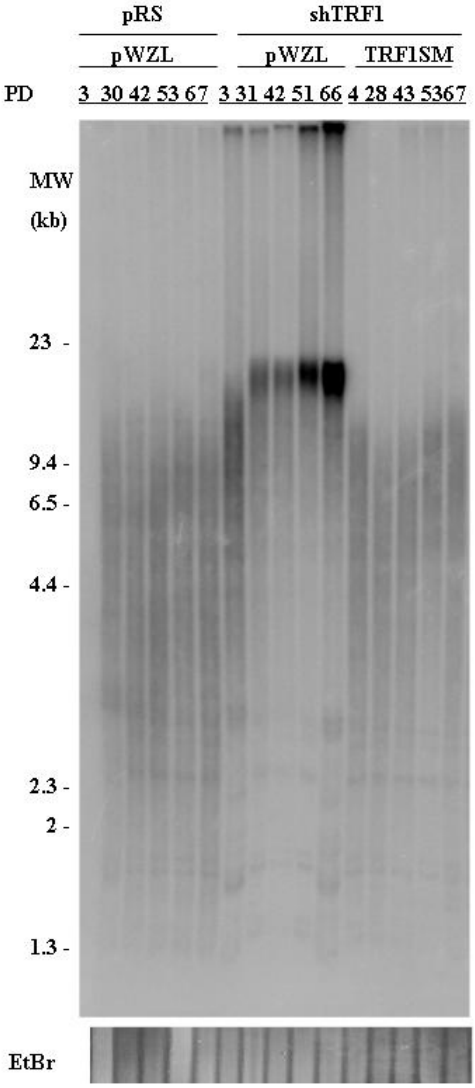
pRS
shTRF1
pWZL
pWZL
TRF1SM
PD
3 30 42 53 67
3 31 42 51 66
4 28 43 53 67
MW
(kb)
23 -
9.4 -
6.5 -
4.4 -
2.3 -
2 -
1.3 -
EtBr

D

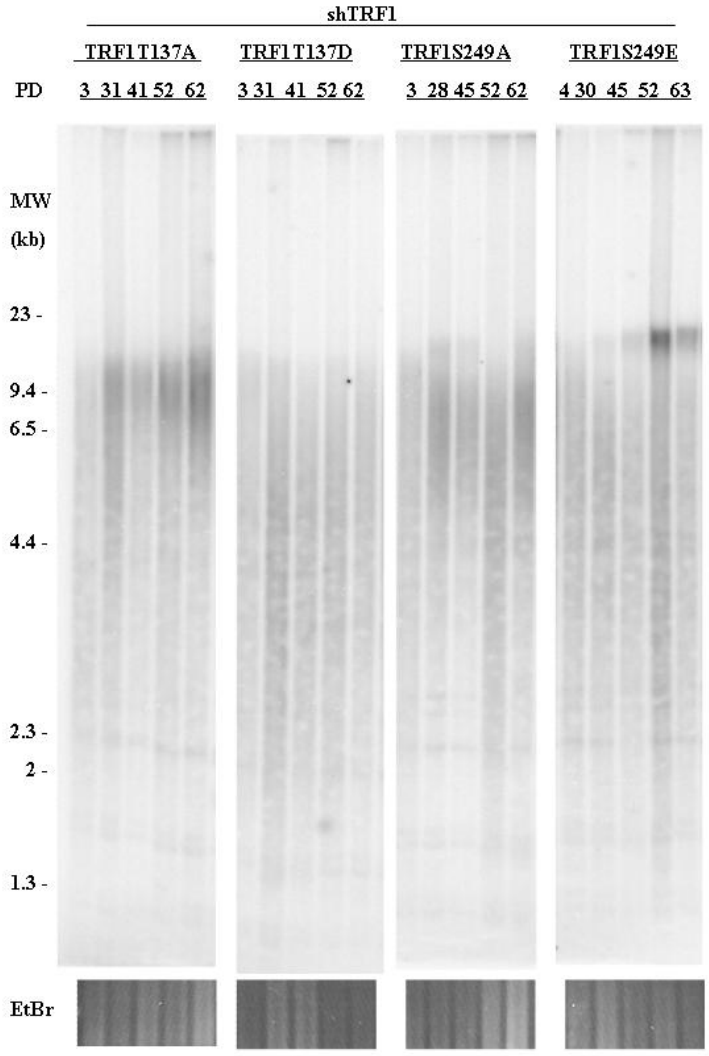
shTRF1
TRF1 T137A
TRF1 T137D
TRF1S249A
TRF1S249E
PD
3 31 41 52 62
3 31 41 52 62
3 28 45 52 62
4 30 45 52 63
MW
(kb)
23 -
9.4 -
6.5 -
4.4 -
2.3 -
2 -
1.3 -
EtBr

E

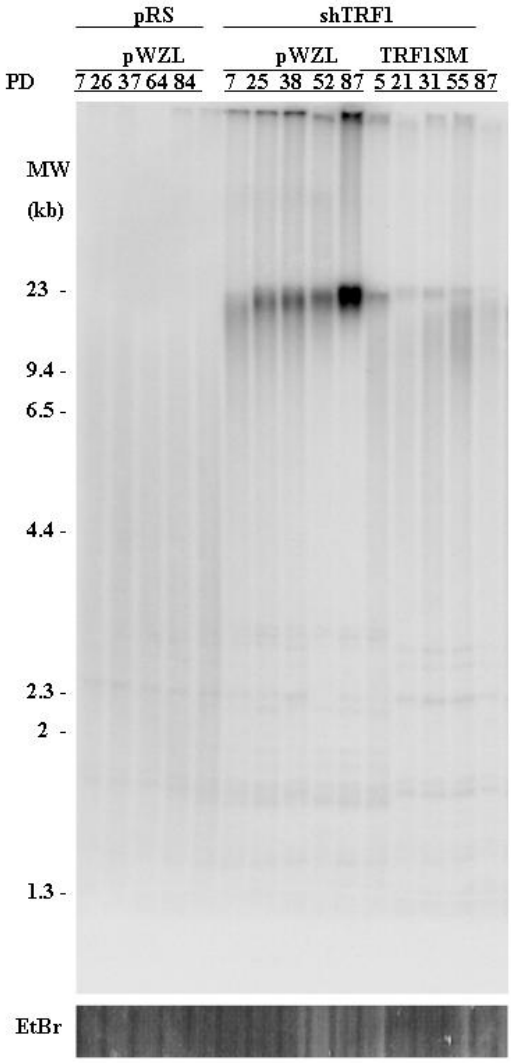
pRS
shTRF1
pWZL
pWZL
TRF1SM
PD
7 26 37 64 84
7 25 38 52 87
5 21 31 55 87
MW
(kb)
23 -
9.4 -
6.5 -
4.4 -
2.3 -
2 -
1.3 -
EtBr

F

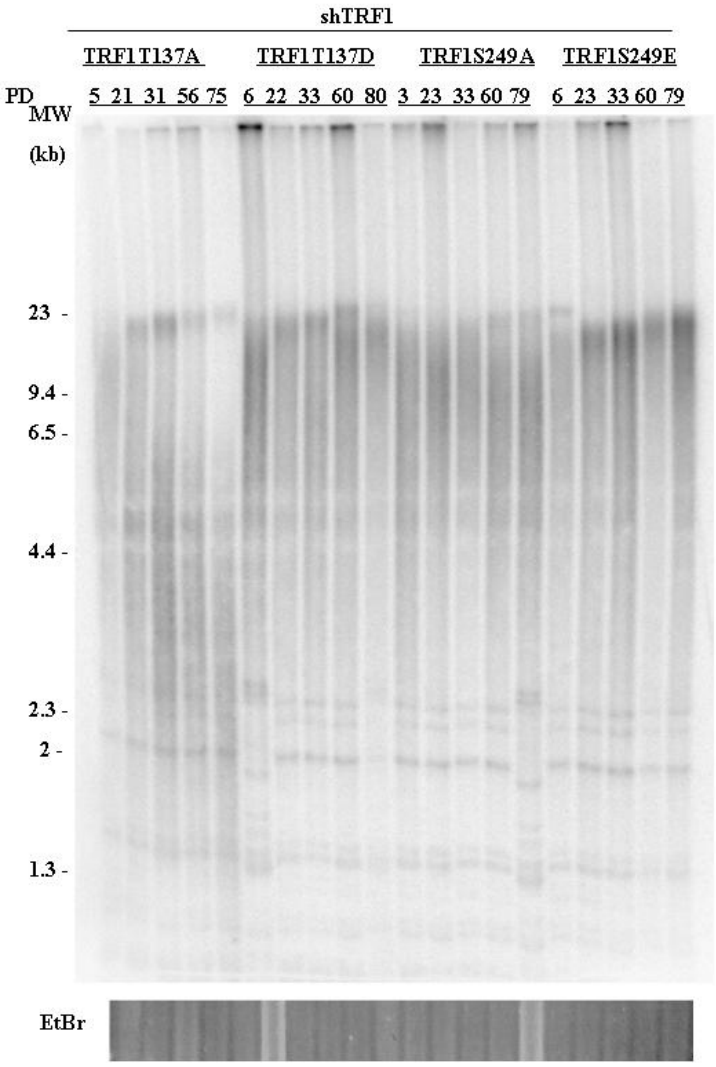
shTRF1
TRF1T137A
TRF1T137D
TRF1S249A
TRF1S249E
PD
5 21 31 56 75
6 22 33 60 80
3 23 33 60 79
6 23 33 60 79
MW
(kb)
23 -
9.4 -
6.5 -
4.4 -
2.3 -
2 -
1.3 -
EtBr

G

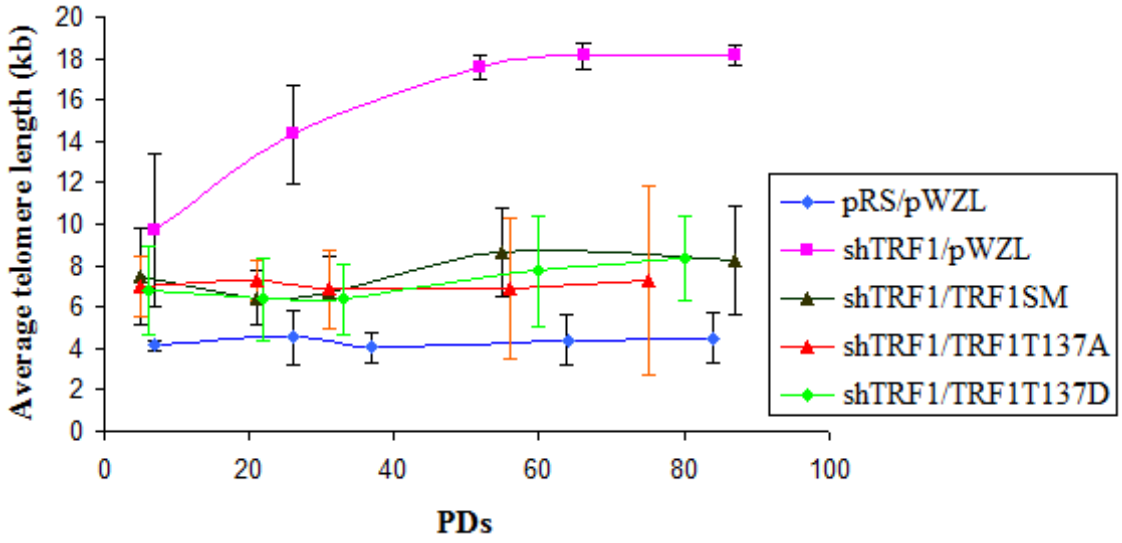
Average telomere length (kb)
0
2
4
6
8
10
12
14
16
18
20
0
20
40
60
80
100
PDs
pRS/pWZL
shTRF1/pWZL
shTRF1/TRF1SM
shTRF1/TRF1T137A
shTRF1/TRF1T137D

H

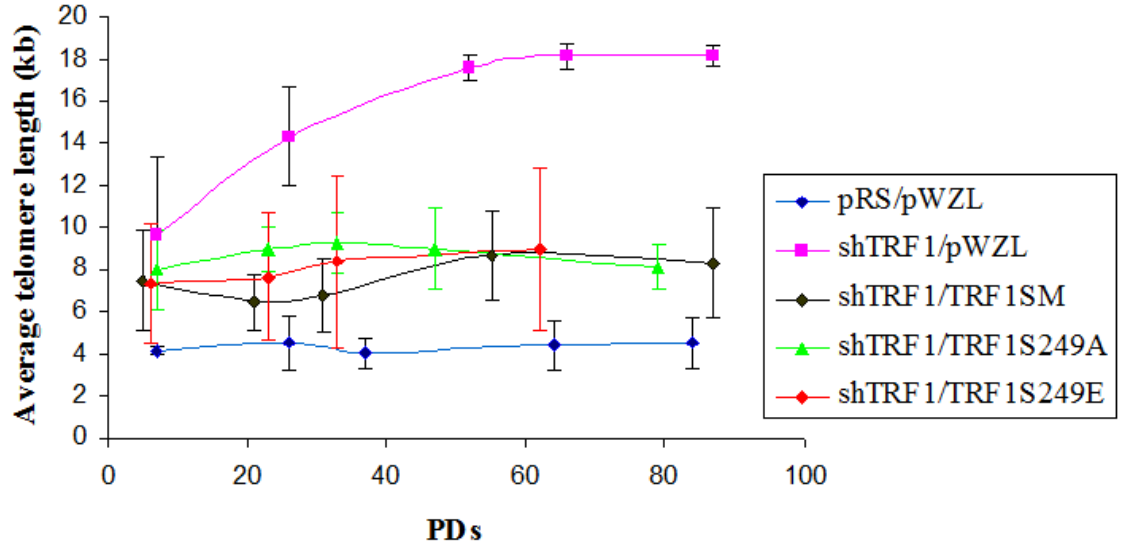
Average telomere length (kb)
0
2
4
6
8
10
12
14
16
18
20
0
20
40
60
80
100
PDs
pRS/pWZL
shTRF1/pWZL
shTRF1/TRF1SM
shTRF1/TRF1S249A
shTRF1/TRF1S249E

Figure 3.6: T137 or S249 of TRF1 is not required for TRF1 interaction with TIN2. The interaction of Myc-tagged wild type TRF1 and TRF1 mutants with endogenous TIN2 in HeLaII-shTFR1 cells was assessed by immunoprecipatation in the same stable cell lines used for long-term culturing at their early PDs (before PD 15). Proteins were immunoprecipitated with anti-Myc antibody. pWZL-N-Myc served as a negative control. The presence of endogenous TIN2 in immunoprecipitates was analyzed by Western blot using TIN2 antibody. Western blot using anti-Myc served as a loading control. 5% of input was loaded. (The arrow indicates the position of endogenous TIN2).

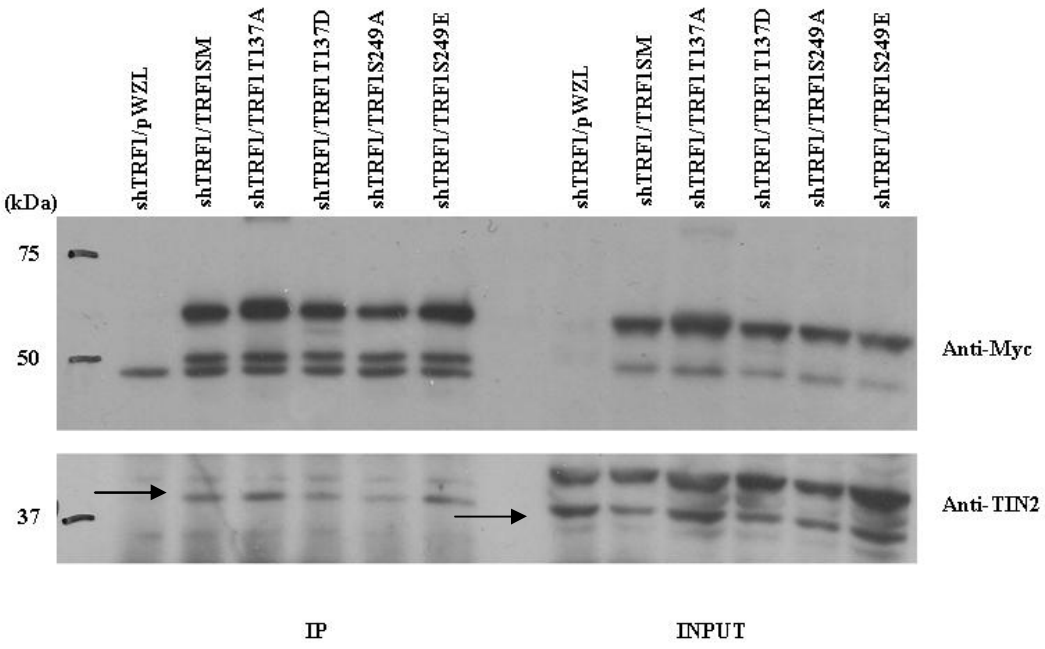
shTRF1/pWZL
shTRF1/TRF1SM
shTRF1/TRF1T137A
shTRF1/TRF1T137D
shTRF1/TRF1S249A
shTRF1/TRF1S249E
shTRF1/pWZL
shTRF1/TRF1SM
shTRF1/TRF1T137A
shTRF1/TRF1T137D
shTRF1/TRF1S249A
shTRF1/TRF1S249E
(kDa)
75
50
37
Anti-Myc
Anti-TIN2
IP
INPUT

Figure 3.7: T137 and S249 are not important for TRF1 binding to telomere DNA. Gel-shift assays using bacteria-expressed recombinant TRF1 proteins to assess telomeric DNA binding affinity of wild type TRF1 and mutants were conducted in triplicates. Samples were loaded at the indicated concentration (60 ng to 360 ng), and the free probe lane served as a control for unbound DNA (188 bp). Gel-shift assays comparing telomeric binding affinity of wild type TRF1, phosphomimic and alanine mutant of TRF1 at site T137 (A) and site S249 (B) were depicted. The percentage of TRF1-bound probe was plotted against protein concentration (C) and (D) Standard deviations derived from three independent experiments were indicated.

A

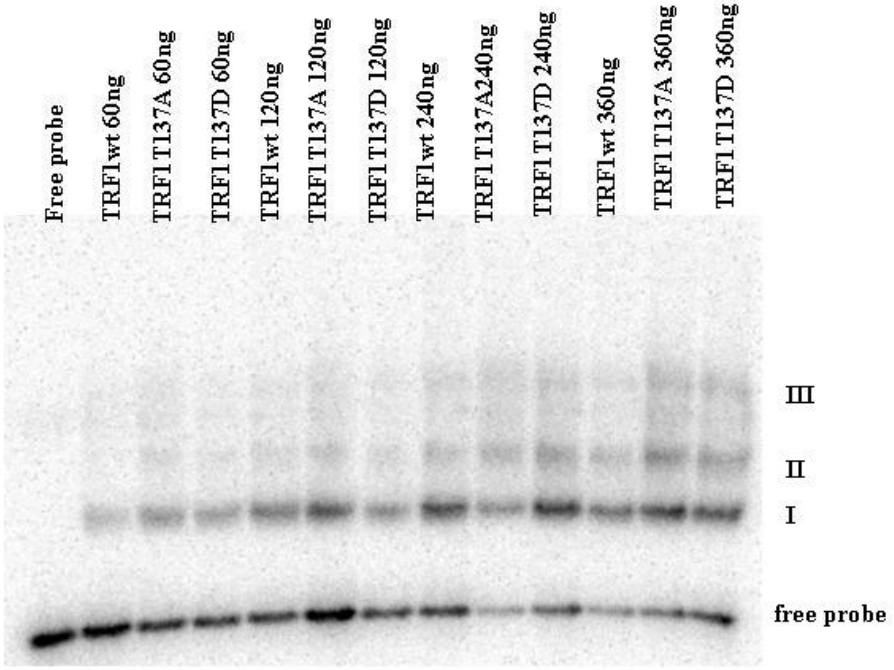
Free probe
TRF1wt 60ng
TRF1 T137A 60ng
TRF1 T137D 60ng
TRF1wt 120ng
TRF1 T137A 120ng
TRF1 T137D 120ng
TRF1wt 240ng
TRF1 T137A240ng
TRF1 T137D 240ng
TRF1wt 360ng
TRF1 T137A 360ng
TRF1 T137D 360ng
III
II
I
free probe

B

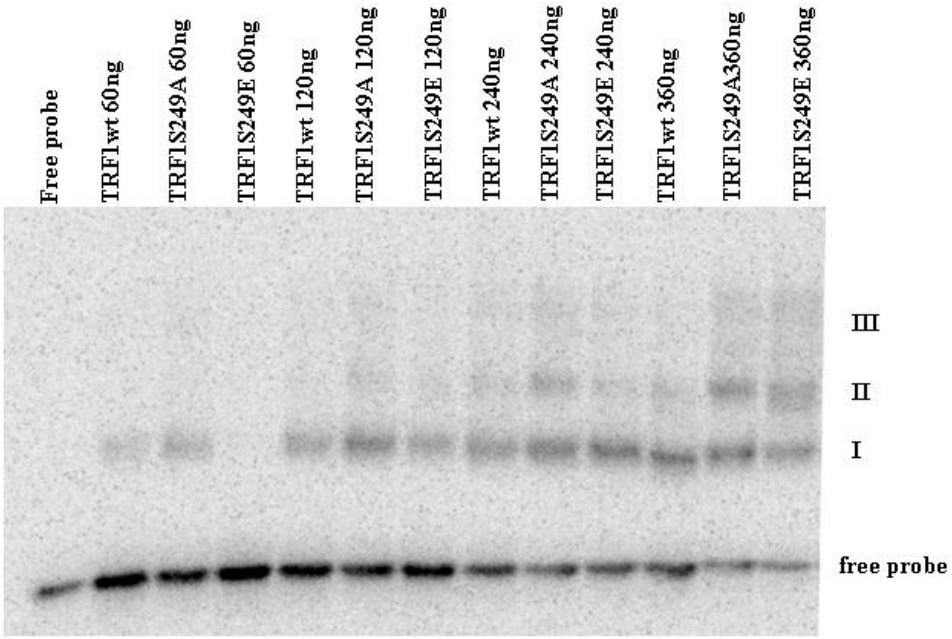
Free probe
TRF1wt 60ng
TRF1S249A 60ng
TRF1S249E 60ng
TRF1wt 120ng
TRF1S249A 120ng
TRF1S249E 120ng
TRF1wt 240ng
TRF1S249A 240ng
TRF1S249E 240ng
TRF1wt 360ng
TRF1S249A360ng
TRF1S249E 360ng
III
II
I
free probe

C

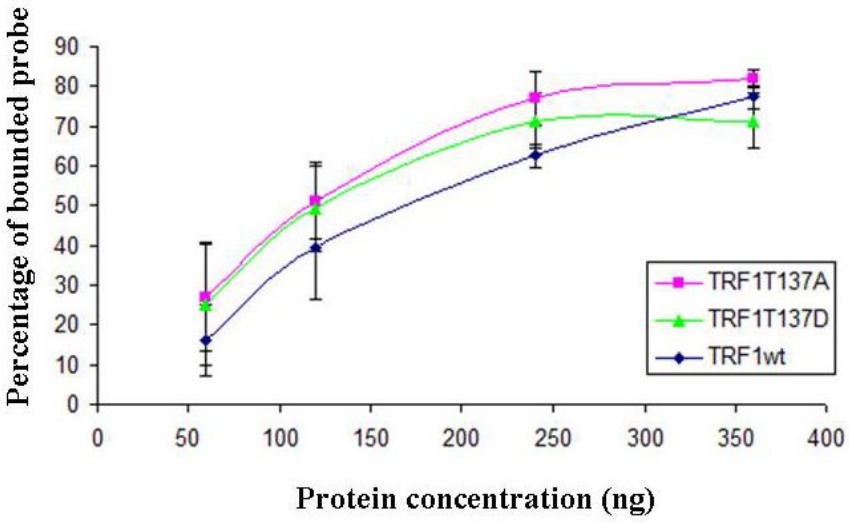
Percentage of bounded probe
90
80
70
60
50
40
30
20
10
0
0
50
100
150
200
250
300
350
400
Protein concentration (ng)
TRF1T137A
TRF1T137D
TRF1wt

D

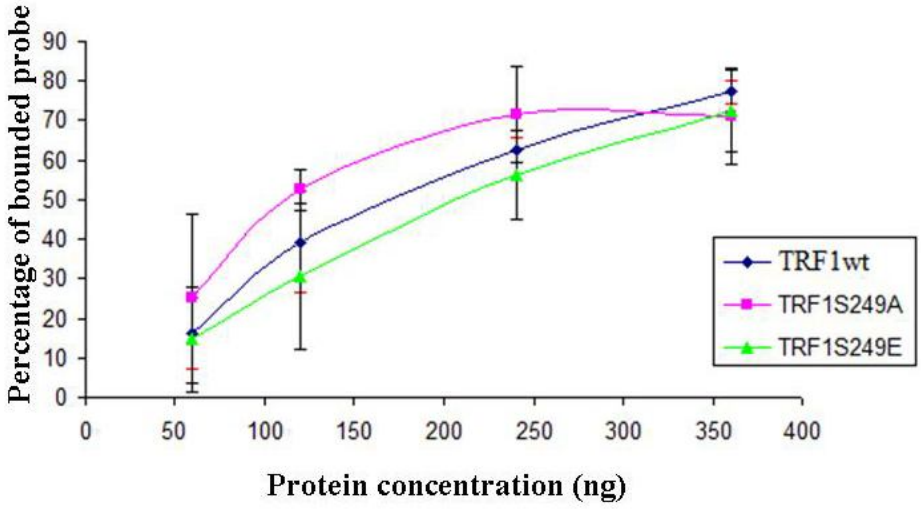
Percentage of bounded probe
90
80
70
60
50
40
30
20
10
0
0
50
100
150
200
250
300
350
400
Protein concentration (ng)
TRF1wt
TRF1S249A
TRF1S249E

Chapter 4-Results and Discussion: Analysis the Role of hEst1A (SMG6) in Telomere Length Maintenance

Human Est1A (hEst1A/SMG6) consists of two EBM (exon junction complex binding motif) motifs at its N-terminus, a RID domain (RNA interaction domain), a 14-3-3 like domain and a PIN (PilT N- terminal) domain at its C-terminus. SMG6 functions at the crossroad of NMD and telomeres. The N-terminus, the 14-3-3 domain and the PIN domain have been shown to be involved in NMD. Coexpression of hEst1A with hTERT results in telomere lengthening, suggesting that hEst1A plays a role in telomere length maintenance. However, the domain(s) of hEst1A involved in telomere length maintenance has not been fully characterized.

4.1 Human Est1A Domain Structure and Cloned hEst1A Constructs

Human Est1A contains an N-terminus, a RID domain, a linker region, 14-3-3 like domain, a linker region, and a PIN domain as depicted in Figure 4.1. To analyze the role of various domains of hEst1A in telomere length maintenance, I generated a number of deletion constructs (Fig. 4.1A), and they are hEst1A#5: missing PIN domain (AA^{1-1238}); #6: missing N-terminus and RID domain ($AA^{413-1419}$); #7: missing N-terminus amino acid 1 to 220 ($AA^{221-1419}$), and a full length construct (AA^{1-1419}). All constructs were derived from pWZL-N-Myc hEst1A ($AA^{32-1419}$) and were cloned into pLPC-N-Myc vector.

4.2 Overexpression of hEst1A Alleles Doesn't Appear to Affect Cell Proliferation in HT1080 Cells

Overexpression of wild type hEst1A has been shown to result in chromosome fusions, anaphase bridges and genomic instability in HTC75 cells (Reichenbach et al.,

2003). To assess the effect of overexpression of various deletion mutants of hEst1A on cell proliferation, pLPC-N-Myc, pLPC-Myc-tagged hEst1A#5, pLPC-Myc-tagged hEst1A #6, pLPC-Myc-tagged hEst1A#7, and pLPC-Myc-tagged hEst1Awt were each retrovirally introduced into HT1080 cells, giving rise to five stable cell lines. These cell lines were cultured continuously for 60 PDs to analyze their growth dynamics and telomere length dynamics. Overexpression of deletion mutant didn't affect cell proliferation in HT1080 as the growth curves showed that cells expressing various hEst1A mutants grew similar to those expressing the vector alone (Fig. 4.2). In addition, there was no detectable growth defect in HT1080 cells stably expressing wild type hEst1A. Western analysis confirmed that wild type hEst1A was expressed (Fig. 4.3C and Fig. 4.4C). These results are in contrast to previous findings that overexpression of wild type hEst1A induced apoptosis in HeLa cells, HT1080 cells and HLF cells (Reichenbach et al., 2003).

4.3 Overexpression of Wild Type hEst1A Doesn't Appear to Promote Telomere Elongation in HT1080 Cells

It has been shown that overexpression of hEst1A ($AA^{32\text{-}1419}$) results in telomere shortening, but lengthening while co-expressed with hTERT in 293 cells (Snow et al., 2003). To determine whether overexpression of wild type hEst1A ($AA^{1\text{-}1419}$) promotes telomere elongation, telomerase positive HT1080 cells stably expressing pLPC-N-Myc or Myc-tagged hEst1Awt were cultured up to 40 PDs, and telomere length dynamics were analyzed by Southern blot. Southern analysis revealed that overexpression of hEst1Awt had no effect on telomere length dynamics compared to that of expressing vector alone

(Fig. 4.3A). The average telomere length in cells stably expressing vector control maintained little changed from early to late PDs (Fig. 4.3B). The average telomere length in cells stably expressing wild type hEst1A remained little changed from PD 4 to PD 33, however, there appeared to be a slight increase in average telomere length from PD 33 to PD 41 (Fig. 4.3C). Western analysis detected a decrease of protein expression from PD 2 to PD 39 (Fig. 4.3C). These results suggested that overexpression of wild type hEst1A may not play a role in telomere length maintenance.

4.4 Overexpression of hEst1A#7 Seems to Promote Telomere Elongation

4.4.1 Expression Level of hEst1A#6, #7, and wt (up to 60 PDs) Is Maintained During the Long-term Culturing

To determine the effect of overexpression of hEst1A deletion mutants on telomere length maintenance, HT1080 cells stably expressing the vector alone, Myc-tagged hEst1A#5 (missing PIN domain), Myc-tagged hEst1A#6 (missing N-terminus and RID domain), Myc-tagged hEst1A#7 (missing N-terminus) and Myc-tagged hEst1Awt were cultured up to 80 PDs. Various hEst1A proteins were expressed at a comparable level at an early time point (PD3, Fig. 4.4A). hEst1A#11 is a construct missing the first 556 amino acids, but it produced degradation products (data not shown), thus, cell lines stably expressing hEst1A#11 were dropped. Expression of hEst1A#6, #7 and wild type (up to 60PDs) was well-maintained, whereas the expression of hEst1A#5 decreased from PD 20 to PD 40 and became undetectable at PD 80 (Fig 4.4B and C).

4.4.2 Overexpression of hEst1A#6 Has No Effect on Telomere Dynamics in HT1080 Cells

To assess whether overexpression of hEst1A#5, #6, and #7 in HT1080 cells may play a role in telomere length maintenance, the average telomere length in these cell lines were measured by Southern blotting. Cells stably expressing hEst1Awt or the vector alone didn't appear to affect telomere length dynamics in HT108 cells (Fig. 4.4D, 4.4E, 4.4F, and 4.4G), consistent with earlier findings.

Southern analysis indicated that overexpression of hEst1A#5 didn't alter telomere length dynamics in HT1080 cells (Fig. 4.4D and 4E), implicating that the PIN domain of hEst1A may be not involved in telomere length maintenance. However, the expression of hEst1A#5 decreased in HT1080 cells, which may mask the role of overexpression of hEst1A#5 in telomere length maintenance. The same experiment was repeated, however, a decrease in protein expression from PD 20 to PD 40 was also detected by Western (data not shown).

Southern analysis showed that overexpression of hEst1A#6 didn't appear to affect telomere length dynamics (Fig. 4.4D). The average telomere length in this cell line stayed fairly constant, similar to that of vector control (Fig. 4.4E). Western analysis demonstrated the expression of hEst1A#6 was well-maintained from early to late PDs (Fig. 4.4B). Taken together, these results suggest that hEst1A#6 doesn't play a role in telomere length maintenance when overexpressed.

4.4.3 Overexpression of hEst1A#7 Appears to Promote Telomere Elongation in HT1080 Cells

Southern analysis showed that overexpression of hEst1A#7 appeared to promote telomere lengthening compared to overexpression of wild type hEst1A or vector alone

(Fig. 4.4F), and the average telomere length in this cell line increased at a rate of 12.5 bp/PD (Fig. 4.4G). To further investigate the effect of overexprssion of hEst1A#7 on telomere length maintenance, cells expressing the vector alone, hEst1A#7 or hEst1Awt were cultured for additional 20 PDs, and then Southern blot was performed. Southern analysis revealed that the average telomere length continued to increase with increasing population doublings in cells stably expressing hEst1A#7. Telomere length was maintained fairly constant in cells expressing the vector alone. The average telomere length decreased from PD 60 to PD 80 in cells expressing wild type hEst1A (Fig. 4.4H and 4.4I). Western blotting showed that the level of expression of hEst1A#7 was not changed. The expression of hEst1Awt decreased from PD 60 to PD 80 (Fig 4.4B). These results suggestion that overexpression of hEst1A#7 promotes telomere lengthening in HT1080 cells.

4.5 Conclusions and Discussion: The N-terminus and RID Domain of hEst1A May Play a Role in Regulating Telomere Length Maintenance

Overexpression of hEst1A ($AA^{32\text{-}1419}$) or ($AA^{661\text{-}1419}$) has been suggested to cause telomere shortening in 293 cells, but both of them promoted telomere lengthening when co-expressed with hTERT (Snow et al., 2003), implicating that overexpression of the C-terminal of hEst1A in telomerase positive cells may have similar telomere length phenotype as that of wild type, however, telomere length dynamics wasn't assessed in their paper.

My results indicate that overexpression of wild type hEst1A ($AA^{1\text{-}1419}$) in HT1080 (telomerase positive) cells doesn't appear to promote telomere elongation (up to

PD 40 in Fig. 4.3, and Fig. 4.4D and 4.4E, up to PD 60 in Fig. 4.4F and 4.4G), neither does the N-terminal deletion construct hEst1A#6 (Fig. 4.4D and 4.4E). On the contrary, overexpression of hEst1A#7 seems to promote telomere lengthening (Fig. 4.4F-4I). Taken together, these results suggest the N-terminal of hEst1A may play a role in regulating telomere length maintenance.

Human Est1A has been shown to be associated with hTERT in a protein-RNA dependant manner which is mediated by the RID domain of hEst1A and hTR and a specific protein-protein interaction which is RNA independent (Redon et al., 2007). Overexpression of hEst1A#6 (lack of RID domain compared to hEst1A#7) failed to elongate telomeres, implicating that the RID domain of hEst1A may positively regulate telomere length maintenance since the RID domain establishes hEst1A and hTR interaction, both of which are the components of telomerase holoenzyme.

Overexpression of hEst1A #7 promotes telomere elongation, indicating that the-N-terminal region spanning amino acid 1-220 of hEst1A may be a negative mediator of telomere length maintenance. The amino acids 1-208 at the N-terminus have been suggested to be a DNA binding domain (Redon et al., 2007). Recently, two EBM (exon junction complex motif) motifs have been identified in this region which mediates a direct interaction of SMG6 (hEst1A) with exon junction complex. Such interaction is required for the function of SMG6 in NMD. In addition, deletion of the first 556 amino acids of hEst1A (SMG6) disrupts the interaction of SMG6 with any NMD factor and SMG6 itself (Kashima et al., 2010), suggesting that the N-terminal is important for SMG6

(hEst1A) function. It is likely the N-terminus of hEst1A may also play a role in regulating telomere length maintenance.

Figure 4.1: Schematic diagram of various hEst1A constructs. (A) Cloned hEst1A constructs. All constructs were derived from pWZL-N-Myc hEst1A ($AA^{32\text{-}1419}$) and cloned into pLPC-N-Myc vector. (B) Domain organization of hEst1A: N-terminus, RID domain (or TRID, RNA interaction domain, interaction with telomerase RNA), linker region, 14-3-3 domain with a 14-3-3 like fold, linker region, and PIN domain.

A

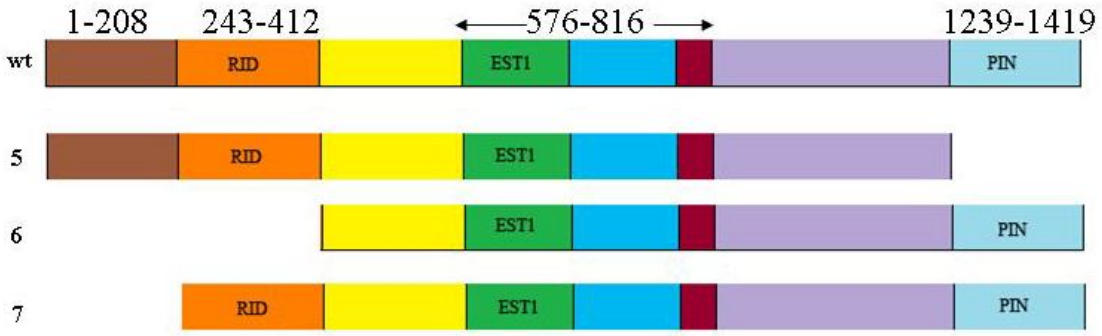
1-208
243-412
576-816
1239-1419
wt
RID
EST1
PIN
5
RID
EST1
6
EST1
PIN
7
RID
EST1
PIN

B

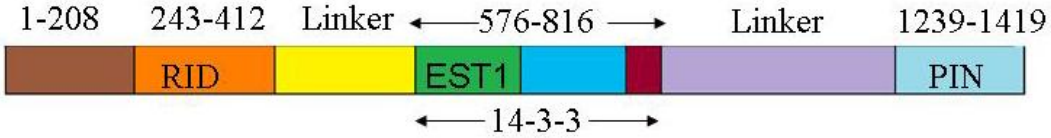
1-208
243-412
Linker
576-816
Linker
1239-1419
RID
EST1
PIN
14-3-3

Fig 4.2: Effect of overexpression of various hEst1A alleles on cell proliferation. HT1080 cells stably expressing pLPC-N-Myc, pLPC-N-Myc-hEst1A #5, pLPC-N-Myc-hEst1A#6, pLPC-N-Myc-hEst1A#7 and pLPC-N-Myc-hEst1Awt were cultured up to 60 PDs. The number of population doublings was plotted against days in culture.

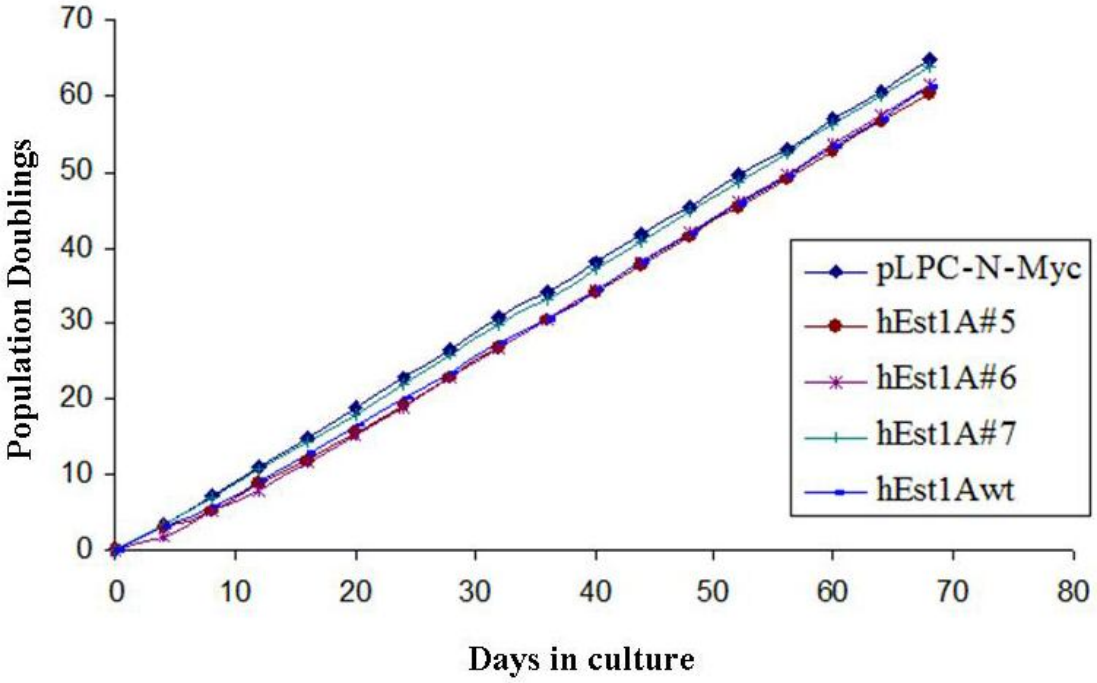
Population Doublings
70
60
50
40
30
20
10
0
0
10
20
30
40
50
60
70
80
Days in culture
pLPC-N-Myc
hEst1A#5
hEst1A#6
hEst1A#7
hEst1Awt

Figure 4.3: The effect of overexpression of wild type hEst1A (hEst1Awt) on telomere length maintenance. HT1080 cells stably expressing the vector alone (pLPC-N-Myc) or Myc-tagged wild type hEst1A were cultured for up 40 population doublings. Southern blotting was performed to examine the effect of overexpression of wild type hEst1A on telomere length dynamics. Genomic DNA isolated from different population doublings was digested with HinfI and RsaI. DNA was run on a 0.7% agarose gel. The gel was dried, denatured, and hybridized with a radioactively labeled telomere specific probe. (A) Southern analysis. (B) The quantification. Average telomere length of HT1080 cells expressing vector alone or hEst1Awt was plotted against PDs. Error bars were derived from three different gels. Loading control (ethidium bromide staining) is shown below the Southern blot. (C) Western analysis of wild type hEst1A expression at early and late population doublings. Immunoblotting was carried out with anti-Myc antibody. The γ-tubulin blot was used as a loading control. Protein extracts prepared from $1.8x10^5$ cells of each sample were loaded on an 8% SDS-PAGE gel. EV: pLPC-N-Myc.

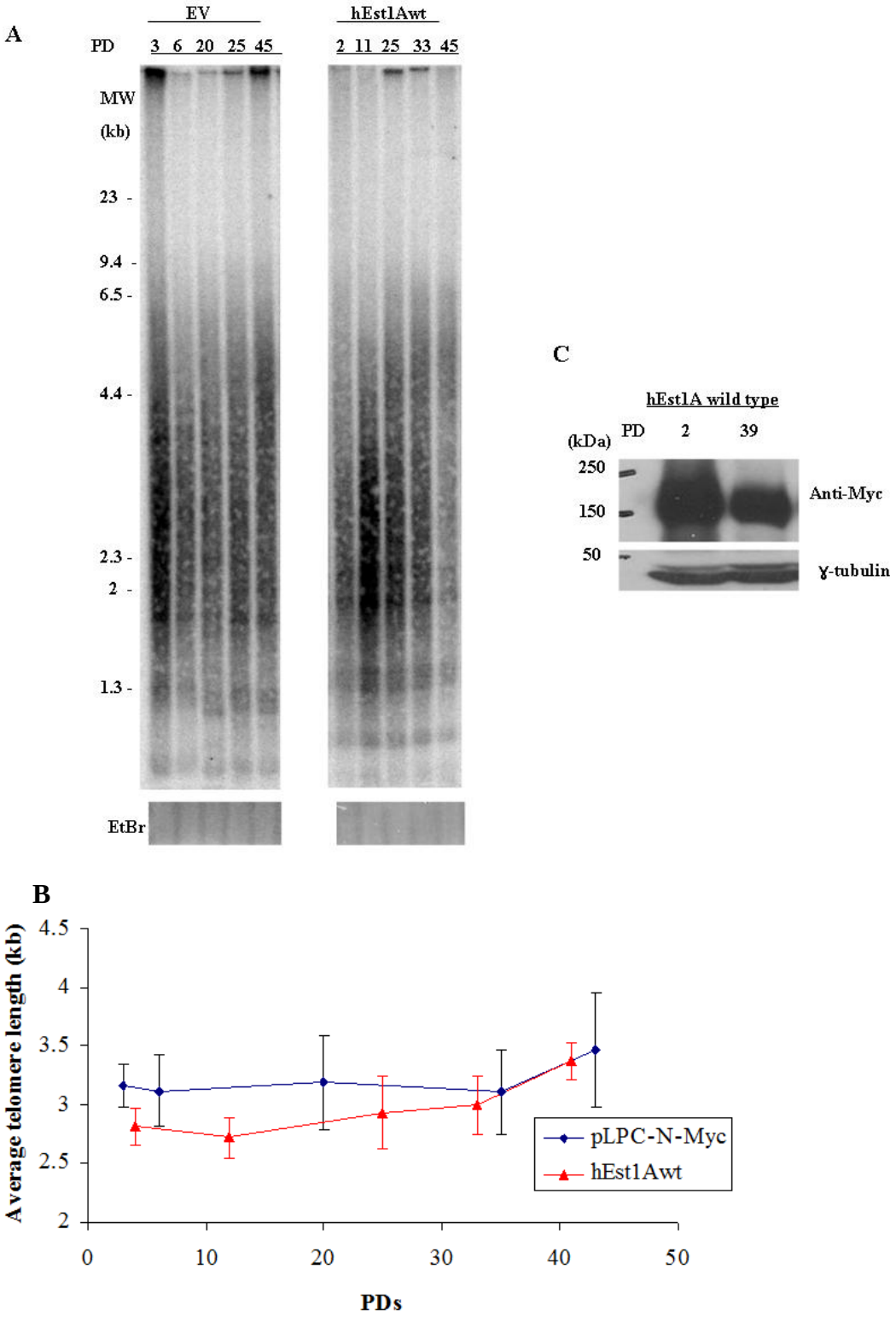
A
EV
hEst1Awt
PD
3 6 20 25 45
2 11 25 33 45
MW
(kb)
23
9.4
6.5
4.4
2.3
2
1.3
EtBr
C
hEst1A wild type
(kDa)
PD
2
39
250
150
50
Anti-Myc
γ-tubulin
B
Average telomere length (kb)
4.5
4
3.5
3
2.5
2
0
10
20
30
40
50
PDs
pLPC-N-Myc
hEst1Awt

Fig4.4: Effect of overexpression of various hEst1A alleles on telomere length maintenance. HT1080 cells stably expressing pLPC-N-Myc, pLPC-N-Myc-hEst1A#5, pLPC-N-Myc-hEst1A#6, pLPC-N-Myc-hEst1A#7 or pLPC-N-Myc-hEst1Awt were cultured for long-term, and their telomere length dynamics were measured by Southern blotting. The expression of various hEst1A proteins was analyzed by Western blot using anti-Myc antibody. The γ-tubulin blot served as a loading control. (A) Western analysis of expression of various hEst1A proteins at an early time point (PD 3). Protein extracts prepared from $1.8x10^5$ cells of each sample was loaded on an 8% SDS-PAGE gel. (B) and (C) Western analysis of expression of the hEst1A#5,#6, #7 and wild type at indicated population doublings. Protein extracts prepared from $1x10^5$ cells of each sample were loaded on an 8% SDS-PAGE gel. (D) Southern analysis of the effect of overexpression of hEst1A#5 and #6 on telomere length maintenance. (E) The quantification. (F) and (H) Southern analysis of the effect of overexpression of hEst1A#7 on telomere length maintenance. (G) and (I) The quantification. Loading control (ethidium bromide staining) is shown below the Southern blot. EV: pLPC-N-Myc.

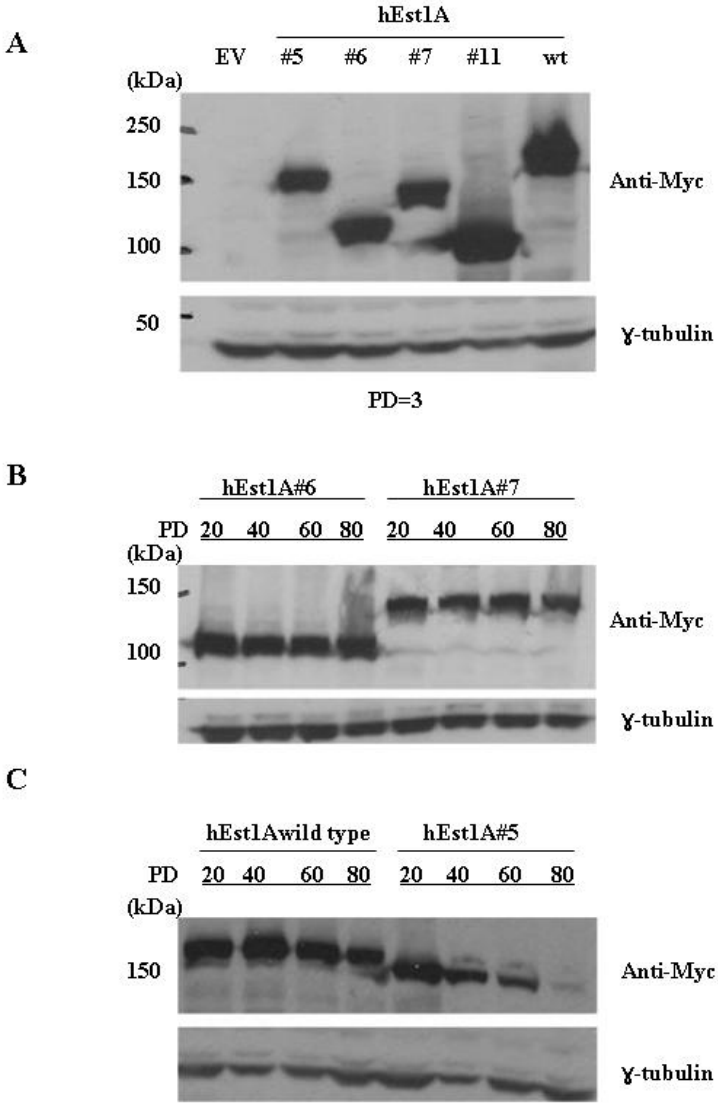
A
hEst1A
EV
#5
#6
#7
#11
wt
(kDa)
250
150
100
50
Anti-Myc
γ-tubulin
PD=3
B
hEst1A#6
hEst1A#7
PD 20 40 60 80 20 40 60 80
(kDa)
150
100
Anti-Myc
γ-tubulin
C
hEst1Awild type
hEst1A#5
PD 20 40 60 80 20 40 60 80
(kDa)
150
Anti-Myc
γ-tubulin

D

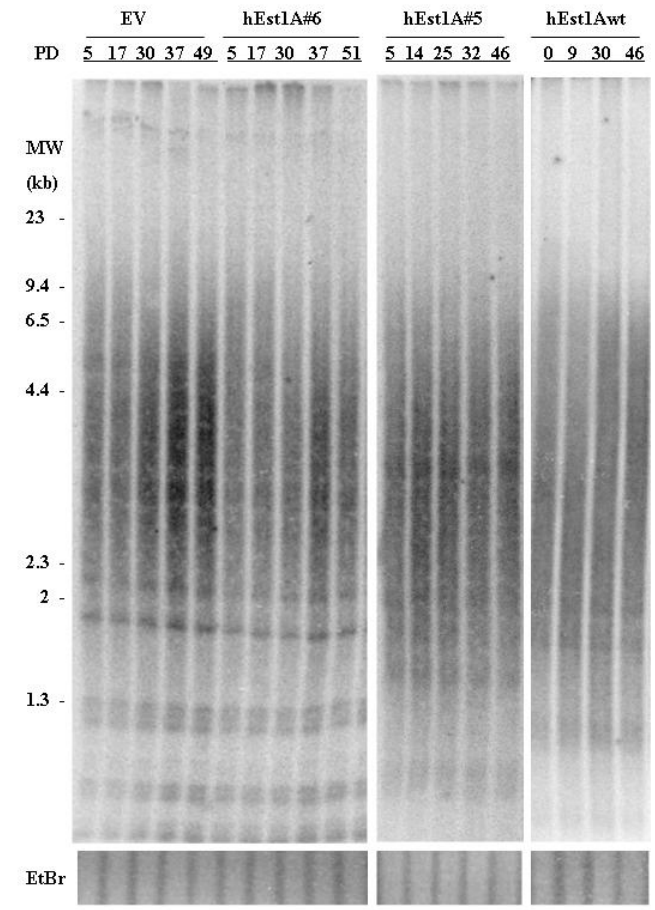
EV
hEst1A#6
hEst1A#5
hEst1Awt
PD
5 17 30 37 49
5 17 30 37 51
5 14 25 32 46
0 9 30 46
MW
(kb)
23
9.4
6.5
4.4
2.3
2
1.3
EtBr

E

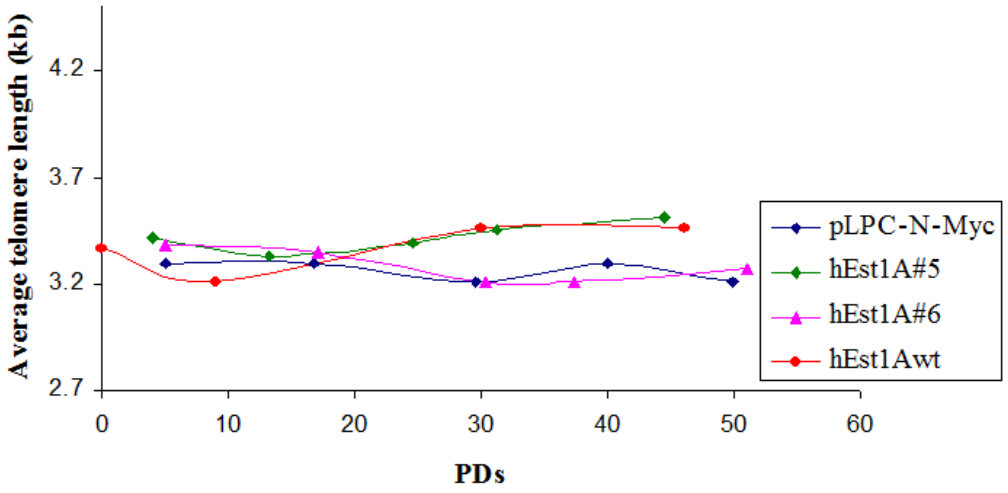
Average telomere length (kb)
4.2
3.7
3.2
2.7
0
10
20
30
40
50
60
PDs
pLPC-N-Myc
hEst1A#5
hEst1A#6
hEst1Awt

F

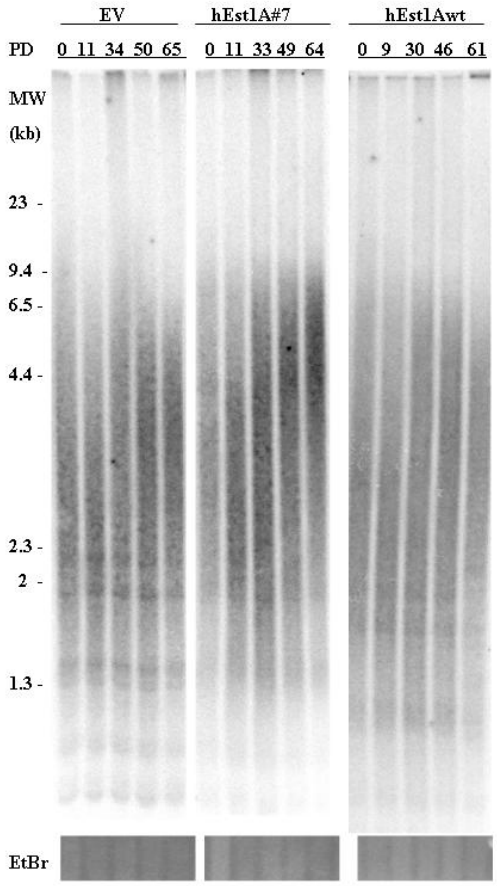
EV
hEst1A#7
hEst1Awt
PD
0 11 34 50 65
0 11 33 49 64
0 9 30 46 61
MW
(kb)
23 -
9.4 -
6.5 -
4.4 -
2.3 -
2 -
1.3 -
EtBr

G

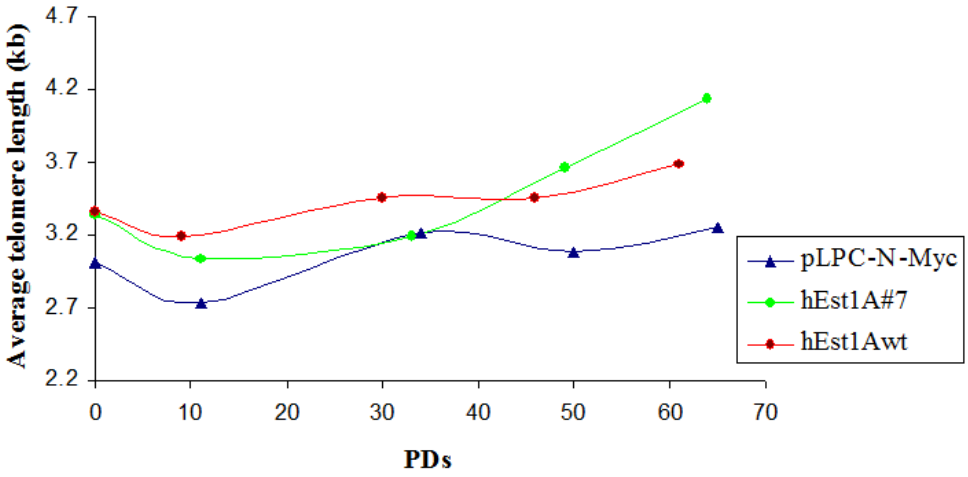
Average telomere length (kb)
4.7
4.2
3.7
3.2
2.7
2.2
0
10
20
30
40
50
60
70
PDs
pLPC-N-Myc
hEst1A#7
hEst1Awt

H

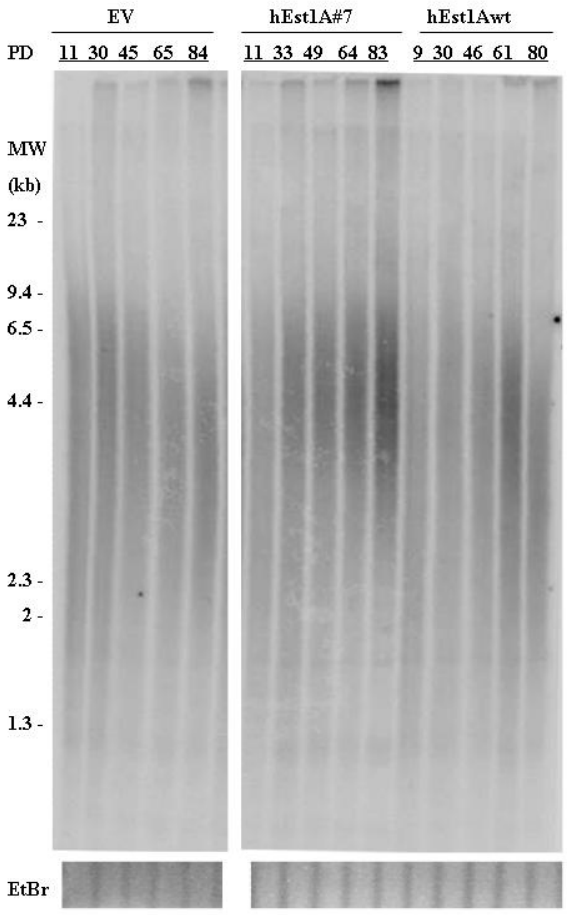
EV
hEst1A#7
hEst1Awt
PD
11 30 45 65 84
11 33 49 64 83
9 30 46 61 80
MW
(kb)
23 -
9.4 -
6.5 -
4.4 -
2.3 -
2 -
1.3 -
EtBr

I

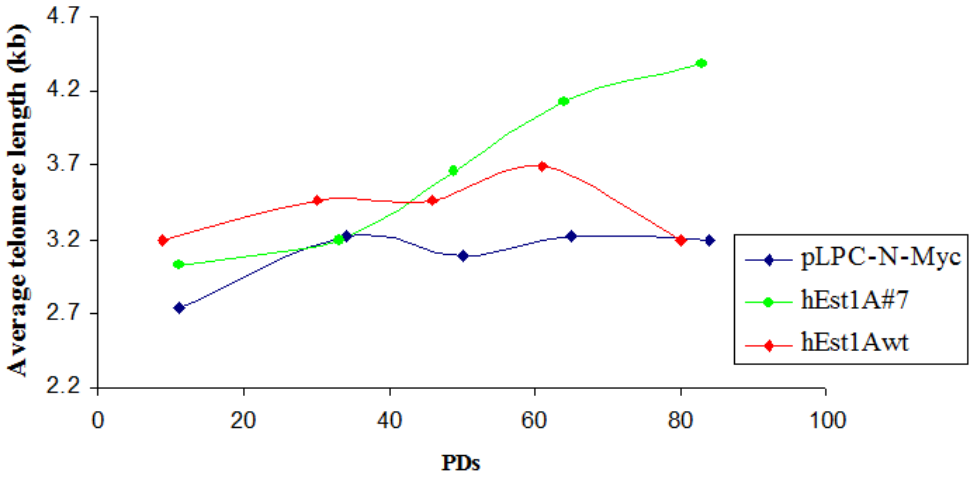
Average telomere length (kb)
4.7
4.2
3.7
3.2
2.7
2.2
0
20
40
60
80
100
PDs
pLPC-N-Myc
hEst1A#7
hEst1Awt

Chapter 5-Results and Discussion: Analysis of the Role of *C.elegans* SMG-6 in Telomere Length Maintenance

Est1 recruits telomerase (Est2) to telomeres in *S.cerevisiae* is Tel1 (ATM-1 in *C. elegans*) and MRX dependent. Deletion the homolog of ATM *in S.cerevisiae* (Tel1) resulted in ever shorter telomeres (Ritchie et al, 1999). The Est1 protein is conserved from yeast to humans (Reichenbach et al., 2003; Snow et al., 2003). Whether the role ATM and SMG6 in telomere length maintenance conserved in *C.elegans* is not assessed, and whether *atm-1* and *smg-6* function in the same genetic pathway of telomere length regulation is not determined.

5.1 Generation of *atm-1* and *smg-6* Double Mutant

To determine whether *atm-1* and *smg-6* act in the same genetic pathway in regulating telomere length, *atm-1*; *smg-6* double mutants were generated, and their telomere length was analyzed and compared to the respective single mutants.

To generate *atm-1* and *smg-6* double mutant, one *atm-1(gk186)* and three *smg-6* single mutant strains were used to set up for crosses. *Atm-1 (gk186)* carries a 548 bp deletion at its N-terminus, *smg-6 (tm1308)* carries a 1056 bp deletion at its N-terminus, and *smg-6 (ok1794)* carries a 920 bp deletion at its C-terminus (Fig. 5.1). *Smg-6 (r896)* strain carries a point mutation generated by ethylmethanesulphonate (EMS). This allele has abnormal vulva (Hodgkinet al., 1989).

Positive F2 double mutants for *atm-1*; *smg-6 (tm1308)* or *(ok1794)* produced by self-crossed of F1 heterozygous hermaphrodites were screened by PCR using *atm-1* specific primers to amplify *atm-1*, and *smg*-6 specific primers to amplify *smg-6*. PCR

results showed that there was about a 500 bp deletion in *atm-1*; smg-*6* double mutants and *atm-1* single mutant strain compared to wild type N2 (Fig. 5.2A lane 1-4), about a 1 kb deletion in *atm-1*; *smg-6 (tm1308)* , and *smg-6 (tm1308*) strain compared to wild type N2 (Fig. 5.2A lane 5-7), and about a 900 bp deletion in *atm-1*; *smg-6 (ok1794)* and *smg-6 (ok1794)* strain compared to wild type N2 (Fig. 5.2A lane 8-10). *Atm-1* deletion in two *atm-1*; *smg-6 (r896)* clones was verified by PCR (Fig. 5.2B lane 1-4). *Smg-6 (r896)* was determined by selecting the F1 worms *(atm-1*$^{+}$*/atm-1*$^{-}$ genotype) without protrusive vulva to generate F2 since *atm-1* mutant doesn't exhibit morphological abnormalities, and F2 worms with protrusive vulva were selected to screen for *atm-1* deletion. All together, these results indicated that three of *atm-1*; *smg-6* double mutant strains were generated.

5.2 *Atm*-1 Appears to Function Upstream of *smg-6* in Regulating Telomere Length Maintenance

5.2.1 Deletion of ATM-1 Promotes Telomere Shortening

Wild type worm N2, single mutant strains *atm-1*, *smg-6 (tm1308)*, *smg-6 (ok 1794)*, *smg-6 (r896)* , and double mutant strains *atm-1;smg-6 (tm1308)*, *atm-1; smg-6 (ok1794)*, and *atm-1;smg-6 (r896)* were cultured for a few generations, and their telomere length was determined by Southern blotting. Southern analysis revealed that average telomere length of wild type N2 worms was about 3 kb (Fig. 5.3), which is consistent with the previous finding (Raices et al, 2005). The average telomere length in *atm-1 (gk186)* worms was about 2.2 kb, which is significantly shorter than that of wild type (p= 0.015), suggesting that deletion of ATM-1 promotes telomere shortening in *C.elegans*.

This result is consistent with the role of Tel1 in telomere length maintenance in *S.cerevisiae*, and ATM in human cells.

Southern analysis showed that average telomere length in *smg-6 (ok1794)* and *smg-6 (r896)* worms was 2.8 kb and 3.2 kb respective, similar to that of wild type (Fig. 5. 3). The average telomere length in *smg-6 (tm1308)* worms was about 2.4 kb, and it is significantly shorter than that of wild type (p=0.04), implicating that deletion of SMG-6 resulted in telomere shortening.

5.2.2 *Atm-1* Appears to Function upstream of *smg-6*

The average telomere length of *atm-1; smg-6* double mutant strains was much shorter than that of wild type (P<0.04). It was about 2.3 kb for *atm-1; smg-6 (tm1308)* and *atm-1; smg-6 (ok1794)* worms, 2.1 kb for *atm-1; smg-6 (r896)* worms (Fig. 5.3B). Comparing double mutants to their respective single mutants, the average telomere length of double mutants was similar to that of *atm-1* strain (2.2 kb), implicating that ATM-1 deletion under SMG-6 mutant background causes telomere shortening, since *smg-6 (ok1794)* and *smg-6 (r896)* strains maintained their telomere length at wild type level. It seems *atm-1* acts upstream of *smg-6*. In addition, the average telomere length of smg-*6 (tm1308)* strain was similar to *atm-1* strain; however, *Atm-1* and SMG-6 *(tm1308)* double deletion didn't further reduce telomere length. Taken together, these results implicate that *atm-1* and *smg-6* may function in the same genetic pathway to regulate telomere length maintenance.

5.3 Discussion

Homolog of ATM-1 (ATM in human, Tel 1 in budding yeast) has been shown to play a role in telomere length maintenance. Deletion of Tel1 causes telomere shortening in *S.cerevisiae*, and Est1 mediated telomerase recruitment to telomeres is Tel1-dependent. In human, mutation of *ATM* gene results in ataxia-telangectasia (AT) like syndrome, and cells from AT patients have short telomeres and increased level of aberrant telomeres as well (Abraham, 2001; Savitsky et al., 1995). It appears the role of ATM in telomere length maintenance is conserved in *C.elegans.*

The Est1 proteins are conserved from yeast to human (Reichenbach et al., 2003; Snow et al., 2003) . Human Est1A (SMG6) functions at telomeres and NMD. Analysis the telomere length of *atm-1*, *smg-6* single mutant strains, and *atm-1*/*smg-6* double mutant strains reveals that ATM-1 mutation results in telomere shortening, and *atm-1* appears to function upstream of *smg-6*. A point mutation (G582 to R582) at 14-3-3 domain of SMG-6 *(r896)* was identified by Nazmuas Sakib (private communication from Dr. Bhagwati Gupta: Dept. of Biology, McMaster University). This mutation shows defect in vulva development (Hodgkinet al., 1989), but didn't appear to affect telomere length maintenance. *Smg-6 (ok1794)* carries a deletion at C-terminal, it may encode a C-terminal truncated protein, or its mRNA may be degraded by NMD machinery, however, this strain has an average telomere length as that of wild type. *Smg-6 (tm1308)* carries a deletion (exon 3 and 4) at its N-terminal (Fig. 5.1), and it has shorter telomeres compared to wild type, implicating that deletion of SMG-6 causes telomere shortening. It seems that deletion of ATM-1, or SMG-6 causes telomere shortening, and it appears *atm-1* and *smg-6* function in the same genetic pathway of regulation telomere length. However, whether

these single mutants and double mutants affect telomere length dynamics has not been assessed. Whether *smg-6* genetically interacts *with C.elegans* telomerase *trt-1* is yet to be defined.

Figure 5.1: Schematic of *smg-6* gene structure and domain structure of Est1-related proteins. (A) *Smg-6* and *atm-1* gene structure: *smg-6 (tm1308)* carries a 1056 bp deletion, and *smg-6 (ok1794)* carries a 920 bp deletion, *atm-1 (gk186)* carries a 548 bp deletion. Adapted from online wormbase (www.wormbase.sanger.ac.uk). (B) Domain architecture of Est1-related proteins.14-3-3 like domain consists of EST1 and TPR (Reichenbach et al., 2003). (C) Sequence analysis of SMG-6 and hEst1A. SMG-6 contains one conserved EBM (Exon junction binding motif) motif whereas hEst1A contains two of them at the N-terminus. The 14-3-3 like domain of hEst1A and SMG-6 shares 31% of identity and 51% of similarity, whereas the PIN domain shares 31% identity and 55% of similarity. The identical residues are highlighted in red. (Arrow points to the position of the point mutation of *smg-6(r896)*).

A

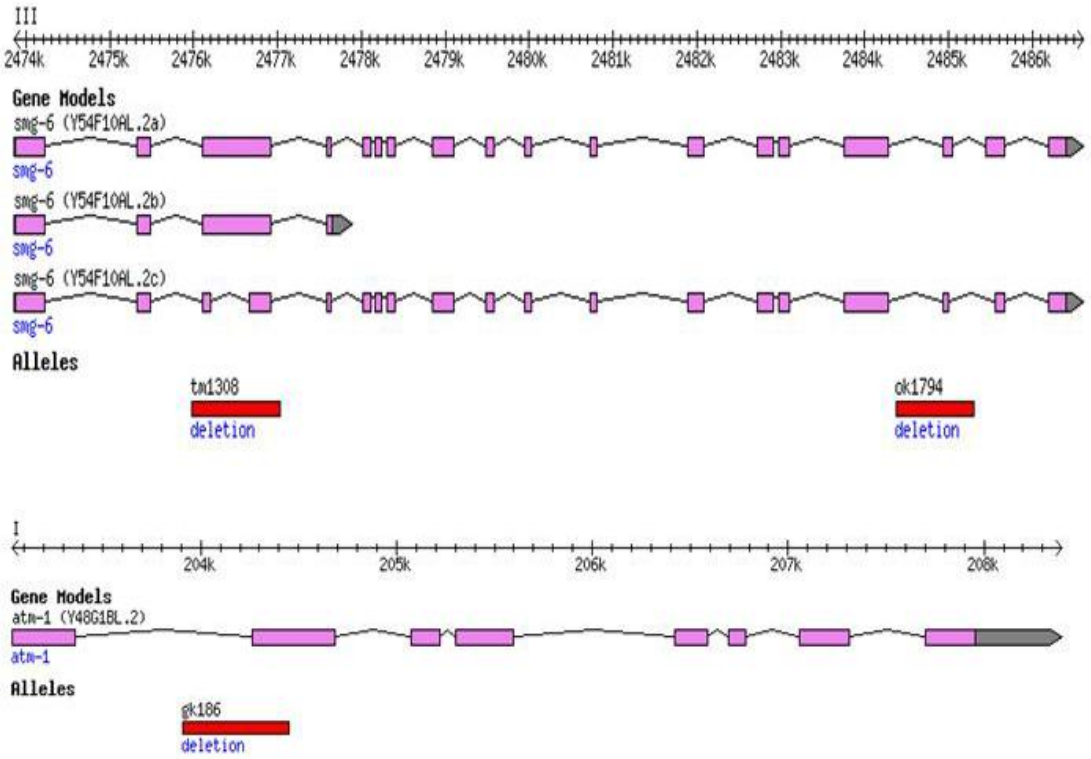
III
2474k
2475k
2476k
2477k
2478k
2479k
2480k
2481k
2482k
2483k
2484k
2485k
2486k
Gene Models
smg-6 (Y54F10AL.2a)
smg-6
smg-6 (Y54F10AL.2b)
smg-6
smg-6 (Y54F10AL.2c)
smg-6
Alleles
tm1308
deletion
ok1794
deletion
I
204k
205k
206k
207k
208k
Gene Models
atm-1 (Y48G1BL.2)
atm-1
Alleles
gk186
deletion

B

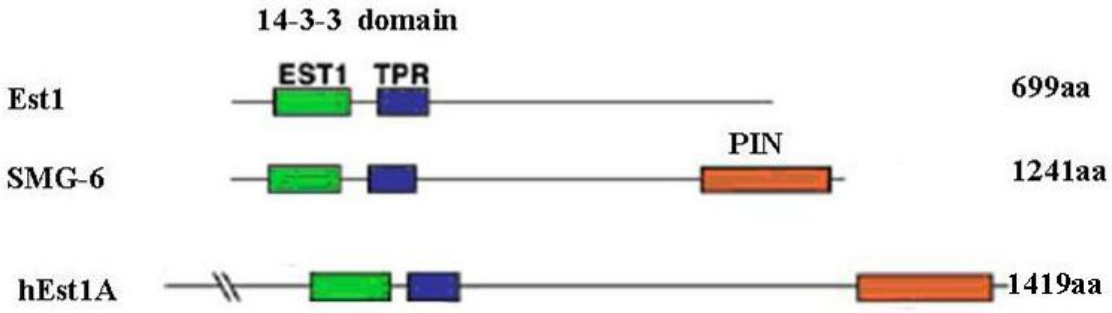
14-3-3 domain
EST1
TPR
Est1
699aa
PIN
SMG-6
1241aa
hEst1A
1419aa

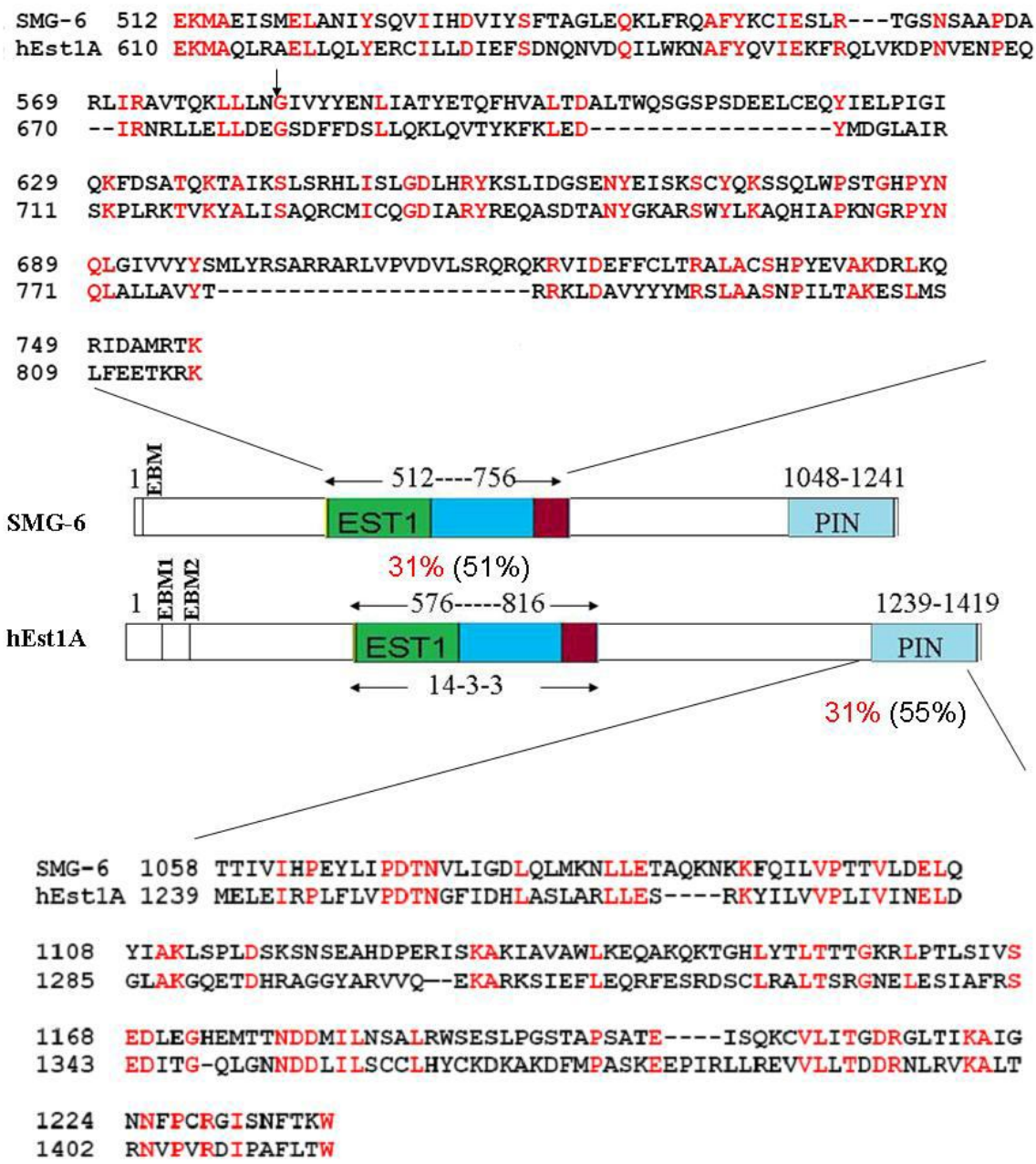
SMG-6 512 EKMAEISMELANIYSQVIIHDVIYSFTAGLEQKLFRQAFYKCIESLR---TGSNSAAPDA
hEst1A 610 EKMAQLRAELLQLYERCILLDIEFSDNQNVDQILWKNAFYQVIEKFRQLVKDPNVENPEQ
569 RLIRAVTQKLLLNGIVYYENLIATYETQFHVALTDALTWQSGSPSDEELCEQYIELPIGI
670 --IRNRLLELLDEGSDFFDSLLQKLQVTYKFKLED----------YMDGLAIR
629 QKFDSATQKTAIKSLSRHLISLGDLHRYKSLIDGSENYEISKSCYQKSSQLWPSTGHPYN
711 SKPLRKTVKYALISAQRCMICQGDIARYREQASDTANYGKARSWYLKAQHIAPKNGRPYN
689 QLGIVVYYSMLYRSARRARLVPVDVLSRQRQKRVIDEFFCLTRALACSHPYEVAKDRLKQ
771 QLALLAVYT----------RRKLDAVYYYMRSLAASNPILTAKESLMS
749 RIDAMRTK
809 LFEETKRK
1
EBM
512----756
1048-1241
SMG-6
EST1
PIN
31% (51%)
1
EBM1
EBM2
576-----816
1239-1419
hEst1A
EST1
PIN
14-3-3
31% (55%)
SMG-6 1058 TTIVIHPEYLIPDTNVLIGDLQLMKNLLETAQKNKKFQILVPTTVLDELQ
hEst1A 1239 MELEIRPLFLVPDTNGFIDHLASLARLLES----RKYILVVPLIVINELD
1108 YIAKLSPLDSKSNSEAHDPERISKAKIAVAWLKEQAKQKTGHLYTLTTTGKRLPTLSIVS
1285 GLAKGQETDHRAGGYARVVQ--EKARKSIEFLEQRFESRDSCLRALTSRGNELESIAFRS
1168 EDLEGHEMTTNDDMILNSALRWSESLPGSTAPSATE----ISQKCVLITGDRGLTIKAIG
1343 EDITG-QLGNNDDLILSCCLHYCKDKAKDFMPASKEEPIRLLREVVLLTDDRNLRVKALT
1224 NNFPCRGISNFTKW
1402 RNVPVRDIPAFLTW

Figure 5.2: Verify *atm-1/smg-6* double mutant strains by single worm PCR. (A) PCR using *atm-1* specific primers and genomic DNA from wild type N2 worms (lane 1), mutant worms (lane 2-4) showed a deletion ~500 bp in size in mutant strains. PCR using *smg-6 (tm1308)* specific primers and genomic DNA from wild type (land 5), and mutant worms (land 6-7) indicated a deletion ~ 1000 bp in size in mutants. PCR using *smg-6 (ok1794)* specific primers and genomic DNA from wild type (land 8) and mutant worms (lane 9-10) showed ~900 bp deletion in mutant strains. (B) PCR using *atm-1* specific primers and genomic DNA from wild type N2 worms (lane 1), mutant worms (lane 2-4) showed a deletion ~500 bp in size in mutant strains. Hermaphrodites of *smg-6 (r896)* have an abnormal protrusive vulva. Two clones derived from one putative positive F_2 hermaphrodite with *smg-6 (r896)* phenotype were used to extract genomic DNA. All the PCR has been repeated at least 3 times. (N2: wild type strain)

A

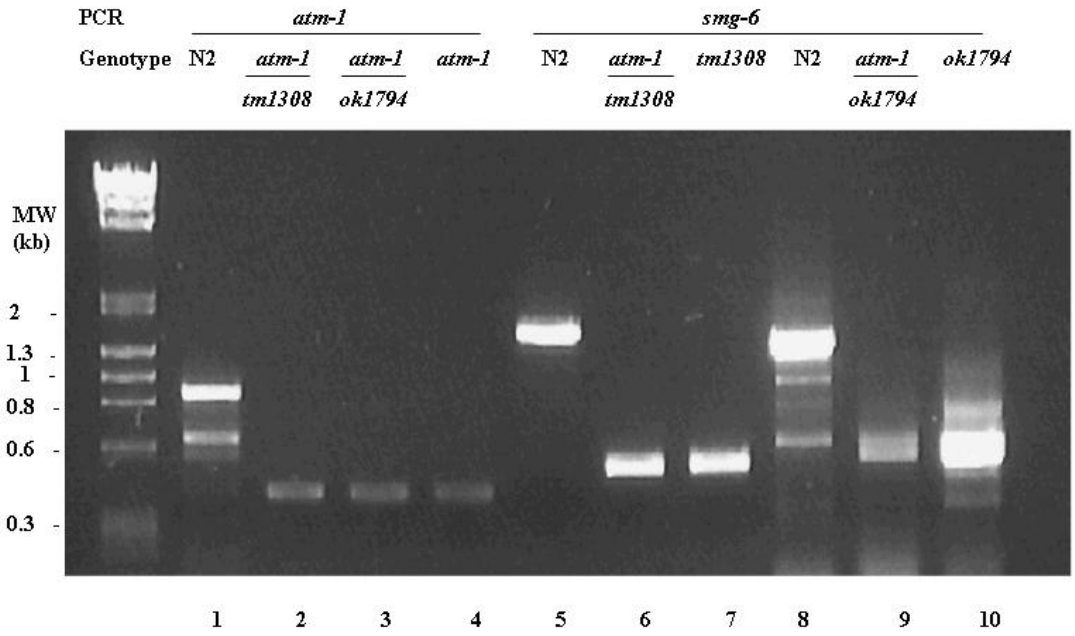
PCR
atm-1
smg-6
Genotype
N2
atm-1 tm1308
atm-1 ok1794
atm-1
N2
atm-1 tm1308
tm1308
N2
atm-1 ok1794
ok1794
MW (kb)
2
1.3
1
0.8
0.6
0.3
1
2
3
4
5
6
7
8
9
10

B

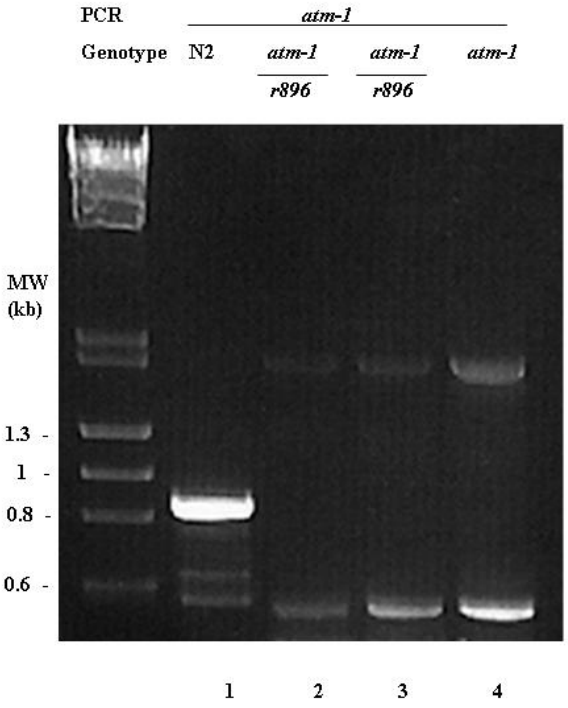
PCR
atm-1
Genotype
N2
atm-1
r896
atm-1
r896
atm-1
MW
(kb)
1.3
1
0.8
0.6
1
2
3
4

Figure 5.3: Effect of ATM-1 and SMG-6 on the *C.elegans* telomere length maintenance. (A) Southern analysis of *C.elegans* telomere length under denature condition. Genomic DNAs isolated from N2 (wild type), single mutant strain *atm-1 (gk186), smg-6 (ok1794, tm1308, r896),* and double mutants *atm-1/smg-6 (tm1308), atm-1/smg-6 (ok1794), atm-1/smg-6 (r896)* was digested and separated by 0.7% agarose gel as described (Raices et al, 2005). The gel was dried at 50˚C, and then hybridized with radioactively labeled $(GCCTAA)_4$. A loading control (ethidium bromide staining) is shown below the Southern blot. (B) The telomere length of each strain was quantified. Standard deviations derived from four independent gels were indicated. (** $p < 0.05$)

A

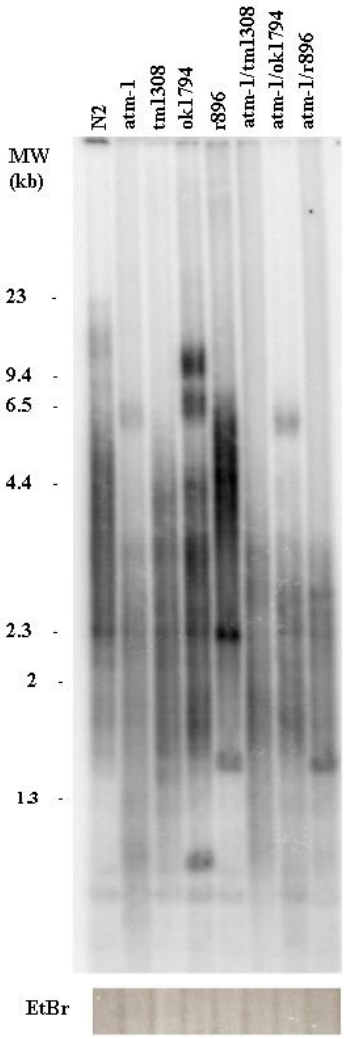
N2
atm-1
tm1308
ok1794
r896
atm-1/tm1308
atm-1/ok1794
atm-1/r896
MW
(kb)
23
9.4
6.5
4.4
2.3
2
1.3
EtBr

B

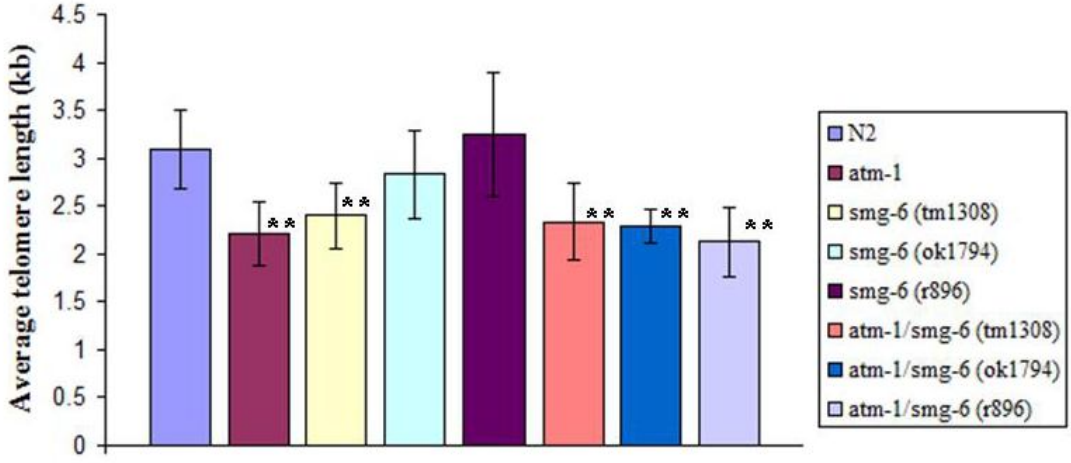
Average telomere length (kb)
4.5
4
3.5
3
2.5
2
1.5
1
0.5
0
**
**
**
**
**
N2
atm-1
smg-6 (tm1308)
smg-6 (ok1794)
smg-6 (r896)
atm-1/smg-6 (tm1308)
atm-1/smg-6 (ok1794)
atm-1/smg-6 (r896)

Chapter 6-Discussion and Future Directions

6.1 TRF1 Phosphorylation

Casine kinase 2-mediated T122 (located in helix 3 of TRFH) phosphorylation has been suggested to affect TRF1 dimerization and regulates telomere length maintenance (Kim et al., 2008). In response to DNA damage, ATM phosphorylates S219 (located in helix 7) of TRF1 which suppresses apoptosis (Kishi et al., 2001). Phosphorylation of T149 (located in helix 4) can be recognized by PIN1 (Lee et al., 2009). It appears all the identified phopshorylation sites important for TRF1 function at TRFH are located in the helices. T137 is located outside of helices outside of helix 3, and S249 is located at the C-terminal of helix 8 (Fairall et al., 2001). Phosphorylation of TRF1 at T137 and S249 doesn't appear to modulate TRF1 function in telomere length maintenance. However, whether simultaneous phosphorylation of these two sites at the dimerization domain of TRF1 may affect TRF1 function has not been characterized.

6.2 Human Est1A in Telomere Length Maintenance

HT1080 cells experienced difficulty to maintain hEst1A#5 (lack of PIN domain) at the same level during the course of long-term culturing. Whether the PIN domain may play a role in telomere length maintenance is inconclusive. The PIN domain of hEst1A (SMG6) has been suggested to be required for its association with SMG5 (hEst1B), a protein functions in NMD and also associates with telomerase activity (Snow et al., 2003; Kashima et al., 2010). Furthermore, overexpression of SMG6 carrying mutations at the catalytic residues of PIN domain has been shown to inhibit NMD in a dominant negative manner (Huntzinger et al., 2008). I would predict the same phenotype in NMD upon

expression of hEst1A#5 (PIN domain deleted) since it is the N-terminal of SMG6 mediated SMG6 interaction with itself (Kashima et al., 2010).

It is clear that wild type hEst1A can be stably expressed in HT1080 cells and cultured for a long period of time without a detectable growth defect. Overexpression of hEst1A has been suggested to induce apoptosis as a result of chromosome end to end fusions and anaphase bridges. This phenotype was characterized in HTC75 cells using an inducible system within 72 hours after the induction of the protein expression. While generating the stable cell lines by retroviral infection, I observed about 30% of cell death after 12-14 hours selection in cells expression of wild type hEst1A and 5 % of cell death in the vector control cells. However, cells expressing hEst1A recovered after 24 hours of selection. Since hEst1A is a large protein containing 1419 amino acids, cells may need time to adapt in order to be forced to express such a huge protein.

Human Est1A has been suggested to negatively regulate TERRA association with telomeric DNA without affecting either the half life of TERRA or total TERRA levels (Azzalin et al., 2007). TERRA has been suggested to associate with the telomerase RNA template and may be a competitive inhibitor for telomerase association with telomeric DNA *in vitro* as well as *in vivo* (Redon *et al.*, 2010). Depletion of TERRA by siRNA causes a defect in telomere heterochromatin and induces dysfunctional telomere foci, implicating that TERRA may be a component of telomeric heterochromatin (Deng et al., 2009). Overexpression of hEst1A #7 may be sufficient to displace TERRA from telomeres and increase telomerase accessibility. Alternatively, deletion of the N-terminal 220 amino acids would result in the exposure of RID domain which mediates the

interaction of hEst1A with hTR. The exposure of the RID domain may enhance telomerase recruitment and promotes telomere elongation.

Since hEst1A#7 doesn't contain the EMB motifs, presumably this protein is not involved in NMD pathway. It is unknown whether the function of hEst1A at NMD and at telomeres can be separated. Elucidating the mechanism of overexpression of hEst1A#7 promoting telomere elongations may provide a mean to separate the hEst1A function at different pathways. Overexpression hEst1A#7 may cause the disassociation of TERRA from telomeres. RNA-FISH and RNA-ChIP analysis (using anti-Myc antibody) can be performed to assess whether overexpression of hEst1A#7 may affect telomeric association of TERRA. The *in vitro* transcribed hTR appears to contain several binding sites for the RID domain of hEst1A (Redon et al., 2007). RNA-FISH using antibody against hTR can be performed to examine whether overexpression of hEst1A#7 may enhance the recruitment of hTR to telomeres.

To further understand the role of hEst1A at telomeres, it is worth to introduce hEst1A deletion mutant under endogenous hEst1A depleted background which is the approach also utilized for identifying the domain of SMG6 involved in NMD (Kashima et al., 2010). Knockdown of hEst1A results in sister telomere fusion, and sudden lose of entire telomere tract at some chromosome ends (Azzalin et al., 2007). It is of interest to illustrate which domain of hEst1A is responsible for such detrimental phenotypes. However, knockdown of hEst1A generates a cell cycle arrest and induces DNA damage response (Chawla & Azzalin, 2008). It seems unfeasible to introduce shRNA resistant hEst1A deletion mutants into endogenous hEst1A depleted cells. However, it may be

possible to co-expression of hEst1A (wild type or deletion mutants) with sh-hEst1A to generate stable cell lines. If any of this stable cell line could be made, domain(s) of hEst1A important for hEst1A function in maintaining telomere integrity could be further characterized.

6.3 *C.elegans* SMG-6 in Telomere Length Maintenance

C. elegans (tm1308) carries a deletion at its N-terminus. This strain has shorter telomeres compared to wild type strain N2. It appears that the role of Est1 in telomere length maintenance is conserved in *C.elegan*. SMG-6 *(r896)* carries a point mutation at 14-3-3 domain (G to R at residue 582) and this mutant has abnormal vulva (Hodgkinet al., 1989). The 14-3-3 proteins are a family of signal transduction proteins that specifically recognize and bind to phosphorylated serine or threonine residues (Tzivion et al., 2001). The average telomere length of this strain is similar to that of wild type strain. However, whether this mutation may affect telomere length dynamics has not been assessed. This site (correspond to G681 of hEst1A) is conserved between hEst1A and SMG-6, raising the question as to whether G681 may be important for the function of hEst1A for telomere length maintenance and NMD.

Bibliography

Abraham, R. T. (2001). Cell cycle checkpoint signaling through the ATM and ATR kinases. *Genes & Development, 15*, 2177-2196.

Abreu, E., Aritonovska, E., Reichenbach, P., Cristofari, G., Culp, B., Terns, R. M., et al. (2010). TIN2-tethered TPP1 recruits human telomerase to telomeres in vivo. *Molecular and Cellular Biology, 30*, 2971-2982.

Amiard, S., Doudeau, M., Pinte, S., Poulet, A., Lenain, C., Faivre-Moskalenko, C., et al. (2007). A topological mechanism for TRF2-enhanced strand invasion. *Nature Structural & Molecular Biology, 14*, 147-154.

Ancelin, K., Brunori, M., Bauwens, S., Koering, C. E., Brun, C., Ricoul, M., et al. (2002). Targeting assay to study the cis functions of human telomeric proteins: Evidence for inhibition of telomerase by TRF1 and for activation of telomere degradation by TRF2. *Molecular and Cellular Biology, 22*, 3474-3487.

Arcus, V. L., Backbro, K., Roos, A., Daniel, E. L., & Baker, E. N. (2004). Distant structural homology leads to the functional characterization of an archaeal PIN domain as an exonuclease. *The Journal of Biological Chemistry, 279*, 16471-16478.

Azzalin, C. M., & Lingner, J. (2006). The human RNA surveillance factor UPF1 is required for S phase progression and genome stability. *Current Biology, 16*, 433-439.

Azzalin, C. M., Reichenbach, P., Khoriauli, L., Giulotto, E., & Lingner, J. (2007). Telomeric repeat containing RNA and RNA surveillance factors at mammalian chromosome ends. *Science, 318*, 798-801.

Baumann, P., & Cech, T. R. (2001). Pot1, the putative telomere end-binding protein in fission yeast and humans. *Science, 292*, 1171-1175.

Behm-Ansmant, I., & Izaurralde, E. (2006). Quality control of gene expression: A stepwise assembly pathway for the surveillance complex that triggers nonsense-mediated mRNA decay. *Genes & Development, 20*, 391-398.

Bianchi, A., Negrini, S., & Shore, D. (2004). Delivery of yeast telomerase to a DNA break depends on the recruitment functions of Cdc13 and Est1. *Molecular Cell, 16*, 139-146.

Bianchi, A., & Shore, D. (2008). How telomerase reaches its end: Mechanism of telomerase regulation by the telomeric complex. *Molecular Cell, 31*, 153-165.

Bianchi, A., Smith, S., Chong, L., Elias, P., & de Lange, T. (1997). TRF1 is a dimer and bends telomeric DNA. *The EMBO Journal, 16*, 1785-1794.

Bilaud, T., Brun, C., Ancelin, K., Koering, C. E., Laroche, T., & Gilson, E. (1997). Telomeric localization of TRF2, a novel human telobox protein. *Nature Genetics, 17*, 236-239.

Blackburn, E. H., Greider, C. W., Henderson, E., Lee, M. S., Shampay, J., & Shippen-Lentz, D. (1989). Recognition and elongation of telomeres by telomerase. *Genome, 31*, 553-560.

Brenner, S. (1974). The genetics of caenorhabditis elegans. *Genetics, 77*, 71-94.

Broccoli, D., Chong, L., Oelmann, S., Fernald, A. A., Marziliano, N., van Steensel, B., et al. (1997). Comparison of the human and mouse genes encoding the telomeric protein, TRF1: Chromosomal localization, expression and conserved protein domains. *Human Molecular Genetics, 6*, 69-76.

Broccoli, D., Young, J. W., & de Lange, T. (1995). Telomerase activity in normal and malignant hematopoietic cells. *Proceedings of the National Academy of Sciences of the United States of America, 92*, 9082-9086.

Brumbaugh, K. M., Otterness, D. M., Geisen, C., Oliveira, V., Brognard, J., Li, X., et al. (2004). The mRNA surveillance protein hSMG-1 functions in genotoxic stress response pathways in mammalian cells. *Molecular Cell, 14*, 585-598.

Buchwald, G., Ebert, J., Basquin, C., Sauliere, J., Jayachandran, U., Bono, F., et al. (2010). Insights into the recruitment of the NMD machinery from the crystal structure of a core EJC-UPF3b complex. *Proceedings of the National Academy of Sciences of the United States of America, 107*, 10050-10055.

Celli, G. B., & de Lange, T. (2005). DNA processing is not required for ATM-mediated telomere damage response after TRF2 deletion. *Nature Cell Biology, 7*, 712-718.

Chang, W., Dynek, J. N., & Smith, S. (2003). TRF1 is degraded by ubiquitin-mediated proteolysis after release from telomeres. *Genes & Development, 17*, 1328-1333.

Chawla, R., & Azzalin, C. M. (2008). The telomeric transcriptome and SMG proteins at the crossroads. *Cytogenetic and Genome Research, 122*, 194-201.

Chen, Y., Yang, Y., van Overbeek, M., Donigian, J. R., Baciu, P., de Lange, T., et al. (2008). A shared docking motif in TRF1 and TRF2 used for differential recruitment of telomeric proteins. *Science, 319*, 1092-1096.

Chen, Y. C., Teng, S. C., & Wu, K. J. (2009). Phosphorylation of telomeric repeat binding factor 1 (TRF1) by akt causes telomere shortening. *Cancer Investigation, 27*, 24-28.

Cheung, I., Schertzer, M., Baross, A., Rose, A. M., Lansdorp, P. M., & Baird, D. M. (2004). Strain-specific telomere length revealed by single telomere length analysis in caenorhabditis elegans. *Nucleic Acids Research, 32*, 3383-3391.

Chiu, S. Y., Serin, G., Ohara, O., & Maquat, L. E. (2003). Characterization of human Smg5/7a: A protein with similarities to caenorhabditis elegans SMG5 and SMG7 that functions in the dephosphorylation of Upf1. *RNA , 9*, 77-87.

Chong, L., van Steensel, B., Broccoli, D., Erdjument-Bromage, H., Hanish, J., Tempst, P., et al. (1995). A human telomeric protein. *Science 270*, 1663-1667.

Cimprich, K. A., & Cortez, D. (2008). ATR: An essential regulator of genome integrity. *Nature Reviews.Molecular Cell Biology, 9*, 616-627.

Clissold, P. M., & Ponting, C. P. (2000). PIN domains in nonsense-mediated mRNA decay and RNAi. *Current Biology, 10*, R888-90.

Conrad, M. N., Wright, J. H., Wolf, A. J., & Zakian, V. A. (1990). RAP1 protein interacts with yeast telomeres in vivo: Overproduction alters telomere structure and decreases chromosome stability. *Cell, 63*, 739-750.

de Lange, T. (2002). Protection of mammalian telomeres. *Oncogene, 21*, 532-540.

de Lange, T. (2005). Shelterin: The protein complex that shapes and safeguards human telomeres. *Genes & Development, 19*, 2100-2110.

Denchi, E. L., & de Lange, T. (2007). Protection of telomeres through independent control of ATM and ATR by TRF2 and POT1. *Nature, 448*, 1068-1071.

Deng, Z., Norseen, J., Wiedmer, A., Riethman, H., & Lieberman, P. M. (2009). TERRA RNA binding to TRF2 facilitates heterochromatin formation and ORC recruitment at telomeres. *Molecular Cell, 35*, 403-413.

Dynek, J. N., & Smith, S. (2004). Resolution of sister telomere association is required for progression through mitosis. *Science . 304*, 97-100.

Eberle, A. B., Lykke-Andersen, S., Muhlemann, O., & Jensen, T. H. (2009). SMG6 promotes endonucleolytic cleavage of nonsense mRNA in human cells. *Nature Structural & Molecular Biology, 16*, 49-55.

Fairall, L., Chapman, L., Moss, H., de Lange, T., & Rhodes, D. (2001). Structure of the TRFH dimerization domain of the human telomeric proteins TRF1 and TRF2. *Molecular Cell, 8*, 351-361.

Feng, J., Funk, W. D., Wang, S. S., Weinrich, S. L., Avilion, A. A., Chiu, C. P., et al. (1995). The RNA component of human telomerase. *Science, 269*, 1236-1241.

Fouche, N., Cesare, A. J., Willcox, S., Ozgur, S., Compton, S. A., & Griffith, J. D. (2006). The basic domain of TRF2 directs binding to DNA junctions irrespective of the presence of TTAGGG repeats. *The Journal of Biological Chemistry, 281*, 37486-37495

Fukuhara, N., Ebert, J., Unterholzner, L., Lindner, D., Izaurralde, E., & Conti, E. (2005). SMG7 is a 14-3-3-like adaptor in the nonsense-mediated mRNA decay pathway. *Molecular Cell, 17*, 537-547.

Gehen, S. C., Staversky, R. J., Bambara, R. A., Keng, P. C., & O'Reilly, M. A. (2008). hSMG-1 and ATM sequentially and independently regulate the G1 checkpoint during oxidative stress. *Oncogene, 27*, 4065-4074.

Glavan, F., Behm-Ansmant, I., Izaurralde, E., & Conti, E. (2006). Structures of the PIN domains of SMG6 and SMG5 reveal a nuclease within the mRNA surveillance complex. *The EMBO Journal, 25*, 5117-5125.

Greider, C. W., & Blackburn, E. H. (1985). Identification of a specific telomere terminal transferase activity in tetrahymena extracts. *Cell, 43*, 405-413.

Greider, C. W., & Blackburn, E. H. (1987). The telomere terminal transferase of tetrahymena is a ribonucleoprotein enzyme with two kinds of primer specificity. *Cell, 51*, 887-898.

Greider, C. W., & Blackburn, E. H. (1989). A telomeric sequence in the RNA of tetrahymena telomerase required for telomere repeat synthesis. *Nature, 337*, 331-337.

Griffith, J., Bianchi, A., & de Lange, T. (1998). TRF1 promotes parallel pairing of telomeric tracts in vitro. *Journal of Molecular Biology, 278*, 79-88.

Griffith, J. D., Comeau, L., Rosenfield, S., Stansel, R. M., Bianchi, A., Moss, H., et al. (1999). Mammalian telomeres end in a large duplex loop. *Cell, 97*, 503-514.

Harley, C. B., Futcher, A. B., & Greider, C. W. (1990). Telomeres shorten during ageing of human fibroblasts. *Nature, 345*, 458-460.

Hockemeyer, D., Palm, W., Else, T., Daniels, J. P., Takai, K. K., Ye, J. Z., et al. (2007). Telomere protection by mammalian Pot1 requires interaction with Tpp1. *Nature Structural & Molecular Biology, 14*, 754-761.

Hodgkin, J., Papp, A., Pulak, R., Ambros, V., & Anderson, P. (1989). A new kind of informational suppression in the nematode caenorhabditis elegans. *Genetics, 123*, 301-313.

Houghtaling, B. R., Cuttonaro, L., Chang, W., & Smith, S. (2004). A dynamic molecular link between the telomere length regulator TRF1 and the chromosome end protector TRF2. *Current Biology, 14*, 1621-1631.

Hughes, T. R., Evans, S. K., Weilbaecher, R. G., & Lundblad, V. (2000). The Est3 protein is a subunit of yeast telomerase. *Current Biology, 10*, 809-812.

Huntzinger, E., Kashima, I., Fauser, M., Sauliere, J., & Izaurralde, E. (2008). SMG6 is the catalytic endonuclease that cleaves mRNAs containing nonsense codons in metazoan. *RNA, 14*, 2609-2617.

Karlseder, J., Broccoli, D., Dai, Y., Hardy, S., & de Lange, T. (1999). p53- and ATM-dependent apoptosis induced by telomeres lacking TRF2. *Science, 283*, 1321-1325.

Karlseder, J., Kachatrian, L., Takai, H., Mercer, K., Hingorani, S., Jacks, T., et al. (2003). Targeted deletion reveals an essential function for the telomere length regulator Trf1. *Molecular and Cellular Biology, 23*, 6533-6541.

Kashima, I., Jonas, S., Jayachandran, U., Buchwald, G., Conti, E., Lupas, A. N., et al. (2010). SMG6 interacts with the exon junction complex via two conserved EJC-binding motifs (EBMs) required for nonsense-mediated mRNA decay. *Genes & Development, 24*, 2440-2450.

Kedde, M., le Sage, C., Duursma, A., Zlotorynski, E., van Leeuwen, B., Nijkamp, W., et al. (2006). Telomerase-independent regulation of ATR by human telomerase RNA. *The Journal of Biological Chemistry, 281*, 40503-40514.

Kelleher, C., Kurth, I., & Lingner, J. (2005). Human protection of telomeres 1 (POT1) is a negative regulator of telomerase activity in vitro. *Molecular and Cellular Biology, 25*, 808-818.

Kim, M. K., Kang, M. R., Nam, H. W., Bae, Y. S., Kim, Y. S., & Chung, I. K. (2008). Regulation of telomeric repeat binding factor 1 binding to telomeres by casein kinase 2-mediated phosphorylation. *The Journal of Biological Chemistry, 283*, 14144-14152.

Kim, N. W., Piatyszek, M. A., Prowse, K. R., Harley, C. B., West, M. D., Ho, P. L., et al. (1994). Specific association of human telomerase activity with immortal cells and cancer. *Science, 266*, 2011-2015.

Kim, S. H., Davalos, A. R., Heo, S. J., Rodier, F., Zou, Y., Beausejour, C., et al. (2008). Telomere dysfunction and cell survival: Roles for distinct TIN2-containing complexes. *The Journal of Cell Biology, 181*, 447-460.

Kim, S. H., Kaminker, P., & Campisi, J. (1999). TIN2, a new regulator of telomere length in human cells. *Nature Genetics, 23*, 405-412.

Kishi, S., & Lu, K. P. (2002). A critical role for Pin2/TRF1 in ATM-dependent regulation. inhibition of Pin2/TRF1 function complements telomere shortening, radiosensitivity, and the G(2)/M checkpoint defect of ataxia-telangiectasia cells. *The Journal of Biological Chemistry, 277*, 7420-7429.

Kishi, S., Wulf, G., Nakamura, M., & Lu, K. P. (2001). Telomeric protein Pin2/TRF1 induces mitotic entry and apoptosis in cells with short telomeres and is down-regulated in human breast tumors. *Oncogene, 20*, 1497-1508.

Kishi, S., Zhou, X. Z., Ziv, Y., Khoo, C., Hill, D. E., Shiloh, Y., et al. (2001). Telomeric protein Pin2/TRF1 as an important ATM target in response to double strand DNA breaks. *The Journal of Biological Chemistry, 276*, 29282-29291.

Lee, T. H., Perrem, K., Harper, J. W., Lu, K. P., & Zhou, X. Z. (2006). The F-box protein FBX4 targets PIN2/TRF1 for ubiquitin-mediated degradation and regulates telomere maintenance. *The Journal of Biological Chemistry, 281*, 759-768.

Lee, T. H., Tun-Kyi, A., Shi, R., Lim, J., Soohoo, C., Finn, G., et al. (2009). Essential role of Pin1 in the regulation of TRF1 stability and telomere maintenance. *Nature Cell Biology, 11*, 97-105.

Lendvay, T. S., Morris, D. K., Sah, J., Balasubramanian, B., & Lundblad, V. (1996). Senescence mutants of saccharomyces cerevisiae with a defect in telomere replication identify three additional EST genes. *Genetics, 144*, 1399-1412.

Levin, I., Schwarzenbacher, R., Page, R., Abdubek, P., Ambing, E., Biorac, T., et al. (2004). Crystal structure of a PIN (PilT N-terminus) domain (AF0591) from archaeoglobus fulgidus at 1.90 A resolution. *Proteins, 56*, 404-408.

Li, B., & de Lange, T. (2003). Rap1 affects the length and heterogeneity of human telomeres. *Molecular Biology of the Cell, 14*, 5060-5068.

Li, B., Oestreich, S., & de Lange, T. (2000). Identification of human Rap1: Implications for telomere evolution. *Cell, 101*, 471-483.

Lingner, J., Hughes, T. R., Shevchenko, A., Mann, M., Lundblad, V., & Cech, T. R. (1997). Reverse transcriptase motifs in the catalytic subunit of telomerase. *Science, 276*, 561-567.

Liu, D., O'Connor, M. S., Qin, J., & Songyang, Z. (2004). Telosome, a mammalian telomere-associated complex formed by multiple telomeric proteins. *The Journal of Biological Chemistry, 279*, 51338-51342.

Loayza, D., & De Lange, T. (2003). POT1 as a terminal transducer of TRF1 telomere length control. *Nature, 423*, 1013-1018.

Loayza, D., Parsons, H., Donigian, J., Hoke, K., & de Lange, T. (2004). DNA binding features of human POT1: A nonamer 5'-TAGGGTTAG-3' minimal binding site, sequence specificity, and internal binding to multimeric sites. *The Journal of Biological Chemistry, 279*, 13241-13248.

Lundblad, V., & Szostak, J. W. (1989). A mutant with a defect in telomere elongation leads to senescence in yeast. *Cell, 57*, 633-643.

Makarov, V. L., Hirose, Y., & Langmore, J. P. (1997). Long G tails at both ends of human chromosomes suggest a C strand degradation mechanism for telomere shortening. *Cell, 88*, 657-666.

Mallory, J. C., & Petes, T. D. (2000). Protein kinase activity of Tel1p and Mec1p, two saccharomyces cerevisiae proteins related to the human ATM protein kinase. *Proceedings of the National Academy of Sciences of the United States of America, 97*, 13749-13754.

McKerlie, M., & Zhu, X. D. (2011). Cyclin B-dependent kinase 1 regulates human TRF1 to modulate the resolution of sister telomeres. *Nature Communications, 2*, 371.

Meier, B., Clejan, I., Liu, Y., Lowden, M., Gartner, A., Hodgkin, J., et al. (2006). Trt-1 is the caenorhabditis elegans catalytic subunit of telomerase. *PLoS Genetics, 2*, e18.

Metcalfe, J. A., Parkhill, J., Campbell, L., Stacey, M., Biggs, P., Byrd, P. J., et al. (1996). Accelerated telomere shortening in ataxia telangiectasia. *Nature Genetics, 13*, 350-353.

Meyerson, M., Counter, C. M., Eaton, E. N., Ellisen, L. W., Steiner, P., Caddle, S. D., et al. (1997). hEST2, the putative human telomerase catalytic subunit gene, is up-regulated in tumor cells and during immortalization. *Cell, 90*, 785-795.

Moyzis, R. K., Buckingham, J. M., Cram, L. S., Dani, M., Deaven, L. L., Jones, M. D., et al. (1988). A highly conserved repetitive DNA sequence, (TTAGGG)n, present at the telomeres of human chromosomes. *Proceedings of the National Academy of Sciences of the United States of America, 85*, 6622-6626.

Nakamura, M., Zhou, X. Z., Kishi, S., & Lu, K. P. (2002). Involvement of the telomeric protein Pin2/TRF1 in the regulation of the mitotic spindle. *FEBS Letters, 514*, 193-198.

Nugent, C. I., Hughes, T. R., Lue, N. F., & Lundblad, V. (1996). Cdc13p: A single-strand telomeric DNA-binding protein with a dual role in yeast telomere maintenance. *Science, 274*, 249-252.

O'Connor, M. S., Safari, A., Xin, H., Liu, D., & Songyang, Z. (2006). A critical role for TPP1 and TIN2 interaction in high-order telomeric complex assembly. *Proceedings of the National Academy of Sciences of the United States of America, 103*, 11874-11879.

Ohnishi, T., Yamashita, A., Kashima, I., Schell, T., Anders, K. R., Grimson, A., et al. (2003). Phosphorylation of hUPF1 induces formation of mRNA surveillance complexes containing hSMG-5 and hSMG-7. *Molecular Cell, 12*, 1187-1200.

Oganesian, L., & Karlseder, J. (2011). Mammalian 5' C-rich telomeric overhangs are a mark of recombination-dependent telomere maintenance. *Molecular Cell, 42*, 224-236.

Olovnikov, A. M. (1973). A theory of marginotomy. the incomplete copying of template margin in enzymic synthesis of polynucleotides and biological significance of the phenomenon. *Journal of Theoretical Biology, 41*, 181-190.

Palm, W., & de Lange, T. (2008). How shelterin protects mammalian telomeres. *Annual Review of Genetics, 42*, 301-334.

Pennock, E., Buckley, K., & Lundblad, V. (2001). Cdc13 delivers separate complexes to the telomere for end protection and replication. *Cell, 104*, 387-396.

Qi, H., & Zakian, V. A. (2000). The saccharomyces telomere-binding protein Cdc13p interacts with both the catalytic subunit of DNA polymerase alpha and the telomerase-associated est1 protein. *Genes & Development, 14*, 1777-1788.

Raices, M., Maruyama, H., Dillin, A., & Karlseder, J. (2005). Uncoupling of longevity and telomere length in C. elegans. *PLoS Genetics, 1*, e30.

Raices, M., Verdun, R. E., Compton, S. A., Haggblom, C. I., Griffith, J. D., Dillin, A., et al. (2008). C. elegans telomeres contain G-strand and C-strand overhangs that are bound by distinct proteins. *Cell, 132*, 745-757.

Redon, S., Reichenbach, P., & Lingner, J. (2007). Protein RNA and protein protein interactions mediate association of human EST1A/SMG6 with telomerase. *Nucleic Acids Research, 35*, 7011-7022.

Reichenbach, P., Hoss, M., Azzalin, C. M., Nabholz, M., Bucher, P., & Lingner, J. (2003). A human homolog of yeast Est1 associates with telomerase and uncaps chromosome ends when overexpressed. *Current Biology, 13*, 568-574.

Ritchie, K. B., Mallory, J. C., & Petes, T. D. (1999). Interactions of TLC1 (which encodes the RNA subunit of telomerase), TEL1, and MEC1 in regulating telomere length in the yeast saccharomyces cerevisiae. *Molecular and Cellular Biology, 19*, 6065-6075.

Sarthy, J., Bae, N. S., Scrafford, J., & Baumann, P. (2009). Human RAP1 inhibits non-homologous end joining at telomeres. *The EMBO Journal, 28*, 3390-3399.

Schoeftner, S., & Blasco, M. A. (2008). Developmentally regulated transcription of mammalian telomeres by DNA-dependent RNA polymerase II. *Nature Cell Biology, 10*, 228-236.

Seto, A. G., Livengood, A. J., Tzfati, Y., Blackburn, E. H., & Cech, T. R. (2002). A bulged stem tethers Est1p to telomerase RNA in budding yeast. *Genes & Development, 16*, 2800-2812.

Sfeir, A., Kabir, S., van Overbeek, M., Celli, G. B., & de Lange, T. (2010). Loss of Rap1 induces telomere recombination in the absence of NHEJ or a DNA damage signal. *Science, 327*, 1657-1661.

Sfeir, A., Kosiyatrakul, S. T., Hockemeyer, D., MacRae, S. L., Karlseder, J., Schildkraut, C. L., et al. (2009). Mammalian telomeres resemble fragile sites and require TRF1 for efficient replication. *Cell, 138*, 90-103.

Shen, M., Haggblom, C., Vogt, M., Hunter, T., & Lu, K. P. (1997). Characterization and cell cycle regulation of the related human telomeric proteins Pin2 and TRF1 suggest a role in mitosis. *Proceedings of the National Academy of Sciences of the United States of America, 94*, 13618-13623.

Singer, M. S., & Gottschling, D. E. (1994). TLC1: Template RNA component of saccharomyces cerevisiae telomerase. *Science, 266*, 404-409.

Smith, S., Giriat, I., Schmitt, A., & de Lange, T. (1998). Tankyrase, a poly(ADP-ribose) polymerase at human telomeres. *Science, 282*, 1484-1487.

Smogorzewska, A., & de Lange, T. (2004). Regulation of telomerase by telomeric proteins. *Annual Review of Biochemistry, 73*, 177-208.

Smogorzewska, A., van Steensel, B., Bianchi, A., Oelmann, S., Schaefer, M. R., Schnapp, G., et al. (2000). Control of human telomere length by TRF1 and TRF2. *Molecular and Cellular Biology, 20*, 1659-1668.

Snow, B. E., Erdmann, N., Cruickshank, J., Goldman, H., Gill, R. M., Robinson, M. O., et al. (2003). Functional conservation of the telomerase protein Est1p in humans. *Current Biology, 13*, 698-704.

Stansel, R. M., de Lange, T., & Griffith, J. D. (2001). T-loop assembly in vitro involves binding of TRF2 near the 3' telomeric overhang. *The EMBO Journal, 20*, 5532-5540.

Taggart, A. K., Teng, S. C., & Zakian, V. A. (2002). Est1p as a cell cycle-regulated activator of telomere-bound telomerase. *Science, 297*, 1023-1026.

Takeshita, D., Zenno, S., Lee, W. C., Saigo, K., & Tanokura, M. (2006). Crystallization and preliminary X-ray analysis of the PIN domain of human EST1A., *Structural Biology and Crystallization Communications, 62*, 656-658.

Tzivion, G., Shen, Y. H., & Zhu, J. (2001). 14-3-3 proteins; bringing new definitions to scaffolding. *Oncogene, 20*, 6331-6338.

Unterholzner, L., & Izaurralde, E. (2004). SMG7 acts as a molecular link between mRNA surveillance and mRNA decay. *Molecular Cell, 16*, 587-596.

van Steensel, B., & de Lange, T. (1997). Control of telomere length by the human telomeric protein TRF1. *Nature, 385*, 740-743.

van Steensel, B., Smogorzewska, A., & de Lange, T. (1998). TRF2 protects human telomeres from end-to-end fusions. *Cell, 92*, 401-413.

Verdun, R. E., Crabbe, L., Haggblom, C., & Karlseder, J. (2005). Functional human telomeres are recognized as DNA damage in G2 of the cell cycle. *Molecular Cell, 20*, 551-561.

Virta-Pearlman, V., Morris, D. K., & Lundblad, V. (1996). Est1 has the properties of a single-stranded telomere end-binding protein. *Genes & Development, 10*, 3094-3104.

Watson, J. D. (1972). Origin of concatemeric T7 DNA. *Nature: New Biology, 239*, 197-201.

Wellinger, R. J., & Sen, D. (1997). The DNA structures at the ends of eukaryotic chromosomes. *European Journal of Cancer, 33*, 735-749.

Wellinger, R. J., Wolf, A. J., & Zakian, V. A. (1993). Saccharomyces telomeres acquire single-strand TG1-3 tails late in S phase. *Cell, 72*, 51-60.

Wil Wright, W. E., & Shay, J. W. (2002). Historical claims and current interpretations of replicative aging. *Nature Biotechnology, 20*, 682-688.

Wilkinson, M. F. (2003). The cycle of nonsense. *Molecular Cell, 12*, 1059-1061.

Wu, L., Multani, A. S., He, H., Cosme-Blanco, W., Deng, Y., Deng, J. M., et al. (2006). Pot1 deficiency initiates DNA damage checkpoint activation and aberrant homologous recombination at telomeres. *Cell, 126*, 49-62.

Wu, Z. Q., Yang, X., Weber, G., & Liu, X. (2008). Plk1 phosphorylation of TRF1 is essential for its binding to telomeres. *The Journal of Biological Chemistry, 283*, 25503-25513.

Xin, H., Liu, D., Wan, M., Safari, A., Kim, H., Sun, W., et al. (2007). TPP1 is a homologue of ciliate TEBP-beta and interacts with POT1 to recruit telomerase. *Nature, 445*, 559-562.

Yamashita, A., Kashima, I., & Ohno, S. (2005). The role of SMG-1 in nonsense-mediated mRNA decay. *Biochimica Et Biophysica Acta, 1754*, 305-315.

Ye, J. Z., & de Lange, T. (2004). TIN2 is a tankyrase 1 PARP modulator in the TRF1 telomere length control complex. *Nature Genetics, 36*, 618-623.

Ye, J. Z., Donigian, J. R., van Overbeek, M., Loayza, D., Luo, Y., Krutchinsky, A. N., et al. (2004). TIN2 binds TRF1 and TRF2 simultaneously and stabilizes the TRF2 complex on telomeres. *The Journal of Biological Chemistry, 279*, 47264-47271.

Ye, J. Z., Hockemeyer, D., Krutchinsky, A. N., Loayza, D., Hooper, S. M., Chait, B. T., et al. (2004). POT1-interacting protein PIP1: A telomere length regulator that recruits POT1 to the TIN2/TRF1 complex. *Genes & Development, 18*, 1649-1654.

Zhang, M. L., Tong, X. J., Fu, X. H., Zhou, B. O., Wang, J., Liao, X. H., et al. (2010). Yeast telomerase subunit Est1p has guanine quadruplex-promoting activity that is required for telomere elongation. *Nature Structural & Molecular Biology, 17*, 202-209.

Zhong, Z., Shiue, L., Kaplan, S., & de Lange, T. (1992). A mammalian factor that binds telomeric TTAGGG repeats in vitro. *Molecular and Cellular Biology, 12*, 4834-4843.

Zhou, X. Z., Perrem, K., & Lu, K. P. (2003). Role of Pin2/TRF1 in telomere maintenance and cell cycle control. *Journal of Cellular Biochemistry, 89*, 19-37.

Zhu, X. D., Kuster, B., Mann, M., Petrini, J. H., & de Lange, T. (2000). Cell-cycle-regulated association of RAD50/MRE11/NBS1 with TRF2 and human telomeres. *Nature Genetics, 25*, 347-352.